The LINNEAN SOCIETY of London ZOOLOGICAL Journal of the Linnean Society

Zoological Journal of the Linnean Society, 2011, **163**, 1157–1198. With 24 figures

A new basal ornithopod dinosaur (Frenchman Formation, Saskatchewan, Canada), and implications for late Maastrichtian ornithischian diversity in North America

CALEB MARSHALL BROWN[1]*, CLINT A. BOYD[2] and ANTHONY P. RUSSELL FLS[1]

[1]*Department of Biological Sciences, University of Calgary, 2500 University Drive N.W., Calgary, AB T2N 1N4, Canada*
[2]*Jackson School of Geosciences, The University of Texas at Austin, 1 University Station C1100, Austin, TX 78712, USA*

Received 5 November 2010; revised 20 January 2011; accepted for publication 24 January 2011

A small, articulated basal ornithopod skeleton from the Frenchman Formation (late Maastrichtian) of Saskatchewan (RSM P 1225.1), previously referred to the taxon *Thescelosaurus*, differs from both recognized species of this taxon (*Thescelosaurus neglectus* and *Thescelosaurus garbanii*). The differences are taxonomically informative and we recognize this specimen as the holotype of a new species, ***Thescelosaurus assiniboiensis* sp. nov.**, diagnosed by the presence of two autapomorphies, and displaying plesiomorphic traits more similar to those of *Parksosaurus*, than to those of the other *Thescelosaurus* species. The Frenchman Formation also harbours an intriguing faunal assemblage in which *Thescelosaurus* represents one of the most abundant dinosaur taxa, and preserves a relatively high proportion of small (putatively juvenile and subadult) specimens of many dinosaur taxa. Further work that increases the faunal sample from this formation, and that permits quantitative comparisons with contemporary formations, will determine whether or not these differences are well supported, and will determine their ultimate palaeobiological significance. Identification of a third species of *Thescelosaurus* from the late Maastrichtian of North America suggests that this taxon was more diverse than previously recognized, and shows an increase in diversity from the Campanian through the late Maastrichtian, contrasting the trends seen in most other ornithischian clades.

doi: 10.1111/j.1096-3642.2011.00735.x

ADDITIONAL KEYWORDS: *Thescelosaurus* – *Parksosaurus* – Cretaceous – Systematics – Osteology.

INTRODUCTION

As the largest and latest occurring (late Maastrichtian) member of the traditional 'Hypsilophodontidae', *Thescelosaurus* is an intriguing basal ornithopod with a convoluted taxonomic and systematic history (Sues & Norman, 1990; Weishampel & Heinrich, 1992; Sues, 1997; Boyd *et al*., 2009). Hypsilophodontidae has been historically characterized as containing small, lightly built ornithopod dinosaurs with widespread occurrence, both geographically and statigraphically, through the latter half of the Mesozoic (Galton, 1973, 1974a, b; Sereno, 1986; Sues & Norman, 1990; Weishampel & Heinrich, 1992). Recent cladistic analyses, however, have failed to recover this group and have suggested that its constituent taxa form successive sister taxa to Iguanodontoidea, with a trend towards increasing size and herbivorous specialization (Scheetz, 1998, 1999; Winkler, Murry & Jacobs, 1998; Norman *et al*., 2004;

*Corresponding author. Current address: Department of Ecology and Evolutionary Biology, University of Toronto. E-mail: caleb.brown@utoronto.ca

Butler, Upchurch & Norman, 2008; Boyd *et al*., 2009). Although the taxon Hypsilophodontidae is no longer considered valid, a clade consisting of the Late Cretaceous North American basal ornithopods was recovered by Boyd *et al*. (2009).

There is also uncertainty surrounding the systematic relationships of *Thescelosaurus* (Sereno, 1998; Scheetz, 1999; Butler, 2005; Butler *et al*., 2008; Boyd *et al*., 2009). In the context of large-scale phylogenetic analyses of ornithischian relationships (e.g. Butler *et al*., 2008), support for the traditional placement of *Thescelosaurus* within Ornithopoda is ambiguous when strict concensus cladograms are presented (e.g. Butler *et al*., 2008: fig. 2). However, no strong evidence has yet been presented to contradict the traditional view of *Thescelosaurus* as an ornithopod, and, therefore, we tentatively place *Thescelosaurus* within Ornithopoda. Throughout this study we use the term 'basal ornithopod' to refer to non-iguanodontoid ornithopods, pending more precise and robust systematic resolution. Additionally, we restrict the term 'basal neornithischian' to those taxa definitively placed outside of Ornithopoda but that fall within Neornithischia in the strict consensus tree of Butler *et al*.(2008: fig. 2).

Much of the confusion regarding the taxonomy and systematics of *Thescelosaurus* has resulted from a lack of well-preserved material, with few of these specimens being represented by comparable parts of the skeleton (see discussion in Boyd *et al*., 2009). As such, the recognition of discrete apomorphies diagnosing *Thescelosaurus* and its constituent species has been problematic. The type species, *Thescelosaurus neglectus* Gilmore, 1913, is based on an articulated holotype lacking the head and neck (USNM 7757, Fig. 1E) and a fragmentary paratype (USNM 7758, Fig. 1F) from the late Maastrichtian Lance Formation of Wyoming (Gilmore, 1913). Shortly after the type species was described, a second taxon, *Parksosaurus warreni* (Parks, 1926), originally referred to *Thescelosaurus*, was described from the early Maastrichtian Horseshoe Canyon Formation of Alberta, based on a single nearly complete specimen (ROM 804, Fig. 1J). *Parksosaurus warreni* was originally distinguished from *T. neglectus* by its more gracile skeleton, shorter femur, longer tibia, and longer phalanges. Since its discovery, only one additional specimen, an isolated tooth (Larson, Brinkman & Bell, 2010), has been referred to *Parksosaurus*. However, over the succeeding years multiple basal ornithopod skeletons have been recovered from late Maastrichtian deposits, and additional taxa have been described: *Thescelosaurus edmontonensis* Sternberg, 1940 (Fig. 1G), *Thescelosaurus garbanii* Morris, 1976 (Fig. 1B), and *Bugenasaura infernalis* Galton, 1995 (Fig. 1B). The lack

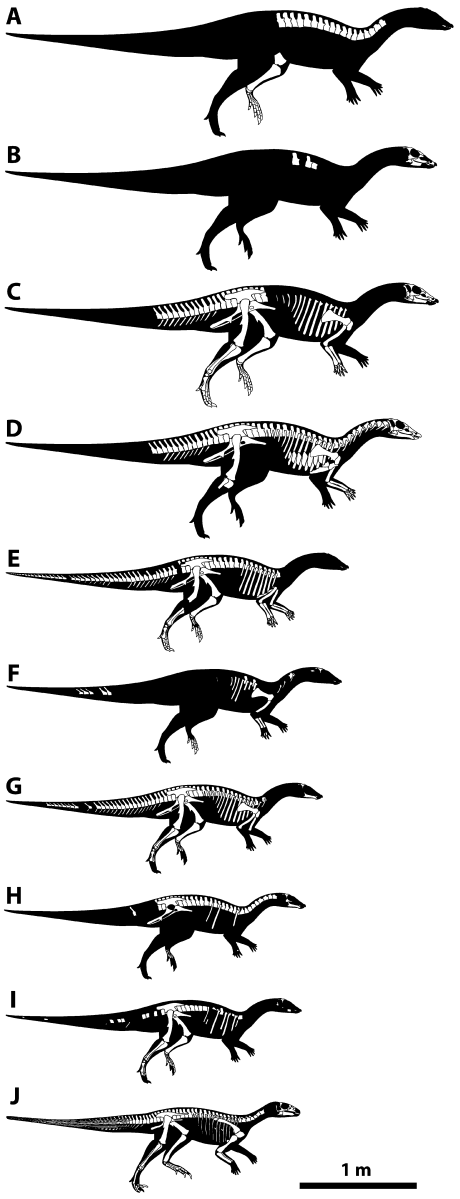

Figure 1. Diagrams of the skeletons of relatively complete articulated *Thescelosaurus* specimens (A–I) and *Parksosaurus* (J), showing their comparative size and degree of completeness. Bones present in each specimen are represented in white. A, LACM 33542; B, SDSM 7210; C, MOR 979; D, NCSM 15728; E, USNM 7757; F, USNM 7758; G, CMN 8537; H, LACM 33543; I, RSM P 1225.1; J, ROM 804. Skeletons are scaled isometrically based on femur and tibia length, when available. Skeletons lacking both tibiae and femora were scaled using the following elements: anteroposterior thickness of orbit for SDSM 7210; length of the dentary for LACM 33543; and length of the humerus for USNM 7758. Proportions for specimens of *Thescelosaurus* represent those of USNM 7757, and do not illustrate proportional changes that would be evident because of allometric scaling. Scale equals 1 m. Modified from Boyd *et al*. 2009.

of cranial material for the type series of *T. neglectus* and the lack of identifiable postcranial autapomorphies have impeded the confident referral of these species (and additional specimens) to *Thescelosaurus*.

The recent discovery of two specimens of *Thescelosaurus* preserving nearly complete skulls and postcranial skeletons (NCSM 15728, Fig. 1D; MOR 979, Fig. 1C; Fisher *et al*., 2000; Horner, 2001), coupled with the recognition of previously unknown cranial material of the paratype of *T. neglectus* (USNM 7758, Fig. 1F), prompted a re-evaluation of all specimens previously referred to the taxa *Thescelosaurus*, *Parksosaurus*, and *Bugenasaura* that preserve cranial material (Boyd *et al*., 2009). A phylogenetic analysis conducted using a modified version of the Scheetz (1999) data set recovered a previously unrecognized clade of exclusively Cretaceous, basal ornithopod taxa from North America (Boyd *et al*., 2009), divided into two smaller clades. One of these contains small-bodied earlier Cretaceous forms with proposed fossorial characterisics (*Zephyrosaurus*, *Oryctodromeus*, and *Orodromeus*; Varricchio, Martin & Katsura, 2007); the other is composed of large-bodied Maastrichtian forms (*Thescelosaurus* and *Parksosaurus*). *Bugenasaura* was determined to be a subjective junior synonym of *Thescelosaurus*, and the validity of *T. neglectus* and *T. garbanii* was upheld. Additionally, preliminary examination of one referred specimen, RSM P 1225.11 (Fig. 1I), revealed differences that distinguish it from both *T. neglectus* and *T. garbanii*, suggesting that a thorough examination and redescription of this specimen was required.

RSM P 1255.1 is a small, partial, articulated skeleton from the Frenchman Formation of Saskatchewan, previously referred to *Thescelosaurus* by Galton (1989). It represents the most complete basal ornithopod skeleton yet recovered from the Frenchman Formation. Although the skull, and specifically the braincase, of RSM P 1225.1 was partially described by Galton (1989, 1997), the postcranial skeleton was not.

Herein we re-evaluate and expand upon the description of the skull of RSM P 1225.1 (Galton, 1997), describe the postcranial skeleton for the first time, and evaluate the putative assignment of this specimen to *Thescelosaurus*. The cranial re-evaluation is conducted in light of the great increase in volume of cranial material for *Thescelosaurus* that is now available, providing insights into the cranial anatomy of this taxon not previously known. A phylogenetic analysis presents the hypothesized relationships of this taxon within the Ornithischia. Additionally, we discuss the late Maastrichtian ornithischian fauna of Saskatchewan, and draw comparisons with contemporaneous formations.

INSTITUTIONAL ABBREVIATIONS

AMNH, American Museum of Natural History, New York, New York, USA; CM, Carnegie Museum, Pittsburgh, Pennsylvania, USA; CMN, Canadian Museum of Nature, Ottawa, Ontario, Canada; EM, Eastend Historical Museum, Eastend, Saskatchewan, Canada; LACM, Natural History Museum of Los Angelas County, California, USA; MCZ, Museum of Comparative Zoology, Harvard University, Harvard, Massachusetts, USA; MB, Museum für Naturkunde, Berlin; MOR, Museum of the Rockies, Bozeman, Montana, USA; NCSM, North Carolina Museum of Natural Sciences, Raleigh, North Carolina, USA; NHMUK, Natural History Museum (formerly British Museum of Natural History), London, UK; ROM, Royal Ontario Museum, Toronto, Ontario, Canada; RSM, Royal Saskatchewan Museum, Regina, Saskatchewan, Canada; SDSM, South Dakota School of Mines and Technology, Rapid City, South Dakota, USA; USNM, National Museum of Natural History, Smithsonian Institution, Washington, D.C., USA.

ANATOMICAL ABBREVIATIONS

a, astragalus; a#, alveolus (numbered from anterior); ac, acetabulum; af, alar flange of quadrate; articulation for illium; ap, anterior process of pubis; asc, anterior semicircular canal; awq, anterior wing of quadrate; bo, basioccipital; bs, basisphenoid; bp, basipterygoid process; brp, brevis process; brs, brevis shelf; c, centrum; cal, calcaneum; cap, capitulum; cc, cnemial crest; ce, cerebral space; ci, crista interfenestralis; cm, crenulated margin; cp, cultriform process; ct, crista tubularis; D#, dorsal vertebra (numbered from anterior); dlt, distal lateral tarsal; ex/op, exoccipital–opisthotic; f, frontal; fi, fibula; fm, foramen magnum; fmt, foramen metoticum; fo, fenestra ovalis; ft, fourth trochanter; gt, greater trochanter; h, head of femur; ica, channel housing internal carotid artery; it, ischial tuberosity; itf, infratemporal fenestra; lc, lateral condyle; lcm, lateral concave margin; ls, laterosphenoid; lt, lesser trochanter; mc, medial condyle; mg, Meckelian groove; mp, medial process of dentary; movm, medial offset ventral margin of jugal; mrp, medial rugosity on palpebral; mwq, medial wing of quadrate; n, neck of femur; nc, neural canal; nf, nutrient foramina; ns, neural spine; o, orbit; ob, trough for olfactory bulb; oc, occipital condyle; or, oblique ridges of ventral jugal; ot, olfactory tract (I); p, parietal; paf, palatine flange; pap, preacetabular process; pet, partially erupted tooth; pfl, posterior flange; pfo, pituitary fossa; po, postorbital; pop, paroccipital process; pp, parapophysis; pr, prootic; prz, prezygapophysis; psc, posterior

semicircular canal; ptf, pterygoid flange; ptz, postzygapophysis; puf, pubic foramen; pup, pubic peduncle; qf, quadrate fossa; qp, quadrate process; rpm, rugose posterior margin; S#, sacral vertebra (numbered from anterior); sa, saccular space; so, supraoccipital; ssbo, sutural surface for basioccipital; ssex, sutural surface for exoccipital; ssi, sutural surface for ilium; ssls, sutural surface for laterosphenoid; ssp sutural surface for parietal; sspf, sutural surface for prefrontal; sspo, sutural surface for postorbital; sspr, sutural surface for prootic; ssq, sutural surface for quadrate; sof, supraoccipital foramen; sr, sacral rib; st, sella turcica; stf, supratemporal fenestra; ti, tibia; tp, transverse process; tub, tuberculum; vcd, canal for vena capitis dorsalis; ve, vestibule.

GEOLOGY AND VERTEBRATE ASSEMBLAGE OF THE FRENCHMAN FORMATION

The Frenchman Formation is the youngest Cretaceous formation that occurs in south-western Saskatchewan. It overlies the late Campanian and Maastrichtian marine shales of the Bearpaw Formation, as well as the terrestrial Eastend, Whitemud, and Battle formations, and is overlain by the Palaeocene Ravenscrag Formation (McIver, 2002) (Fig. 2). The Cretaceous–Palaeogene boundary occurs immediately below or within the basalmost Ravenscrag coal seam, permitting correlation between chronostratigraphic and lithostratigraphic boundaries (McIver, 2002). The top of the Frenchman Formation is defined as the top of the lowest mappable coal seam of the Ravenscrag Formation, and its lower boundary is defined by the upper erosional surface of the Battle Formation (Kupsch, 1957). Its thickness ranges from 8 to 68 metres, depending on the pre-existing level of erosion of the underlying formations (Kupsch, 1957). Palynological (Braman & Sweet, 1999) and magnetostratigraphic (Lerbekmo & Coulter, 1985; Lerbekmo, 1999) data suggest that the Frenchman Formation was deposited in the last one-half million years of the Maastrichtian (McIver, 2002). The Frenchman Formation is, therefore, contemporary with the youngest part of the Hell Creek Formation of Montana, and the lower member of the Scollard Formation of Alberta.

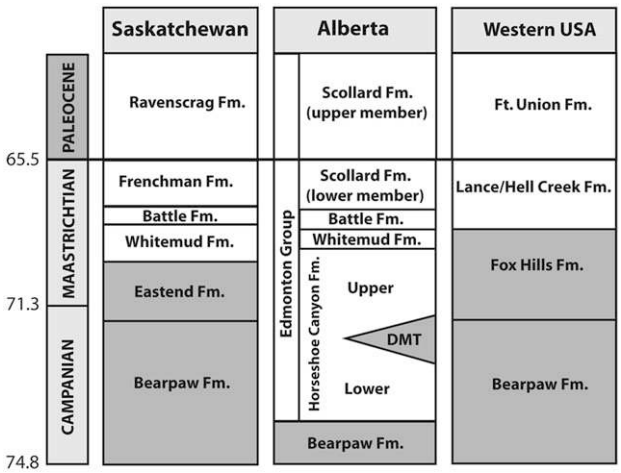

Figure 2. Chronostratigraphy of the Late Cretaceous of Alberta, Saskatchewan, and Montana, Wyoming, and North and South Dakota, showing approximate time equivalence. Numbers on the left are in millions of years before present. Formations in white are terrestrial, and those in grey are marine; DMT, Drumheller Marine Tongue. Complied from Eberth, 2004; Brinkman DB. 2003; Koppelhus EB, Braman DR. 2010; Hamblin and Abrahamson, 1996; McIver 2002.

The Frenchman Formation is characterized by two facies: one dominated by sandstone and the other by claystone. These facies were previously viewed as laterally continuous stratigraphic zones, but are now understood to be regional in distribution, laterally discontinuous, and mutually intertongued (Kupsch, 1957; McIver, 2002). The sandstone facies consists of fine-to-medium grained, loosely cemented sandstone with localized areas of cliff-forming, firmly cemented sandstone. The claystone facies consists of bentonitic clays forming rounded and sparsely vegetated berms (Kupsch, 1957). RSM P 1225.1 was located halfway up the section, in a large (approximately 1 m thick) unconsolidated sandstone lens of the sandstone facies that is capped by a thickened sandstone/ironstone lens.

The vertebrate assemblage of the Frenchman Formation is known primarily from microvertebrate localities, with few articulated or associated skeletons. The osteichthyan fishes *Amia* sp., *Melvius* sp. *Lepisosteus* sp., and *Acipenser* sp., as well as the freshwater ray *Myledaphus* sp., are common, with *Scapanorhychus* sp. and *Lonchidion* sp. being rarer members of the fauna (Tokaryk, 1997a; Gilbert, Tokaryk & Cuggy, 2010). Also present are the amphibians *Scapherpeton tectum* Cope, 1876, *Opisthotriton* sp., and the rare *Habrosaurus* sp., as well as indeterminate Anura and Albanerpetontidae; and the squamates *Iguanavus teres* Marsh, 1892, *Chamops segnis* Marsh, 1892, *Leptochamops denticulatus* (Gilmore, 1928), *Meniscognathus altimani* Estes, 1969, *Haptosphenus placodon* Estes, 1964, *Odaxosaurus piger* (Gilmore, 1928), *Parasaniwa wyomingensis* Gilmore, 1928, *Paraderma bogerti* Estes, 1964, and *Palaeosaniwa* sp. as well as an unindentified iguanid (Tokaryk, 1997a; Tokaryk & Snively 2009). Turtles are well represented by *Compsemys* sp.,

Neurankylus sp., *Plesiobaena* sp., *'Baena' hatcheri* Hay, 1901, *Adocus* sp., *Basilemys praeclara* Hay, 1911, *Thescelus insiliens* Hay, 1908, and *Aspideretes* sp., as well as indeterminate genera of Macrobaenidae, Chelydridae, Plastomeninae, and Trionychinae, and champsosaurs and crocodilians are represented by *Champsosaurus* sp. and *Leidyosuchus* sp. (*Borealosuchus*?), respectively (Tokaryk, 1997a; Tokaryk & Bryant, 2004; Tokaryk & Brinkman, 2009; Tokaryk *et al*. 2009). The mammalian fauna consists of the multituberculates *Catopsalis johnstoni* Fox, 1989, *Catopsalis* sp. cf. *Catopsalis joyneri* Sloan & Van Valen, 1965, *Cimexomys minor* Sloan & Van Valen, 1965, *Cimexomys* sp. cf. *Cimexomys hausoi* Archibald, 1982, *Cimolodon nitidus* (Marsh, 1889), *Cimolomys gracilis* (Marsh, 1889), *Essonodon* sp., *Meniscoessus robustus* (Marsh, 1889), *Mesodma hensleighi* Lillegraven, 1969, *Mesodma formosa* (Marsh, 1889), *Mesodma thompsoni* Clemens, 1964, *Paracimexomys priscus* (Lillegraven, 1969), *Parectypodus foxi* Storer, 1991, *Stygimys cupressus* Fox, 1989, and an indeterminate microsmodontid, the marsulpials *Alphadon jasoni* Storer, 1991, *Didelphodon vorax* (Marsh, 1889), *Glasbius twitchelli* Archibald, 1982, *Pediomys elegans* (Marsh, 1889), *'Pediomys' krejcii* (Clemens, 1966), *'Pediomys'* sp. cf. *'Pediomys' hatcheri* Osborn, 1898, and *Turgidodon petiminis* Storer, 1991, as well as the eutherians *Alostera saskatchewanensis* Fox, 1989, *Baioconodon* sp., *Batodon tenuis* Marsh, 1892, *Gypsonictops illuminatus* Lillegraven, 1969, *Cimolestes incisus* Marsh, 1889, *Cimolestes magnus* Clemens & Russell, 1965, *Cimolestes stirtoni* Clemens, 1973, *Cimolestes* sp. cf. *Cimolestes cerberoides* Lillegraven, 1969, *Cimolestes* sp. cf. *Cimolestes propalaeoryctes* Lillegraven, 1969, *Mimatuta* sp., *Oxyprimus* sp. cf. *Oxyprimus erikseni* (Valen, 1978), *Procerberus* sp. cf. *Procerberus formicarum* Sloan and Van Valen, 1965, *Protungulatum* sp. cf. *Protungulatum donnae* Sloan and Van Valen, 1965, and indeterminate genera of Periptychidae and Hyopsodontidae (Fox, 1997; Tokaryk & Bryant, 2004; Tokaryk *et al*. 2009).

With the exception of *Tyrannosaurus rex* Osborn, 1905, all theropod taxa are known exclusively from isolated elements and/or microvertebrate site fossils. These are *Ornithomimus* sp. and *Chirostenotes* sp., and (the teeth of) *Troodon* sp., *Richardoestesia gilmorei* Currie, Rigby & Sloan, 1990, *Paronychodon* sp., and *Saurornitholestes* sp., with the latter being the most common (Currie, Rigby & Sloan, 1990; Tokaryk, 1997a; Tokaryk *et al*. 2009). *Tyrannosaurus* is represented by numerous isolated elements and a single, fairly complete, associated skeleton. *Cimolopteryx* sp., a charadriiform bird (Tokaryk & James, 1989) and an unidentified hesperornithiiform bird (Tokaryk, 1997a) have been noted to occur, and there are many elements for which convincing identification is still undetermined (Johnston & Fox, 1984; Tokaryk, 1997a).

The ornithischian fauna consists of ceratopsians, hadrosaurs, pachycephalosaurs, ankylosaurs, and thescelosaurs (Tokaryk, 1997a). The ceratopsian *Triceratops horridus* Marsh, 1889 is represented by several complete and nearly complete skulls, as well as isolated teeth from microvertebrate localities. Hadrosaurs are represented by *Edmontosaurus saskatchewanensis* Sternberg, 1926 (considered a subjective junior synonym of *Edmontosaurus annectens* (Marsh, 1892); Prieto-Marquez, 2010), with the holotype consisting of a nearly complete skull and partial postcranial skeleton, and a possible second skeleton preserving skin impressions (Tokaryk, 1997a, b). Although hadrosaurs are also represented by isolated teeth from microvertebrate localities, their abundance is much less than that encountered in other Late Cretaceous terrestrial ecosystems, such as the Hell Creek Formation (Tokaryk, 1997a). Pachycephalosaurs are known from putative isolated teeth from microsites but, interestingly, no domes have yet been found. Isolated dermal scutes suggest the presence of ankylosaurs, but no diagnostic elements or teeth have been recovered.

Thescelosaurus is known from four partial articulated skeletons and numerous isolated elements, making it one of the most common dinosaurs retrieved from the Frenchman Formation, and possibly the most abundant in the faunal assemblage. RSM P 1225.1 represents the smallest known articulated specimen of *Thescelosaurus* for which a significant quantity of the skeleton is preserved. Importantly, this includes the first known braincase for this taxon, although additional material has subsequently been found. A second specimen (RSM P 2415.1) is that of a large animal and preserves the pelvic girdles, proximal femora, and much of the post-scapular axial skeleton; a third (CMN 22039) is the smallest known articulated specimen (although known only from a hind leg); and a fourth (RSM P 3123.1) is a medium-sized specimen that has yet to be prepared. Unfortunately, RSM P 2415.1 and CMN 22039 do not preserve diagnostic areas of the skeleton, and RSM P 3123.1 is awaiting preparation. All specimens of *Thescelosaurus* from Saskatchewan were presumed to represent *T. neglectus*, and indeed, RSM P 1225.1 was employed in the description of the braincase of *T. neglectus* (Galton, 1989, 1995). Tokaryk (1997a) suggested that further research was necessary to determine the correct taxonomic referral of the specimens of *Thescelosaurus* from the Frenchman Formation.

SYSTEMATIC PALAEONTOLOGY

DINOSAURIA OWEN, 1842
ORNITHISCHIA SEELEY, 1887
NEORNITHISCHIA COOPER, 1985
(*SENSU* BUTLER, 2008)
ORNITHOPODA MARSH, 1881 (*SENSU* BULTER, 2008)
THESCELOSAURUS GILMORE, 1913

1995 *Bugenasaura*, Galton: 308, fig. 4; Galton 1999: figs 1–4, pl. 1.

Emended diagnosis: Frontals wider at midorbital level than across posterior end; dorsolaterally directed process on surangular; prominent, horizontal ridge on maxilla, with at least the posterior portion covered by a series of coarse, rounded, obliquely inclined ridges; depressed posterior half of ventral edge of jugal covered laterally with obliquely inclined ridges; foramen in dorsal surface of prefrontal (dorsomedial to articulation surface for palpebral) that opens into the orbit; shafts of anterior dorsal ribs laterally compressed and concave laterally, with the posterior margin of the distal half characterized by a distinct rugose texture and flat surface.

Comments: Two possible autapomorphies of *Thescelosaurus* (for which comparative material with the putative sister taxon, *Parksosaurus*, is unavailable) were identified by Boyd *et al*. (2009: p. 762): palpebral dorsoventrally depressed, with rugosities along medial margin, and an obliquely truncated distal end; and a Y-shaped indentation on the dorsal opisthotics. The putatively diagnostic character 'supraoccipital wedge-shaped and nearly excluded from the dorsal margin of foramen magnum' originally identified by Galton (1997: p. 241) was found to be variable by Boyd *et al*. (2009), and they suggested that further investigation is needed to determine its taxonomic significance. The description of RSM P 1225.1 and comparison with all other pertinent material has revealed that this character is either autapomorphic for *Thescelosaurus* or potentially synapomorphic for *Thescelosaurus* and *Parksosaurus* (Boyd *et al*., 2009) (comparative material for *Parksosaurus* is not available). This condition is more similar to that seen in the Iguanodontia and Hadrosauridae, and displays a reversal of the trend seen in other North American basal ornithopods. This suggests independent evolution of this character state in *Thescelosaurus* and the more derived ornithopods.

THESCELOSAURUS ASSINIBOIENSIS SP. NOV.

1989 *Thescelosaurus neglectus* Galton: pl. 4, figs 1–8; Galton 1995: fig. 4; Galton 1997: figs 3, 4, 10, pl. 1–2.

Diagnosis: Dorsal and posterior margins of the squamosal convex; supraoccipital bearing a distinct median foramen running from the roof of the myelencephalon through to the dorsal surface of the element. Differentiated from *T. garbanii* by the calcaneum not being reduced and thus participating in the mesotarsal joint.

Specific etymology: Named for the District of Assiniboia, a regional administrative unit of the North-West Territories, Canada, from 1882 to 1905 (located between 49° and 51.97°N, and ~101.5 and ~111.5°W). The majority of this district became the southern portion of the modern province of Saskatchewan, with the westernmost area becoming the easternmost portion of the province of Alberta. It encloses the exposures of the Frenchman Formation. This district was named after the Assiniboine First Nations People.

Holotype: RSM P 1225.1, a small, relatively complete skeleton, preserving a partial skull (including a nearly complete braincase), dorsal, sacral, and caudal vertebral series, dorsal ribs, pelvic girdles, and hindlimbs. Based on the 1968 quarry map, the skeleton was found in articulated condition, with the anterior part of the animal extending into the hill, but with the tail exposed.

Locality: Specimen RSM P 1225.1 was discovered on 19 June 1968 and collected by Albert E. Swanston of the Royal Saskatchewan Museum (then the Saskatchewan Museum of Natural History) on 17 July 1968. The original location, stated as 'northwest of Clarks Ranch, from NW 1/4 Sec 35, T 4, R 19, west of the 3rd Meridian, Frenchman River Valley, Saskatchewan', is incorrect. Tim Tokaryk (RSM) relocated the original site in the late 1980s (with the relocation being confirmed by the matching of a rib fragment collected at the site with a rib of the specimen, and residual plaster persisting at the site; T.T. Tokaryk, pers. comm., 2007). Located in LSD 11, Sec 2, T 5, R 19, west of the 3rd Meridian in southwestern Saskatchewan (Fig. 3). The quarry is located on the north side of the Frenchman River Valley on the north-west facing side of a butte extending from the valley wall. Exact locality information is available from the RSM upon request.

Distribution: Frenchman Formation, Saskatchewan – Maastrichtian (65.5–65.0 Mya) (Lerbekmo & Coulter, 1985; Braman & Sweet, 1999; Lerbekmo, 1999) (Fig. 2).

Remarks: Although RSM P 1225.1 is a relatively small specimen that may not be skeletally mature, its recognition as representing a distinct species rests upon two major observations. Firstly, it is only 13%

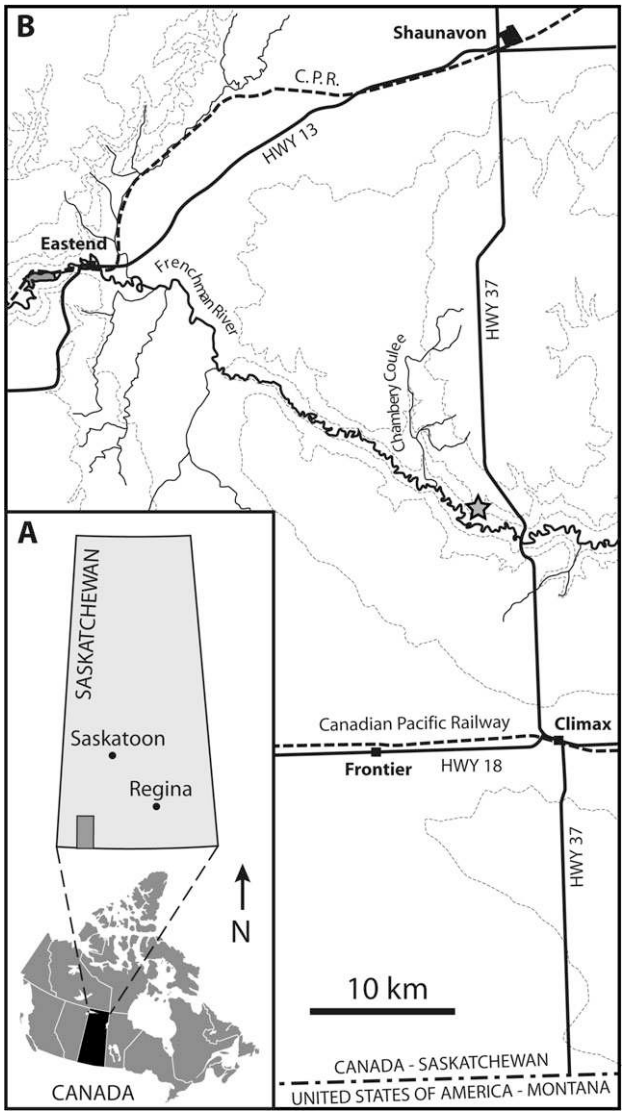

Figure 3. The geographic location of the RSM P 1225.1 quarry. A, the location of the Province of Saskatchewan in Canada, highlighting the area of south-western Saskatchewan illustrated in (B). B, regional map of south-western Saskatchewan with star indicating the location of the quarry on the north side of the Frenchman River Valley near Cambery Coulee.

smaller (based on femur length) than the holotype of *T. neglectus* (USNM 7757), and is less than 9% smaller than both CMN 8537 and LACM 33543. Neither of the latter two specimens, nor the similarly sized paratype of *T. neglectus* (USNM 7758), display the autapomorphies evident in RSM P 1225.1. Secondly, the autapomorphies cited above (presence of the supraoccipital foramen and the shape of the posterior margin of the squamosal) are unlikely to be ontogenetically variable or to vary allometrically by size. In fact, the posterior margin of the squamosal is more deeply concave in immature specimens of *T. neglectus* than it is in adults, which is opposite to the trend that would be required for RSM P 1225.1 to be an immature specimen of *T. neglectus*.

DESCRIPTION

Head Skeleton

Dermatocranium

Frontal: The frontal forms the majority of the dorsal margin of the orbit, and the element is bounded by the parietal posteriorly, postorbital and supraorbital laterally, and nasal and prefrontal anteriorly (Fig. 4). The left and right frontals are both preserved, with only the anteriormost portion being absent from both sides, and the lateral portion missing from the left. As is diagnostic for *Thescelosaurus* (CMN 8537, NCSM 15728, MOR 979; Boyd *et al*., 2009), the widest part of the frontal lies at the midorbital level (Galton, 1974a). The combined maximum midorbital width of both frontals is subequal to their length (~1 : 1). This contrasts sharply with the ratios of other basal ornithopods, including *Dryosaurus* (1.4 : 1; MB R 1378), *Hypsilophodon* (1.7 : 1; BMHN R 2477), *Orodromeus* (1.9 : 1; MOR 294, 473, 623, 995), and *Zephyrosaurus* (2.0 : 1; MCZ 4392). The frontals are flat dorsally, contrasting with the slightly dorsal convex midline conformation of the frontals of *Orodromeus*, *Oryctodromeus*, and *Hypsilophodon*. The lateral aspect of the frontal forms the thin but highly rugose dorsal margin of the orbit (Fig. 4).

Dorsally (Fig. 4A), the midline suture is straight posteriorly, with the two frontals abutting, but anteriorly exhibits overlapping flanges. Posteriorly, the frontals are concave at their junction with the parietal, and the edge of the element is crenulated, a conformation that is reciprocated by the anterior margin of the parietal. Ventrally (Fig. 4B), the suture with the parietal is again crenulated, and lies in the transverse plane, but does not show the distinctly posteriorly concave morphology seen on the dorsal surface. The suture with the postorbital extends anteroposteriorly from the posterolateral margin of the frontal to the dorsal margin of the orbit. Anterolaterally, the frontal bears a dorsally-facing, roughened facet laterally that received the prefrontal along an obtusely angled scarf joint (Fig. 4A). This suture is more dorsally oriented in *Thescelosaurus* than it is in *Dryosaurus* (MB R 1378), *Hypsilophodon* (NHMUK R2477), *Orodromeus* (MOR 294, 473, 623, 995), or *Zephyrosaurus* (MCZ 4392), which all express a more extensive, and more deeply recessed, lateral component of the suture. Medially the frontal extends anterior to at least the posterior extremity of the prefrontal suture, but the limit of this projection cannot be determined as the bone is incomplete.

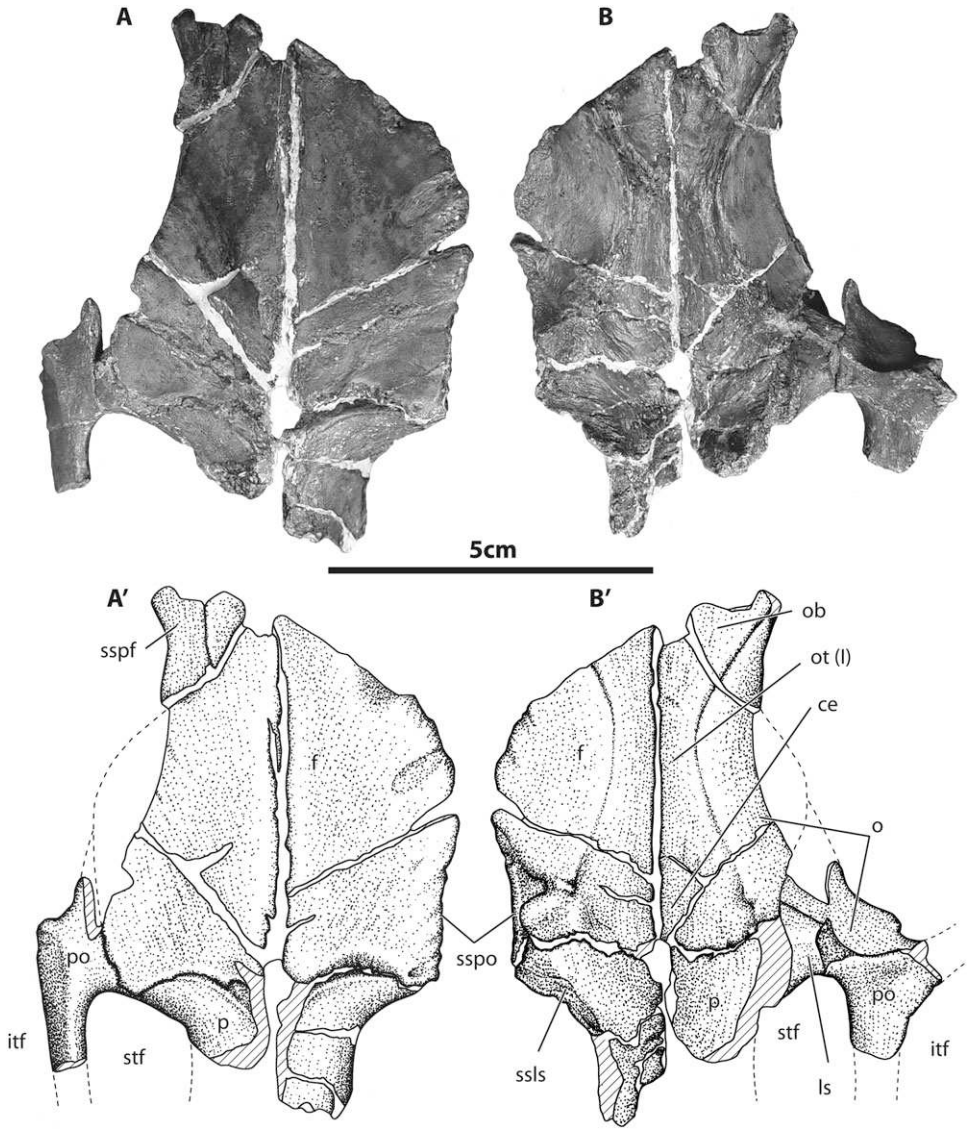

Figure 4. The skull roof of the holotype of ***Thescelosaurus assiniboiensis*** **sp. nov.**, RSM P 1225.1, in dorsal (A) and ventral (B) views. See list in text for an explanation of anatomical abbreviations. Primes indicate illustrations of photographed elements. Dashed lines indicate extrapolated margins of the element. Hatched areas represent incomplete bone surface. White area represents plaster reconstruction.

The ventrolateral surface of the frontal forms the smooth and concave dorsal roof of the orbit (Fig. 4B). The dorsal portion of the orbit is medially separated from the roof of the portion of the skull housing the olfactory tracts, olfactory bulbs, and cerebrum by distinct paired, crescentic ridges (Fig. 4B). Between these ridges, the roof of the interorbital septum, housing the olfactory tract (Hopson, 1979; Starck, 1979; Bellairs & Kamal, 1981; Bubien-Waluszewska, 1981), constitutes an hourglass-shaped, dorsally concave trough that is deeper posteriorly than anteriorly (Galton, 1989, 1997). These ridges are lowest adjacent to the olfactory tract, and anteriorly and posteriorly become higher and more steeply sloped as they curve laterally. The anterior aspect of the mould of the olfactory tract flares laterally to accomodate the olfactory bulbs, and the posterior aspect flares laterally to cradle the anterior portion of the cerebrum. The endocranial mould of the olfactory tract is elongate and narrow relative to that of other ornithischians (Hopson, 1979), but is not as relatively elongate as it is in *Dryosaurus* (MB R 1378), *Orodromeus* (MOR 473, 623, 995), *Zephyrosaurus* (MCZ 4392), or *Hypsilophodon* (NHMUK R2477; Galton, 1989). The

endocranial mould of the cerebrum consists of a slightly dorsally depressed sphere. The morphology is similar to that of the illustrated endocasts of *Dryosaurus* (MB R dy A; Galton, 1989) and *Hypsilophodon* (NHMUK R2477; Galton, 1989), and to that observed in the isolated frontals of *Dryosaurus* (MB R 1378), *Orodromeus* (MOR 473, 623, 995), and *Zephyrosaurus* (MCZ 4392). Subtle vascular imprints (valleculae) are preserved on the dorsolateral surface of the cerebral mould (Fig. 4B). Within the Ornithischia, such valleculae have previously only been reported for the Hadrosauridae and Pachycephalosauridae (Evans, 2005).

The postorbital suture is located at the posterolateral corner of the frontal. Dorsally the sututre is simple, straight, and lies in the parasagittal plane. Ventrally it is more complex, revealing shallow peg-and-socket articulations (one slight lateral projection from the frontal, bounded anteroposteriorly by two invaginations into the frontal). Situated ventral to the postorbital and spanning the frontal and parietal is the gently rounded socket that received the anterior end of the laterosphenoid.

Postorbital: The triradiate left postorbital is almost entirely preserved, missing only the distal tips of all three processes (Fig. 4). This element forms the posterodorsal margin of the orbit and the anterodorsal margin of the lateral temporal fenestra. The anterior process fringes the posterodorsal margin of the orbit, and lies in sutural contact with the frontal medially, whereas the body of the postorbital contacts the posterolateral margin of the frontal, the anterolateral margin of the parietal, and the dorsal head of the laterosphenoid. The posterior process forms the rounded anterolateral margin of the supratemporal fenestra and the much sharper dorsal margin of the infratemporal fenestra. This process is laterally compressed and oblong in cross section. The ventral process of the postorbital is triangular in transverse section, with flattened surfaces facing laterally and anteromedially. The articulation surface for the dorsal process of the jugal is not preserved. A prominent, anterolaterally projecting, rugose process arises from the body of the postorbital and projects into the orbit. This process is also present in other specimens of *Thescelosaurus* (NCSM 15728, CMN 8537), and in the basal ornithopod taxa *Orodromeus* (MOR 473), *Oryctodromeus* (MOR 1642), and *Zephyrosaurus* (MCZ 4392).

Parietal: The anterior portions of the fused parietals are both preserved, but the posterior margin is incomplete (Fig. 4). This compound element is convex dorsally and concave ventrally, and its anterior aspect flares dorsolaterally at its articulation with the frontal. In dorsal view (Fig. 4A) the contour of the frontoparietal suture is convex and directed anteriorly, and its margin exhibits fine-scale crenulations, whereas in ventral view (Fig. 4B) it is slightly concave and has an irregular profile. Posterior to the suture there is a distinct ridge, which is oriented directly laterally in its lateral part, but changes to an anteroposterior orientation as it approaches the midline. The parietal tapers posteriorly, and its lateral margin curves medially, forming the anterior and medial margin of the supratemporal fenestra. Ventrally, the cerebral mould of the parietal is continuous with that of the frontal, and tapers posteriorly, although it is not preserved posterior to the cerebro-cerebellar constriction (Hopson, 1979; Galton, 1989, 1997).

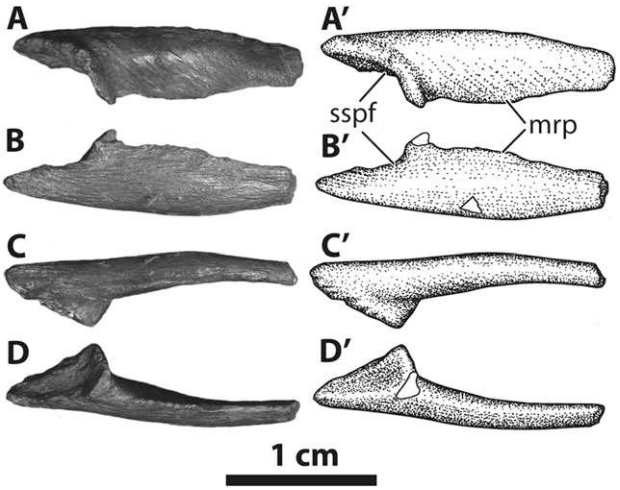

Figure 5. Left palpebral of the holotype of ***Thescelosaurus assiniboiensis* sp. nov.**, RSM P 1225.1, in ventral (A), dorsal (B), lateral (C), and medial (D) views. See list in text for an explanation of anatomical abbreviations. Primes indicate illustrations of photographed elements. Dashed lines indicate extrapolated margins of the element.

Supraorbital: The left supraorbital is preserved in its entirety and is similar to that of *Iguanodon bernissartensis* Boulenger, 1881 (IRSNB 1536; Norman, 1980) and *Oryctodromeus* (MOR 1642) (Fig. 5). As is characteristic for *Thescelosaurus* (NCSM 15728; Boyd *et al*., 2009), the supraorbital is elongate, dorsoventrally depressed, and truncated obliquely. The lateral margin is more rounded in cross section than is the tapered medial margin, and expresses slight rugosities. Anteriorly, the articular facet for the prefrontal is expanded and cup-shaped, with the surface extending at an angle of approximately 40° medially to the long axis of the supraorbital. Its posterior margin is characterized by an abrupt and sloping facet, possibly for articulation with a secondary supraorbital element.

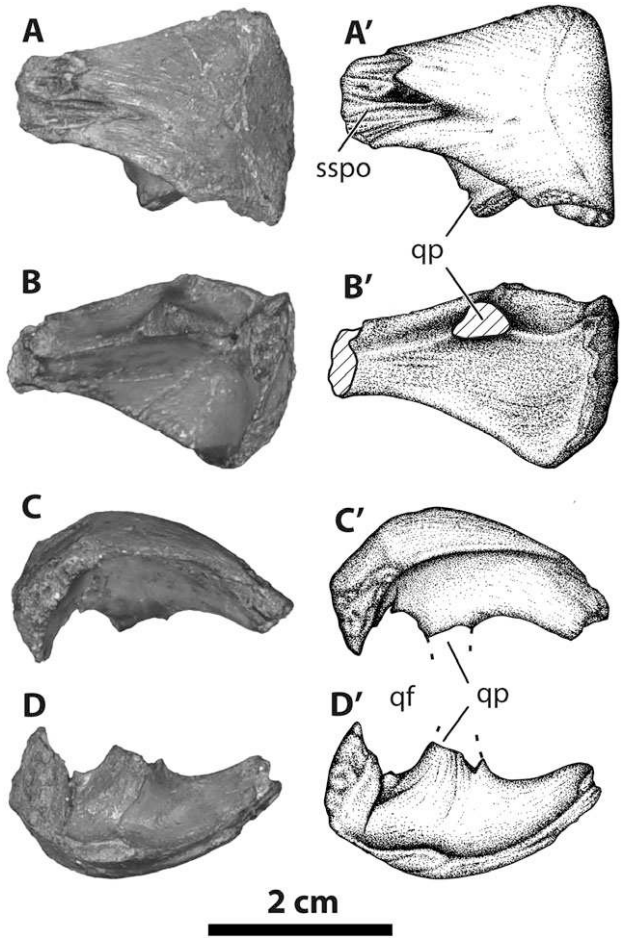

Figure 6. Left squamosal of the holotype of ***Thescelosaurus assiniboiensis* sp. nov.**, RSM P 1225.1, in dorsal (A), ventral (B), medial (C), and lateral (D) views. See list in text for an explanation of anatomical abbreviations. Primes indicate illustrations of photographed elements. Dashed lines indicate extrapolated margins of the element. Hatched areas represent incomplete bone surface. White areas represent plaster reconstruction.

Squamosal: The squamosal forms the posterolateral margin of the supratemporal fenestra, and articulates with the postorbital anteriorly and the quadrate ventrally (Fig. 6). The left squamosal is preserved in its entirety, save for its quadrate process (which is broken off at the base), its small lateral flange (that is broken dorsally), and the ventral portion of the anterior postorbital process. Fragments of the right squamosal are identifiable. Galton (1997) used the left squamosal as the basis of the description of this element for *Thescelosaurus*, but little comparative material was available at that time. Current availability of more comparative material, plus further preparation of the left squamosal, and discovery and reconstruction of the right squamosal, reveals that the squamosals of RSM P 1225.1 are distinctive when compared with those of other species of *Thescelosaurus*, and indeed, with those of all other ornithischians.

The postorbital process of the squamosal is long and narrow, resulting in a relative shift in the location of the postorbital–squamosal suture further anteriorly than that of the paratype of *T. neglectus* (USNM 7758; Boyd *et al*., 2009) and all other specimens. The postorbital process is triangular in cross section, with a flat dorsal surface and a ventral ridge that runs anteroposteriorly along its ventral margin. The anteriormost portion of the postorbital process of the left squamosal is overlain dorsally by the postorbital, forming a prominent lap joint (Fig. 6A). The floor of this suture bears several anteroposterior ridges and grooves that would likely interdigitate with a corresponding set on the postorbital. These are not seen on the right squamosal, and the floor of this suture is more sunken compared with that of the left. The contour of the postorbital suture is jagged, with two long troughs coursing posteriorly, presumably for receipt of posterior processes of the postorbital. The lateralmost trough is the larger, being about three times the length of the smaller trough. Between these troughs an anteriorly directed process projects into the sutural area. This matches the morphology seen in *T. neglectus* (NCSM 15728, USNM 7758).

The ventral ridge of the squamosal ascends as it runs posteriorly and merges with the quadrate process, which is broken at its base. Posterior to the quadrate process the ridge continues to the posterior margin of the element, unequally dividing its ventral surface into a medial fossa and a lateral fossa, occupying two-thirds and one-third of the ventral squamosal, respectively. In both dorsal (Fig. 6A) and lateral (Fig. 6D) views the posterior margin of the squamosal is convex and rounded, in contrast to the condition seen in the paratype of *T. neglectus* (USNM 7758) and all other specimens of *Thescelosaurus* (Boyd *et al*., 2009), in which there is a flat or concave posterior surface in dorsal view, and a concave and angular surface in lateral view. This pattern is repeated by that of the right squamosal.

Jugal: Fragments of both the right and left jugal are preserved, but are too incomplete to enable reconstruction of the overall shape of the element (Fig. 7). Isolated fragments of the posteroventral margin of both the left and right jugals display the autapomorphic condition of *Thescelosaurus* (Boyd *et al*., 2009), a ventromedially offset posteroventral margin with oblique, posteroventrally inclined ridges laterally. Medially the elements are smooth.

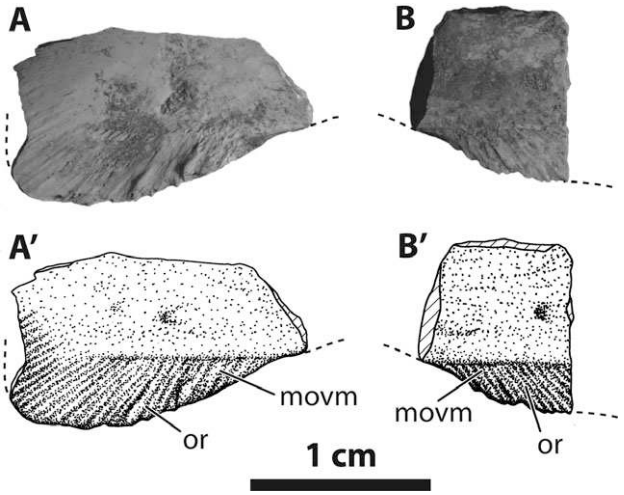

Figure 7. Left jugal of the holotype of ***Thescelosaurus assiniboiensis* sp. nov.**, RSM P 1225.1, in right (A) and left (B) lateral views. See list in text for an explanation of anatomical abbreviations. Primes indicate illustrations of photographed elements. Dashed lines indicate extrapolated margins of the element.

Pterygoid: The central portion of the fragmentary triradiate right pterygoid is preserved, along with much of the plate-like alar process that articulates with the quadrate (Fig. 8). Only the base of the palatine and pterygoid flanges, projecting orthogonal to the alar process, are preserved. The pterygoid is very similar to that of *Zephyrosaurus* (MCZ 4392; Sues, 1980). The central hub of the pterygoid is thick. The alar process is thick, but narrows at its base, becoming wider and thicker further distally. Its dorsal, ventral, and posterolateral extremities are not preserved. The posterolateral surface of the alar process has a distinct rugose texture where it articulates with the quadrate, as in *Hypsilophodon* (Galton, 1974b) (Fig. 8B). Near the base of the alar process, on the medial side, the small, but distinct base of the basipterygoid flange projects medially, normal to the plane of the alar process.

Palatine: Partial left and right palatines are preserved (Fig. 9). The palatal structure of *Thescelosaurus* is unknown, and, although preserved, these partial and disarticulated elements provide relatively little information. The left palatine preserves more of its lateral extremity, but its lateral articulation with the maxilla, jugal, and lacrimal is unclear (Fig. 9A, B). The medial extremity, preserved on the right, thins and tapers to an extremely thin plate (Fig. 9C, D). The anterior margin of the palatine is rounded, with a distinct dorsal ridge running transversely along its medial half. The posterior margin is very thin and attenuated. Its dorsal surface is smooth, and

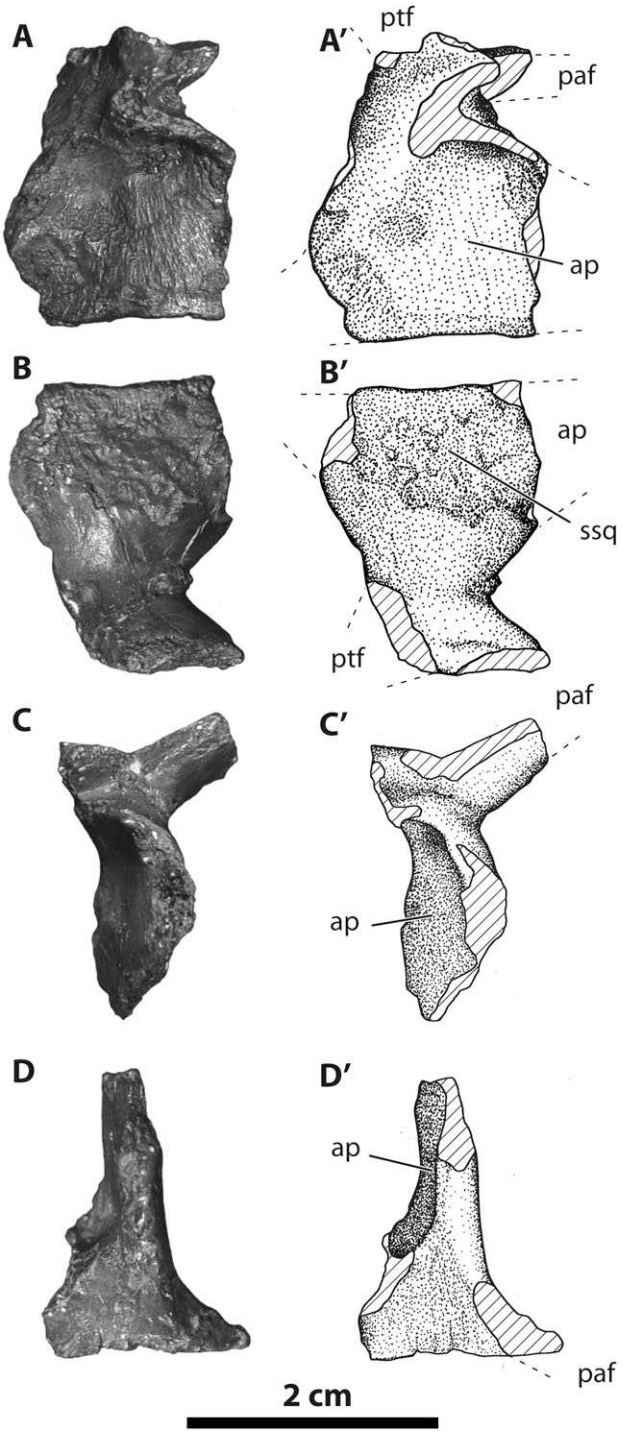

Figure 8. Right pterygoid of the holotype of ***Thescelosaurus assiniboiensis* sp. nov.**, RSM P 1225.1, in medial (A), lateral (B), dorsal (C), and ventral (D) views. See list in text for an explanation of anatomical abbreviations. Primes indicate illustrations of photographed elements. Dashed lines indicate extrapolated margins of the element. Hatched areas represent incomplete bone surface.

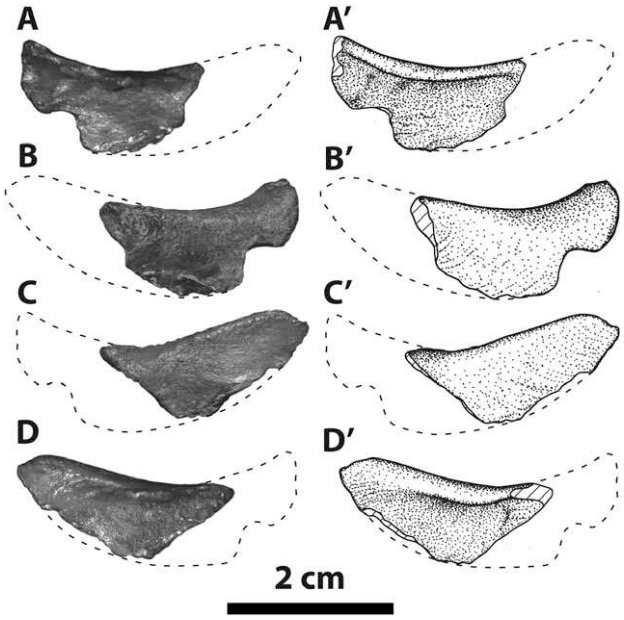

Figure 9. Palatines of the holotype of ***Thescelosaurus assiniboiensis* sp. nov.**, RSM P 1225.1, left palatine in (A) dorsal and (B) ventral view; right palatine in (C) dorsal and (D) ventral view. Primes indicate illustrations of photographed elements. Dashed lines indicate extrapolated margins of the element. Hatched areas represent incomplete bone surface.

its ventral surface is textured at the location of its articulation with the underlying palatine flange of the pterygoid.

Dentary: Only a fragment of the right dentary is preserved (Fig. 10). Its anteriormost aspect exhibits the base of the medial projection that is located posterior to the predentary suture. In cross section the dentary is L-shaped anteriorly, as a result of the ventromedial articular projection, but is oval posteriorly. The six anteriormost alveoli of the lower jaw are preserved. These are deeper laterally than medially, and are positioned closer to the lateral jaw margin than to the medial (Fig. 10B). There is a shallow fossa adjacent to the alveoli on their medial side. Within the extreme medial margin of the second alveolus lies an unerupted tooth, supporting the suggestion of Morris (1976) that this taxon displays a medial to lateral pattern of tooth replacement, as in LACM 33543. Only the extreme apex of the crown of the unerupted tooth is visible, obscuring its morphology. The medial surface of the dentary is flat and its ventral extremity preserves the Meckelian groove (Fig. 10A), which increases in depth posteriorly. The lateral surface is rounded and carries a series of four neurovascular foramina located at the level of the alveolar base (Fig. 10C).

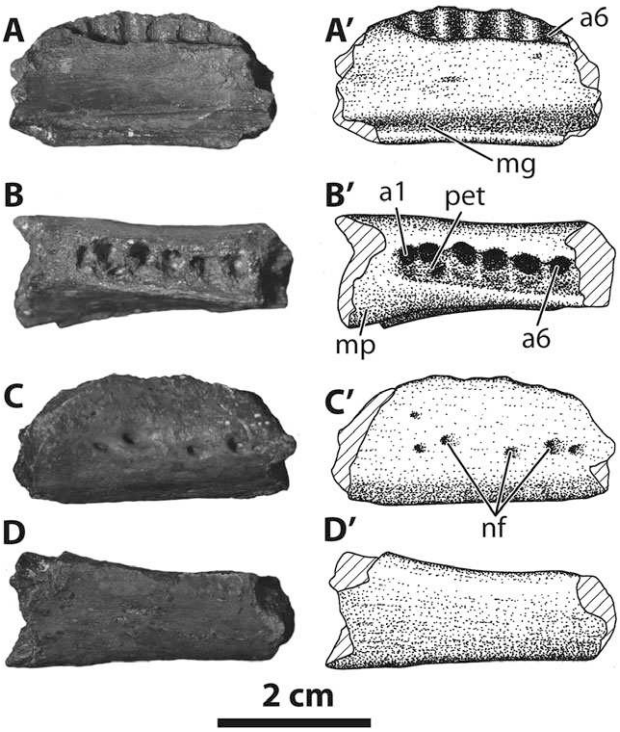

Figure 10. Right dentary of the holotype of ***Thescelosaurus assiniboiensis* sp. nov.**, RSM P 1225.1, in medial (A), dorsal (B), lateral (C), and ventral (D) views. See list in text for an explanation of anatomical abbreviations. Primes indicate illustrations of photographed elements. Hatched areas represent incomplete bone surface.

Chondrocranium

Supraoccipital: The supraoccipital is completely preserved (Fig. 11). Its dorsal surface is pentagonal, with its apex pointing posteriorly, just contacting the dorsal margin of the foramen magnum, and the anterior margin provides a short flat sutural surface for contact with the parietal (Fig. 11F). The sides adjacent to the posterior apex form a butt suture with the exoccipitals at an angle of approximately 116°. The remaining two sides (anterolateral) curve inward to form concave surfaces facing anterolaterally and slightly dorsally (Fig. 11A). Further ventrally, on their lateral surface, these sides flare out laterally as thick wings, the anterior surface of which enters into a butt suture with the laterosphenoid, and the ventral surface of which forms a butt suture with the prootic (Fig. 11A, C). Ventrally, the supraoccipital is contoured into a steep-sided hourglass-shaped trough (Fig. 11C). As is distinctive for *Thescelosaurus*, the supraoccipital is nearly excluded from contact with the dorsal border of the foramen magnum by medial projections of the exoccipital–opisthotic complex (Fig. 11F). This is clearly evident on the skulls of NCSM 15728, LACM 33543, and RSM P 1225.1.

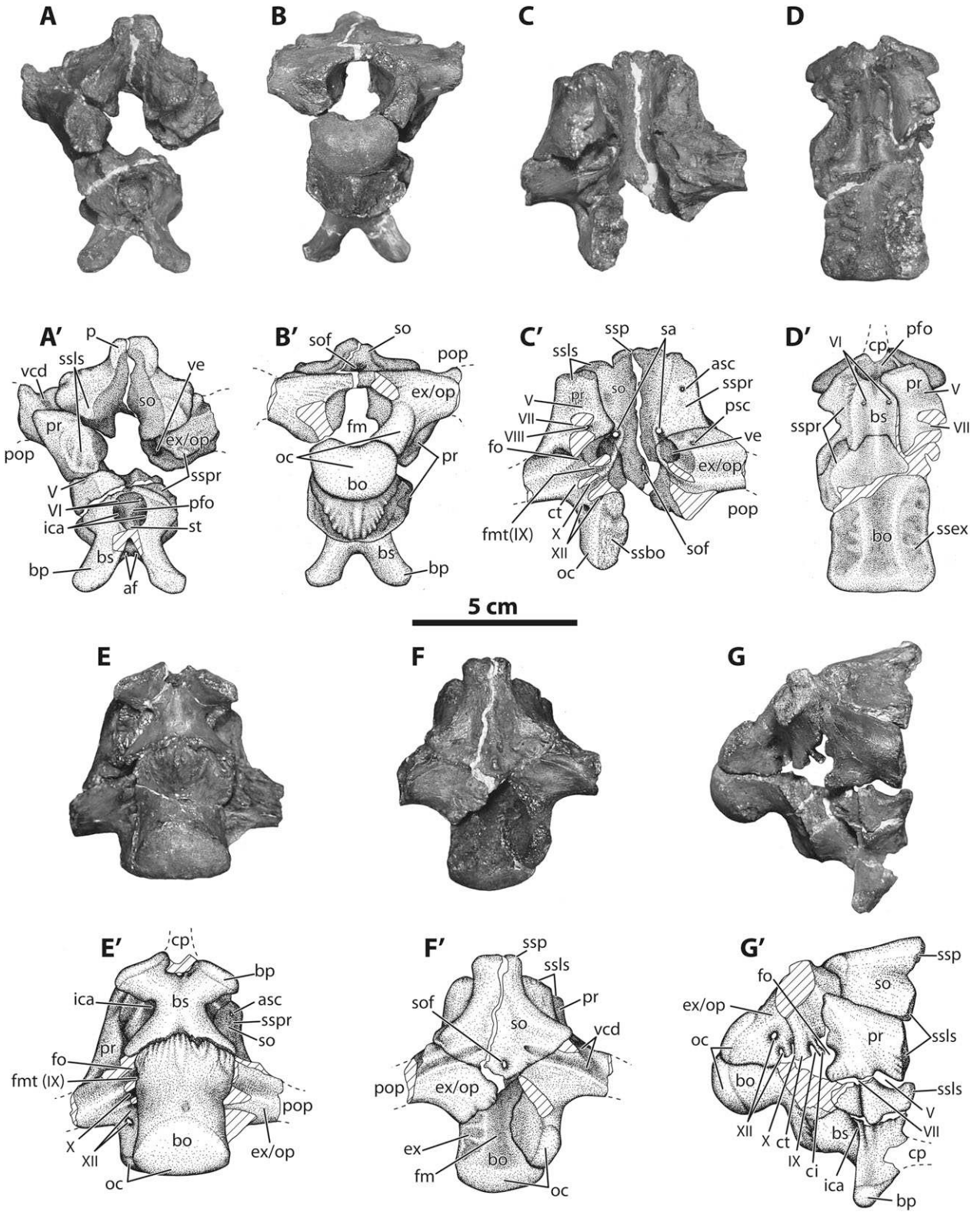

Figure 11. Braincase of the holotype of ***Thescelosaurus assiniboiensis*** **sp. nov.**, RSM P 1225.1, in anterior (A), posterior (B), internal ventral (C), internal dorsal (D), ventral (E), dorsal (F), and left lateral (G) views. See list in text for an explanation of anatomical abbreviations. Dashed lines indicate extrapolated margins of the element. Hatched areas represent incomplete bone surface. White areas represent plaster reconstruction. Roman numerals denote cranial nerve foramina.

The supraoccipitals of *Orodromeus* (MOR 403; Scheetz, 1999), *Oryctodromeus* (MOR 1636; Varricchio *et al.*, 2007) and *Hypsilophodon* (NHMUK R2447; Galton, 1974b) contribute a significant portion of the dorsal margin of the foramen magnum, as is the case for most 'hypsilophodontids' (Currie, 1997).

The dorsal surface is mainly flat, but bears a slight and highly rounded sagittal ridge (less distinct than that of *Oryctodromeus*; MOR 1636) and a prominent swelling at the median distal two-thirds mark (Fig. 11F). Posterior to this swelling, and just anterior to the foramen magnum, there is a large, distinct median foramen that lies in a prominent dorsal fossa, but its ventral extent is limited, barely perforating the dorsal roof of the supraoccipital. This foramen is not encountered in any other ornithischian. Lateral to the median swelling, the shallow trough that extends laterally from the opisthotic courses onto the posterolateral surface of the supraoccipital, and enters the supraoccipital via a small foramen. These troughs were interpreted as those accommodating the vena capitis dorsalis by Galton (1997). This is consistent with the morphology seen in *Orodromeus* (MOR 403), as illustrated by Scheetz (1999). Anteriorly, the dorsalmost and ventralmost surfaces of the supraoccipital form broad contacts for the parietal and laterosphenoid, respectively (Fig. 11A). Between these extremes, however, the anterior margin is thin. Ventrally, the supraoccipital forms a broad straight butt joint with the prootic, penetrated by the anterior semicircular canal (Galton, 1989, 1997). A slight ventral depression on the medial supraoccipital wall, the fossa subarcuata (*sensu* Galton, 1997), which housed the floccular lobe (Hopson, 1979) of the cerebellum (Galton, 1989, 1997), is much less distinct than it is in *Orodromeus* (MOR 403) and *Hypsilophodon* (NHMUK R 2447). Posterior and slightly dorsomedial to the fossa subarcuata, the cavitation for the vestibule is located at the expansive prootic–exoccipital–opisthotic contact (Fig. 11C). The cavitation that housed the crus communis (superior utriculus) arises from the region of the saccule and penetrates dorsally into the extreme ventromedial aspect of the supraoccipital.

Basiocciptial: The robust basioccipital is complete except for its anterodorsal margin, and borders the ventral third of the foramen magnum, forming the majority of the occipital condyle (Fig. 11). It is bordered dorsolaterally by the exoccipital-opisthotic elements, and anteriorly by the basisphenoid. The posterior two-fifths of the element forms the bulbous and globular base of the occipital condyle (Fig. 11E). The basioccipital component of the occipital condyle is wider than high, with the dorsomedial aspect forming the concave border of the foramen magnum, and the dorsolateral surface forming a distinct sutural surface with the exoccipitals (Fig. 11B). The remaining lateral and ventral surfaces are convex. Dorsally, the basioccipital bears a prominent, median hourglass-shaped trough occupying the median third of the basioccipital (Fig. 11D, F). The anterior third of this trough is greatly flared laterally, and is divided by a low median ridge, as is the case in *Orodromeus*. Lateral to this, the dorsal sutural surface for the exoccipital bears distinct, meandering sutural scars.

Ventrally and slightly laterally the basioccipital constricts at its midpoint, anterior to the swelling for the occipital condyle (Fig. 11E). Anterior to this constriction, the basioccipital flares ventrally and slightly laterally, forming a broad convex anterior sutural surface for the basisphenoid. Ventrally, the suture with the basisphenoid forms an intricate and highly interlocking saw-tooth pattern. Dorsally, the basisphenoid suture is simpler and not interdigitated, as it is ventrally (Fig. 11D). A prominent ventrally directed ridge lies in the ventral midline, just posterior to the suture (Fig. 11E), as is the case in *Orodromeus*, *Jeholosaurus*, *Hypsilophodon*, *Zephyrosaurus* and some pachycephalosaurs (Jin *et al.*, 2010). The lateral aspects of the anterodorsal surface are missing. Because of this, description of the sutures with the opisthotic, and the location of cranial nerve foramina is not possible.

Exoccipital–opisthotic: The suture between the exoccipital and opisthotic cannot be determined because of fusion; consequently, these elements are described as a single complex. The ventral margin of the posterior portion of the exoccipital–opisthotic forms a firm interdigitating suture with the basioccipital (Fig. 11C, D, G). Each exoccipital–opisthotic forms the lateral margin and half of the dorsal margin of the foramen magnum (nearly meeting in the midline), contributing about a third of the margin on each side (Fig. 11B, F). The portion of the exoccipital contributing to the occipital condyle is swollen and convex posteriorly. The dorsomedial projections, contributing to the dorsal surface of the foramen magnum, are thin and rugose, and almost meet in the midline, forming a slot by which the supraoccipital just borders the foramen magnum.

The opisthotic region is bordered by the supraoccipital dorsally and the prootic anteriorly, with massive simple sutures between them (Fig. 11F, G). The distal portions of the paroccipital processes are missing, but their bases suggest that they were angled slightly posterodorsally as they project laterally. Also missing is much of the anteroventral region on both sides, where the element is perforated by cranial nerve foramina laterally (Fig. 11G). The dorsal aspect of the base of the paroccipital processes

bear two distinct grooves, one running mainly laterally and slightly posteriorly from the centre of the suture with the supraoccipital, the other running posteriorly and slightly laterally from the intersection of the prootic and supraoccipital (Fig. 11F). These two grooves, the depressions housing the vena capitis dorsalis (*sensu* Galton, 1997), coalesce and run posterolaterally onto the paroccipital process forming the Y-shaped structure diagnostic of *Thescelosaurus*.

The ventral portion of the opisthotic bears multiple perforations. The largest and most anterior of these is the fenestra ovalis, which occurs at the ventralmost point of the suture between the prootic and opsithotic (Fig. 11C, G). The posterior rim of this fenestra is formed by the opisthotic, and the anterior rim by the prootic. The fenestra is confluent medially with the anteroposteriorly expanded cavities for the vestibule, which project both anteriorly and posteriorly into the prootic and opisthotic, respectively. Immediately posterior to the fenestra ovalis lie four foramina for the posterior cranial nerves (IX, X, XI, and XII). This area is incomplete ventrally, and the anterior three of the four are not closed off ventrally, because of a broken bone. For the purpose of description and discussion, the anteriormost of these is referred to as the first, and the posteriormost is referred to as the fourth, with the middle two named accordingly. The first of these foramina (the foramen metotica) is separated from the fenestra ovalis by a thin bony plate (crista interfenestralis) (Galton, 1989, 1997). A central and rounded vertical ridge, the crista tubularis, running down the opisthotic, separates the foramen metotica from the second foramen. The foramen metotica, and those posterior to it, traverse the exoccipital–opisthotic independently, and enter the cerebellar area in series. The third foramen lies posteroventral to the second. The bony rims of both of these foramina are incomplete ventrally, but were probably enclosed entirely within the exoccipital–opisthotic. The fourth foramen lies posterodorsal to the third, is entirely enclosed within the exoccipital–opisthotic and is located at the occipital and paroccipital process regions of this bone.

Using the extant phylogenetic bracket (Bryant & Russell, 1992; Witmer, 1995) to attempt to determine the homology of these foramina results in some ambiguity. In squamates and *Sphenodon* two separate anterior foramina are present for the glossopharyngeal (IX) plus accessory (XI) and vagus (X) nerves, with the posterior foramina (commonly three) carrying branches of the hypoglossal (XII) nerve (Starck, 1979; Bellairs & Kamal, 1981). In crocodilians the anteriormost foramen transmits the glossopharyngeal (IX) and vagus (X) nerves, and the posterior three (sometimes two) carry the hypoglossal (XII) nerve (de Beer, 1937; Iordansky, 1973; Hopson, 1979; Starck, 1979). In birds, however, the anteriormost foramen carries the glossopharyngeal nerve, the second carries the vagus (X) and accessory (XI), and the posterior two (sometimes three) carry branches of the hypoglossal (XII) nerve (de Beer, 1937; Koch, 1973; Bubien-Waluszewska, 1981).

Galton (1989, 1997) interpreted the first foramen as the foramen metoticum (lateral aperture of the recessus scalae tympani) carrying the glossopharyngeal nerve (IX), the second carrying the vagus foramen (X), and the last two (third and fourth) as being for the transmission of the hypoglossal nerve (XII), with the accessory nerve (XI) exiting with either the glossopharyngeal or the vagus nerves. This interpretation of the braincase advocates that the glossopharyngeal (IX) nerve exits through the anteriormost foramen, and the hypoglossal (XII) nerve exits through the posterior two foramina. The location of the vagus and accessory nerves cannot, however, be definitively determined, nor is there certainty as to the identity of the structures passing through the second foramen. Medially, just anterodorsal to the posterior hypoglossal foramen (XII), the foramen for the transmission of the vena cerebralis posterior (Galton, 1989) penetrates laterally into the paroccipital process.

Prootic: The prootic is quadrangular, with the dorsal half of its lateral surface being convex (Fig. 11). It contacts the supraoccipital, and also a limited region of the exoccipital–opisthotic dorsally, and the exoccipital–opisthotic posteriorly (Fig. 11G). The supraoccipital suture is flat, extending in the frontal plane, and is perforated by the anterior semicircular canal (Fig. 11C). The suture with the exoccipital–opisthotic lies in the transverse plane, and is characterized by several transversely oriented grooves laterally and small pits medially, and is perforated by the posterior semicircular canal (Galton, 1989, 1997) (Fig. 11C). The dorsal half of the posterior margin of the prootic participates in this tight suture. The ventral half forms the anterior half of the fenestra ovalis, and the posterior half (although not fully preserved) is contributed to by the opisthotic (Fig. 11G). Within the prootic, confluent with and anterior to the fenestra ovalis, lies the anterior portion of the cavitations that would have housed the vestibule and anterior utriculus (Fig. 11C). Ventral to the fenestra ovalis the prootic is incomplete.

Anteriorly, the prootic enters into a smooth suture in the transverse plane in contacting the laterosphenoid (Fig. 11A). The ventral third of the prootic is broken off from the main body at a large crack connecting two laterally projecting foramina. The anterior of these is the large and dorsoventrally depressed trigeminal foramen (V), and the posterior

is the smaller facial foramen (VII) (Ostrom, 1961; Hopson, 1979; Starck, 1979; Bubien-Waluszewska, 1981; Galton, 1997) (Fig. 11G). The trigeminal foramen is almost entirely enclosed within the prootic, with only the extreme anterior end bordered by the laterosphenoid, and it extends laterally through the anterior margin of the prootic (Bubien-Waluszewska, 1981), similar to the condition seen in *Hypsilophodon* (NHMUK R 2477; Galton, 1989). Because of its size and the existence of only a single foramen, it is concluded that the trigeminal nerve exited through the prootic proximal to its branching into the maxillary (V_2) and mandibular (V_3) rami. The position of the ophthalmic ramus (V_1) relative to the foramen is unknown.

After traversing the prootic laterally, the smaller facial foramen (VII) is continuous, with a ventrally directed groove along the prootic and onto the basisphenoid (Fig. 11G). This groove would have housed the hyomandibular branch of the facial nerve (VII) as it extended ventrally (Bubien-Waluszewska, 1981). It is bordered proximally on its anterior side by a prominent and rugose ridge, and on its posterior side, further ventrally, by an ascending lateral ridge of the basipterygoid process. The other branch of the facial nerve, the palatine branch, would have projected anteriorly, but its path is not marked on the bone.

A small foramen penetrates the bone roofing the facial foramen, within the lateral wall of the prootic, and perforates the prootic dorsally to connect with the cavity of the anterior vestibule (Fig. 11C). This foramen is interpreted as that carrying the anterior ramus ($VIII_a$) of the vestibulocochlear (statoacoustic) nerve (VIII) (Galton, 1989). It follows the path of the facial (VII) nerve proximally, and takes an abrupt dorsal turn halfway along its penetration of the prootic to pierce the cavity of the vestibule. No indication of the path of the posterior ramus ($VIII_p$) is evident. In *Dryosaurus altus* (Galton, 1989) and *Hypsilophodon* (BNMH R 194, 2477), the passage for the anterior ramus ($VIII_a$) is closely associated with the path of the facial nerve proximally, whereas the course of the posterior ramus ($VIII_p$) is located further posteriorly (Galton, 1989). In *Dryosaurus lettowvorbecki* (BM R dy A), however, the pathways of both the anterior and posterior rami follow that of the facial nerve, and then project dorsally (Galton, 1989). Galton (1989, 1995) suggested that *Thescelosaurus* (RSM P 1225.1) exhibits the former condition (similar to that of *Dryosaurus*), but this was declared in the absence of direct evidence of the foramen for the posterior ramus, and so cannot be verified. All three of these nerve foramina (V, VII and VIII) perforate the anterolateral cerebellar area just anterior to the fenestra ovalis.

Basisphenoid: The entire basisphenoid is preserved except for its anteriormost margin, which would have contacted the cultriform process of the presphenoid (Fig. 11). The posterior surface flares laterally, forming the basisphenoid tubera, and participates in a thick and interdigitating suture with the basioccipital, whereas the dorsolateral surface sutures to the prootic (Fig. 11D, E). The dorsal surface is slightly concave and is divided by a central ridge, forming two anteroposteriorly running troughs (Fig. 11D). The small, paired abducens foramina (VI) lie in the centre of these troughs, and the canals of these nerves penetrate anteroventral to the pituitary fossa below (Hopson, 1979; Bellairs & Kamal, 1981; Bubien-Waluszewska, 1981). In the central part of its body, the basisphenoid is constricted laterally and is roughly hourglass shaped in ventral view (Fig. 11D). Located within the constriction, on its lateral aspect, is a large foramen that transmitted the internal carotid artery, which coursed anteromedially to connect with the pituitary fossa, at which point the paired internal carotid arteries anastomosed (Pearson, 1972) (Fig. 11A, D). Anterior to this foramen, a vertical ridge runs from the suture with the prootic to the basipterygoid process. Dorsally this process forms the anterior wall of a trough representing the course of the facial nerve (V) that extends onto the prootic (Fig. 11G). The basipterygoid processes are elliptical, with their long axis running posterolaterally, and arise centrally from the basisphenoid, taper slightly, and then flare as they project ventrolaterally (Fig. 11E). The distal extremities are rounded and rugose. Just medial to the base of these processes, two small paired foramina perforate posterodorsally (Fig. 11A). It is unclear whether these foramina would have transmitted the anterior projections of the trochlear (IV) nerve, abducens (VI) nerve, or a small anterior branch of the internal carotid artery. The lateral surface, dorsal to these processes, is flat and projects anterolaterally and slightly ventrally. Ventral to the dorsal surface of the basisphenoid lies the circular pituitary fossa, which is perforated by the large posterolaterally directed foramina for the internal carotid arteries laterally, and the smaller posterodorsal abducens foramina (VI) dorsally (Fig. 11A). Anteriorly the pituitary fossa opens into a large circular foramen. Ventral to this, the cultriform process is broken off.

Laterosphenoid: Only a fragment of the dorsalmost portion of the left laterosphenoid is preserved (Fig. 4B). It articulates by way of a saddle-shaped suture with the ventral surface of the lateral portion of the frontal and parietal, in the region of the frontoparietal suture. The laterosphenoid fragment is convex ventrally and extends transversely, forming

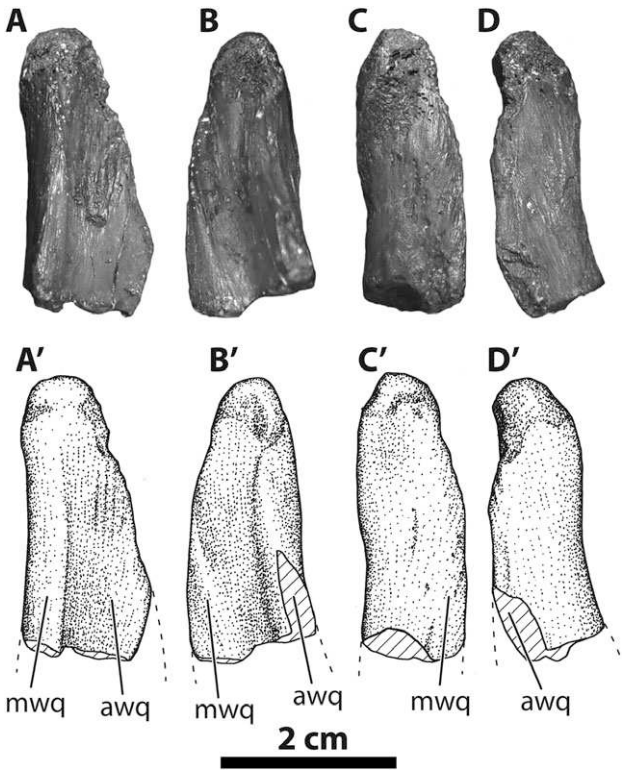

Figure 12. Left quadrate of the holotype of ***Thescelosaurus assiniboiensis* sp. nov.**, RSM P 1225.1, in medial (A), anterior (B), posterior (C), and lateral (D) views. See list in text for an explanation of anatomical abbreviations. Primes indicate illustrations of photographed elements. Dashed lines indicate extrapolated margins of the element. Hatched areas represent incomplete bone surface.

the lateral wall of the cerebral fossa medial to the medial portion of the postorbital suture. Although incomplete, the laterosphenoid would have formed the lateral wall of the braincase medially. Because its anteroventral aspect is missing, and the orbitosphenoid and presphenoid are not preserved, no information is available regarding the positions of foramina for the optic (II), oculomotor (III), or trochlear (IV) nerves.

Splanchnocranium

Quadrate: Only the proximal (dorsal) portion of the left quadrate is preserved (Fig. 12). Dorsally it tapers to form a rounded, highly porous head, triangular in cross section [as in *Hypsilophodon* (Galton, 1974b) and *Zephyrosaurus* (Sues, 1980)], that articulates with the squamosal. The head is slightly concave anteromedially. The anteromedial and medial surfaces of the quadrate bear distinct rugosities and vertically oriented striations (Fig. 12A, B). Two vertically oriented plates project anteriorly and medially, at nearly right angles, from the shaft of the quadrate. The lateral jugal wing (the anterior plate) is slightly larger and thicker than the pterygoid wing (its medial counterpart). Unlike in *Orodromeus* (Scheetz, 1999), these two flanges extended dorsally to the same height on the shaft of the quadrate. Between these two flanges the anteromedial surface is highly concave, fitting closely around the base of the quadrate process of the squamosal. The posterior and lateral margins are straight as they rise vertically and are rounded at the posterolateral angle.

Postcranial skeleton

Vertebrae

The vertebral column is represented by a reasonably complete dorsal and sacral series, and a very fragmentary caudal series.

Dorsal vertebrae: The dorsal series is represented by six anterior dorsal vertebrae (D2–D4 and D6–D8) and seven posterior dorsals (D10–D16) (Fig. 13). As is common for specimens of *Thescelosaurus* (MOR 1106, 1164, 1165, NCSM 15728, and SDSM 7210), the neural arches of the anterior dorsals, with the exception of D6, are separated from their centra. Three isolated centra cannot be confidently associated with their respective neural arches. The neural arch and centrum of D6 was dissociated, but complementary sutural surfaces confirm this match (Fig. 14). With the exception of D6 (which preserves both), the six anterior dorsals preserve only one transverse process, with the other (either left or right) being broken off (Fig. 13A). Only D6 preserves a neural spine (Fig. 14). The seven posterior dorsal vertebrae exhibit articulated sutures between the neural arches and centra, although the sutural line remains visible on some. No neural spines are preserved, and only three transverse processes are represented in the posterior series.

The centra are amphiplatyan to slightly amphicoelous, longer than wide, and slightly wider than high (Fig. 14). Ridges and grooves running anteroposteriorly are located on the anteriormost and posteriormost lateral and ventral surfaces, and form a ring of crenulations around the articular surface (Fig. 14A, B, E). These probably represent the scars of intervertebral muscles or ligaments, and are generally very prominent in basal ornithopods and stem iguanodontoids [*Camptosaurus* (USMN 4697), *Dryosaurus* (CM 21786), *Hypsilophodon* (NHMUK R 196), *Orodromeus* (MOR 473, 623), *Oryctodromeus* (MOR 1636), *Parksosaurus* (ROM 804), *Thescelosaurus* (USNM 7757, NCSM 15728), and *Zephyrosaurus* (MCZ 4392)]. In common with other specimens of *Thescelosaurus* (MOR 1106), and with *Parksosaurus*

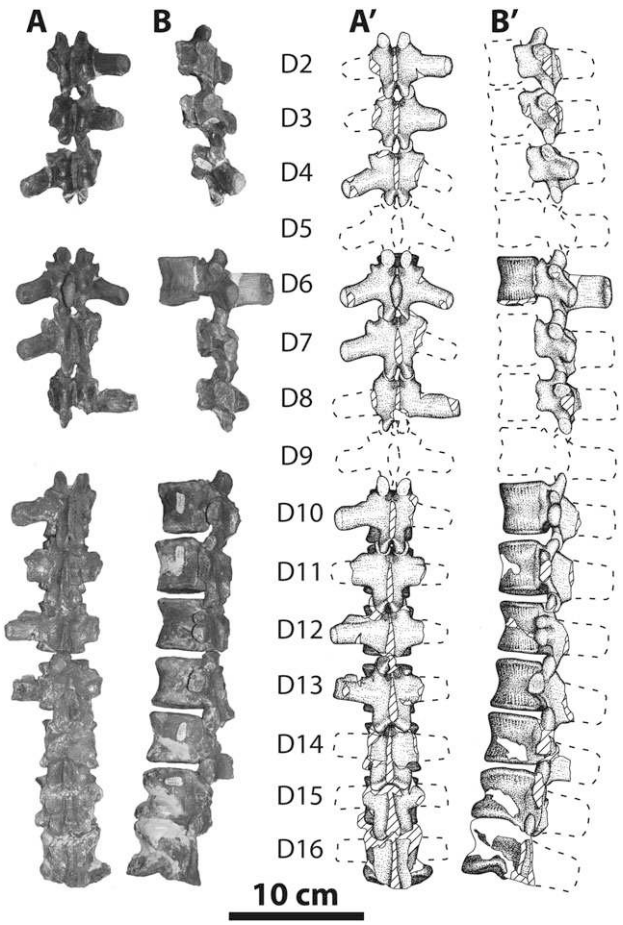

Figure 13. Dorsal vertebral series of the holotype of ***Thescelosaurus assiniboiensis* sp. nov.**, RSM P 1225.1, in dorsal (A) and left lateral (B) views. Anterior vertebrae show the dissociation of neural arches and centra. See list in text for an explanation of anatomical abbreviations. Primes indicate illustrations of photographed elements. Dashed lines indicate extrapolated margins of the element. Hatched areas represent incomplete bone surface. White areas represent plaster reconstruction.

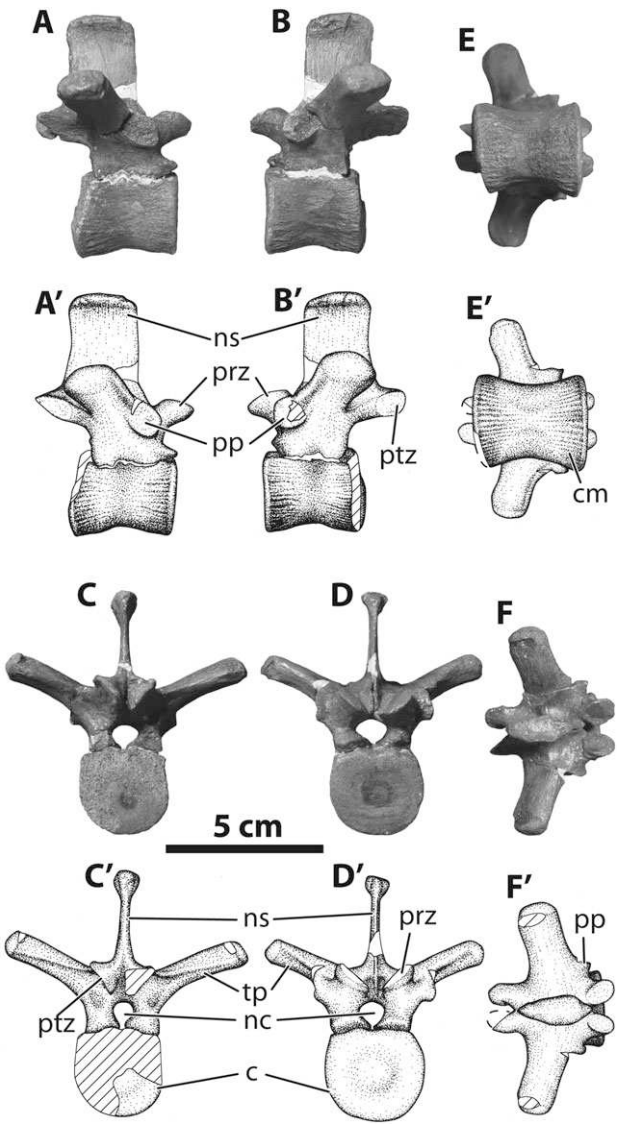

Figure 14. Sixth dorsal vertebra of the holotype of ***Thescelosaurus assiniboiensis* sp. nov.**, RSM P 1225.1, in right lateral (A), left lateral (B), posterior (C), anterior (D), dorsal (E), and ventral (F) views. See list in text for an explanation of anatomical abbreviations. Primes indicate illustrations of photographed elements. Dashed lines indicate extrapolated margins of the element. Hatched areas represent incomplete bone surface. White areas represent plaster reconstruction.

(ROM 804), the floor of the neural canal is not perforated by a large, anteroposteriorly elliptical foramen, a sturucture seen in *Camptosaurus* (USMN 4697), *Dryosaurus* (CM 21786), *Orodromeus* (MOR 623), *Oryctodromeus* (MOR 1636), *Hypsilophodon* (NHMUK R 196), and *Zephyrosaurus* (MCZ 4392).

The neural arches form the lateral and dorsal margins of the cylindrical neural canal (Fig. 14C, D). The lateral surfaces of the neural arches flare dorsally and laterally, forming the parapophyses and transverse processes. On the fourth dorsal, the facet of the parapophysis is a vertical, circular face located on the lateral surface of the neural arch, anterior to, and distinct from, the transverse process (Fig. 14A, B). The transverse processes are elliptical in cross section, with the long axis oriented anteroposteriorly. Their narrow anterior and posterior margins are tapered to form ridges, and their distal extremities are rounded but are not distinctly swollen. The articular surfaces of the pre- and postzygapophyses are smooth and flat, with a rounded outline. The articular faces of the prezygapophyses face dorsome-

dially at an angle of approximately 45°, whereas those of the postzygapophyses face ventrolaterally and incline at a slightly steeper angle (Fig. 14C, D). The postzygapophyses project further posteriorly than do the prezygapophyses anteriorly (Fig. 14A, B). The neural spine is shifted posteriorly relative to those of the other vertebral elements. It is rectangular in lateral view, being higher than long, with straight and parallel anterior and posterior margins. In anterior view the neural spine is thin and of approximately consistent thickness throughout its height, except for a distinct lateral swelling into a bulbous ridge at the dorsal extreme (Fig. 14C, D).

Within the dorsal series there is an increase in centrum height, width, and length from anterior to posterior, with the last dorsal centrum being the widest and longest, although the second last is the highest (Fig. 13). The angle that the transverse processes form with the frontal plane decreases from around 38° anteriorly to nearly zero degrees by the tenth process (Fig. 13A). This pattern agrees with the condition found in the holotype of *T. neglectus* (USNM 7757), and is opposite to that described for CMN 8537 (Sternberg, 1940). Anterior dorsals D1–D10 bear distinct parapophyses laterally, anteroventral to the transverse process, with the diapophyses placed distally on the transverse process (Fig. 13). On D11 and D12 the parapophysis is situated on the anterior margin of the transverse process, with the parapophysis of D12 being placed more distally. On D13 the parapophysis and diapophysis are united into one articular surface on the distal end of the transverse process, indicative of single-headed ribs being borne by D13 and those posterior to it, and double-headed ribs being carried by D12 and those anterior to it. This condition matches that of USNM 7757, CMN 8537, *Orodromeus* (MOR 473) (Scheetz, 1999), and *Hypsilophodon* (NHMUK R 196) (Galton, 1974b).

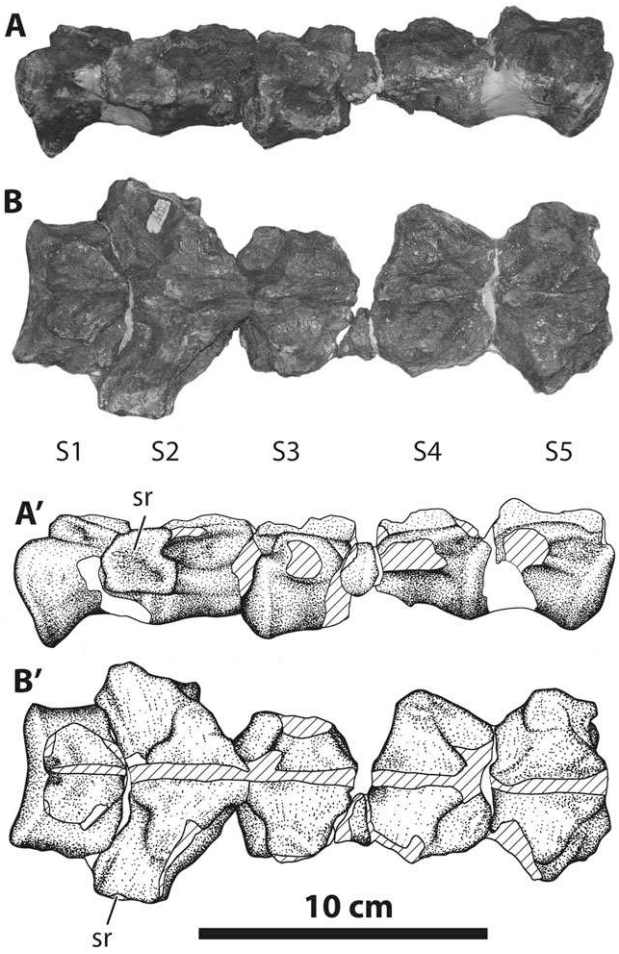

Figure 15. Fused sacral vertebrae of the holotype of ***Thescelosaurus assiniboiensis* sp. nov.**, RSM P 1225.1, in left lateral (A) and dorsal (B) views. See list in text for an explanation of anatomical abbreviations. Primes indicate illustrations of photographed elements. Hatched areas represent incomplete bone surface. White areas represent plaster reconstruction.

Sacral vertebrae: Five sacral centra are preserved, but only the first sacral ribs (and no neural spines) are present (Fig. 15). The first of this series is identified as the dorsosacral (*sensu* Butler *et al*., 2011b), because it does not bear a distinct sacral rib. Instead, the first sacral rib arises intervertebrally along the contact between the dorsosacral and the proceeding first true sacral vertebra, with the latter supporting the majority of the rib (Fig. 15B). This shift of position between the sacral vertebrae and sacral ribs results in one fewer sacral rib than fused vertebrae, characterizing the 'pentapleural' sacrum (Galton, 1974b) that also occurs in *Parksosaurus* (ROM 804), *Thescelosaurus* (USNM 7757), and *Dryosaurus* (Galton, 1981), and is of variable occurrence in *Hypsilophodon* (Galton, 1974b). The articulation between the centra of the dorsosacral and the first true sacral vertebra constitutes the broadest transverse contact along the entire vertebral column. The anterior surface of the dorsosacral displays a distinct heterocoelous articular facet for articulation with the preceding dorsal vertebra.

The first true sacral vertebra is the largest of the sacral series, and the majority of the first sacral rib articulates with the centrum of this vertebra. The subsequent three sacrals are subequal in size, and have no preserved sacral ribs associated with them, and their poor presevation obscures the presence of sacral rib facets. In ventral view, the sacral centra are concave along the midline but flare laterally and ventrally at the points of contact with adjacent vertebrae. The first sacral rib is robust and bears distinct concave articular facets at its lateral end.

The sacrum of the holotype of *T. neglectus* (USNM 7757) was originally thought to consist of five vertebrae (Gilmore, 1915), although the last dorsal, referred to as the 'sacro-dorsal', was described as being transversely expanded posteriorly. Sternberg (1940) noted that the morphology of this 'sacro-dorsal' matched that of the first fused sacral vertebra of the holotype of *T. edmontonensis* (CMN 8537; currently *Thescelosaurus* sp.; Boyd *et al*., 2009), concluding that the 'sacro-dorsal' should be counted as part of the sacrum, resulting in six sacral vertebrae. The subsequent discovery of additional specimens referable to *Thescelosaurus* (e.g. AMNH 117 and NCSM 15728; Galton, 1974a; Boyd *et al*., 2009) and new species of basal ornithopods (e.g. *Orodromeus* and *Changchunsaurus*; Scheetz, 1999; Butler *et al*., 2011) provided further insight into the morphology of the sacrum of basal ornithopods that supports this conclusion. Additionally, all taxa positioned crownward of *Hexinlusaurus* (Boyd *et al*., 2009; fig. 3b) possess at least six sacral vertebrae when the sacrodorsal is included in the sacral count. Thus, the reversal in *T. assiniboiensis* sp. nov. to five sacral vertebrae is unique among derived basal ornithopod taxa. Alternatively, the presence of five sacral vertebrae in RSM P.1225.1 could represent ontogenetic variation. For example, in the holotype of *Parksosaurus warreni* (ROM 804), the posterior three sacral vertebrae are in articulation with each other but unfused, and the anterior three sacral (including the dorsosacral) vertebrae are present as a fused set. If this is indicative of an anteroposterior ontogenetic sequence of fusion, then it would not be unexpected for the last sacral to be unfused to the rest of the sacrum if RSM P 1225.1 is a skeletally immature individual. Given these alternative explanations, confidently determining the number of sacral vertebrae in *T. assiniboiensis* sp. nov. must await the recovery of a specimen that preserves a more completely preserved vertebral column, and that can be definitively determined to be fully skeletally mature.

Caudal vertebrae: Eight isolated caudal centra are preserved, all lacking transverse processes and neural spines. Three large and fragmentary centra are attributed to the proximal region of the tail. A centrum bearing the base of a reduced transverse process on the left side (but not the right) probably corresponds to approximately the tenth caudal, whereas the other centra probably represent caudal vertebrae 12 and 13. Two other fragmentary caudal centra are preserved, and are likely to be attributable to the distal portion of the tail (distal to the 30th caudal). The centra are longer than high, subequal in height and width (except distally where they become dorsoventrally depressed), and spool shaped, with crenulations present on the anterior and posterior rims. Only fragments of chevrons are preserved, but they are preserved with the long, transversely flattened, and spatulate chevron morphology characteristic of *Thescelosaurus* (CMN 8537, USNM 7757), but not with the anteroposteriorly-expanded chevrons of *Parksosaurus* (ROM 804). Only a single fragment of an ossified axial tendon is preserved.

Ribs: Multiple ribs are preserved from both sides of the body, and they bear the same distinctive features as those of other *Thescelosaurus* specimens (CMN 8537, NCSM 15728, USNM 7757) (Fig. 16). The tuberculum is greatly reduced and is represented only as a boss on the angle of the rib (Fig. 16A, B). The capitulum is long and noticeably swollen at its articular end. Immediately distal to the tuberculum the shaft curves sharply ventrally, whereas the remainder of the shaft is only slightly curved. In cross section, proximally the rib shafts are flat laterally with a medial ridge forming a T-shape, and are laterally compressed distally, forming a long ellipse (Fig. 16D). The largest ribs bear a broad thin flange that projects posteriorly from the lateral border of the proximal third, and exhibit a concave lateral surface in their distal third. This concavity is unique to *Thescelosaurus*, and the posterior margins of the ribs in this region are marked with prominent rugosities that are associated with the articulation or juxtaposition of the intercostal plates in many specimens of *Thescelosaurus* (MOR 979, NCSM 15728) and other basal ornithopods [*Hypsilophodon* (NHMUK R 196, 192, 2477, 28707) *Parksosaurus* (ROM 804), *Talenkauen* (MPM 10001)] (Boyd, Cleland & Novas, 2008) (Figs 16B, E and 17). Although such intercostal plates are preserved on other specimens of *Thescelosaurus* (MOR 979, NCSM 15728) and other basal ornithopods [*Hypsilophodon* (NHMUK R 196, 192, 2477, 28707), *Parksosaurus* (ROM 804), and *Talenkauen* (MPM 10001) (Novas, Cambiaso & Ambrosio, 2004; Boyd *et al*., 2008; Butler & Galton, 2008)], they are not preserved here.

Appendicular skeleton

Ilium: Both left and right ilia are preserved, the right being fragmentary and the left being almost complete save for the anterior portion of the preacetabular process and the posterior dorsal margin. Overall, the ilium is most similar to that of *Parksosaurus* (ROM 804), and is distinct from that of *T. neglectus* (USNM 7757) (Fig. 18).

The acetabulum is centrally placed, with a narrow preacetabular process and tall but thin postacetabular area (Fig. 18A). Viewed dorsally the ilium is concave laterally, with the preacetabular process being more curved than the posterior half of the element (Fig. 18C). This differs from the morphology

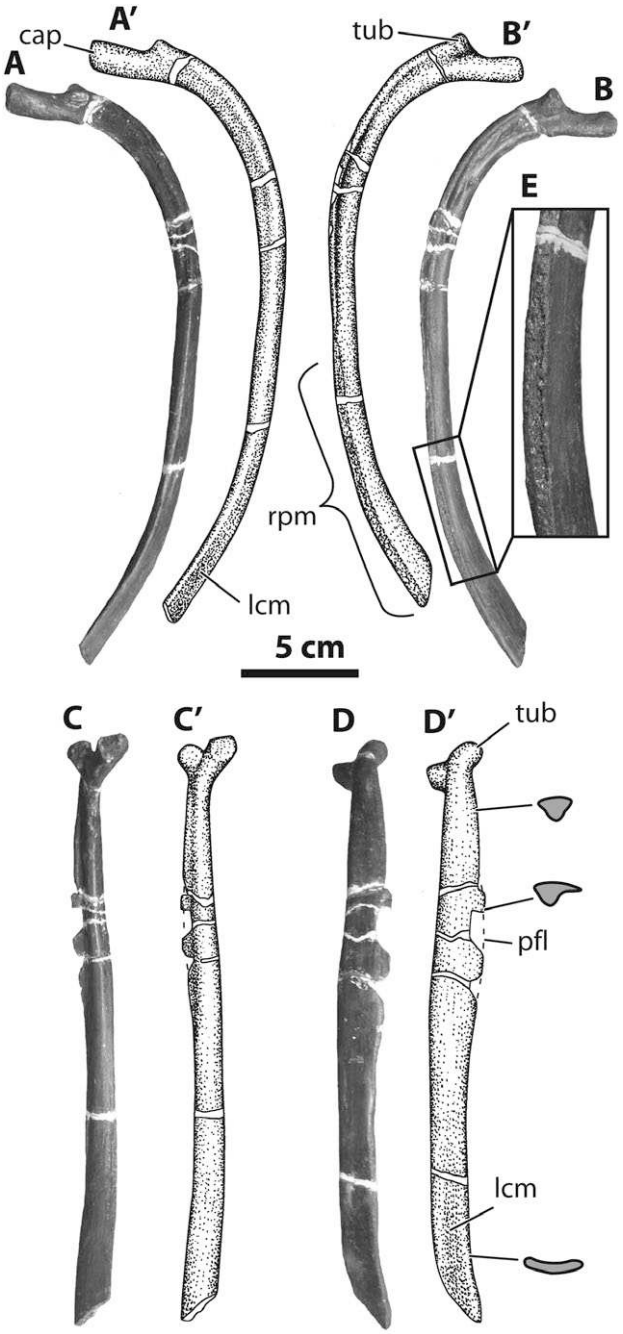

Figure 16. A left rib of the holotype of ***Thescelosaurus assiniboiensis* sp. nov.**, RSM P 1225.1, in anterior (A), posterior (B), medial (C), and lateral (D) views, and showing flattened and rugose posterior margin (E). Lateral view shows cross-sectional shape along the shaft, with the lateral surface facing upwards. See list in text for an explanation of anatomical abbreviations. Primes indicate illustrations of photographed elements. Dashed lines indicate extrapolated margins of the element. White areas represent plaster reconstruction.

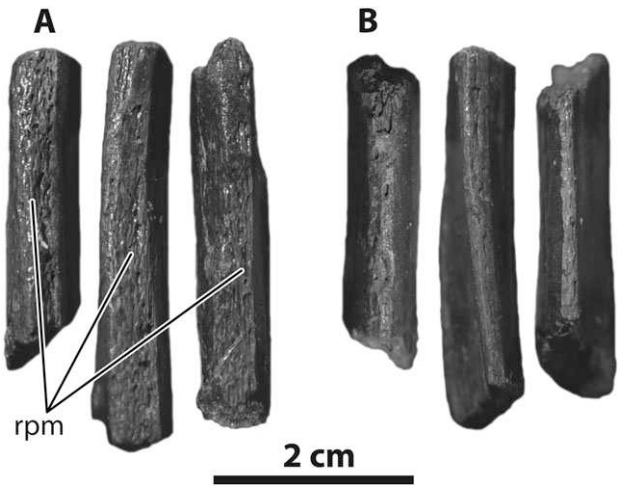

Figure 17. Distal portions of ribs of the holotype of ***Thescelosaurus assiniboiensis* sp. nov.**, RSM P 1225.1, in posterior (A) and anterior (B) views, illustrating rugose texture of posterior margin.

displayed by the ilium of CMN 8537, which is flat laterally. It is evident, however, that the latter is heavily reconstructed, and the original morphology is difficult to ascertain.

The ilium of RSM P 1225.1 is transversely thin and is vertically oriented for most of its length. The preacetabular portion is twisted along its long axis so that its lateral surface lies nearly horizontally and faces dorsally, a condition also seen in CMN 8537 (Sternberg, 1940) and in *Hypsilophodon* (Galton, 1974b). The pubic peduncle is incomplete and, as in USNM 7757, the ischiadic peduncle is distinctly swollen, and projects orthogonal to the main axis of the ilium.

The iliac blade is thin and its posterior portion is vertically oriented. Its highest point is located dorsal to the acetabulum, and its height decreases markedly towards its anterior and posterior extremes (Fig. 18A). This contrasts sharply with the morphology displayed by the iliac blade of other specimens of *Thescelosaurus*. In USNM 7757 the postacetabular portion of the blade is of consistent height in the area preserved, and rises dorsally near its posterior margin prior to the point at which it is broken off. In CMN 8537 the highest point lies close to the posterior margin. The posterior margin of the iliac blade of RSM P 1225.1 is also more rounded than that of USNM 7757 and CMN 8537. The decreasing height and rounded posterior aspect are more similar to the morphology exhibited by *Parksosaurus* than by *Thescelosaurus*.

The brevis shelf projects medially in the frontal plane. In *T. neglectus* (USNM 7757) this shelf forms a thin sheet that extends to the posterior margin of

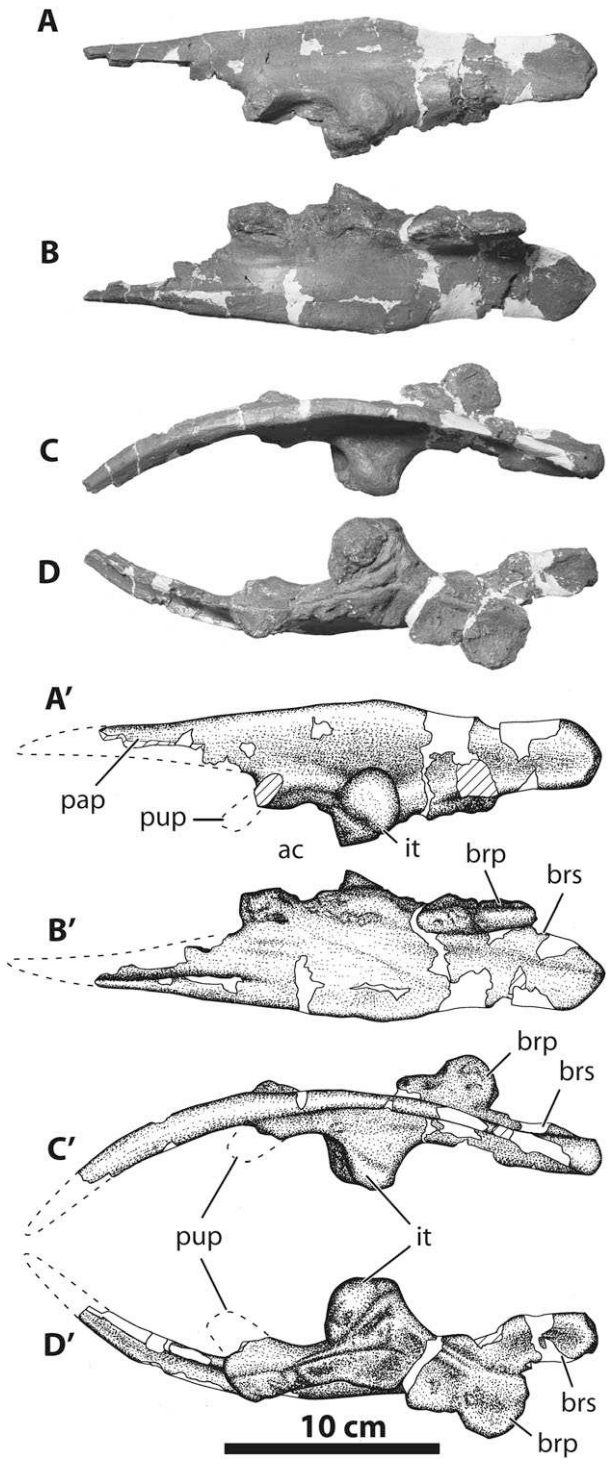

Figure 18. Left ilium of the holotype of ***Thescelosaurus assiniboiensis* sp. nov.**, RSM P 1225.1, in lateral (A), medial (B), dorsal (C), and ventral (D) views. Dashed lines indicate extrapolated margins of the element. See list in text for an explanation of anatomical abbreviations. Primes indicate illustrations of photographed elements. Hatched areas represent incomplete bone surface. White areas represent plaster reconstruction.

the ilium (Gilmore, 1915), and angles ventromedially. In contrast, the brevis shelf of RSM P 1225.1 is a very thick projection, posteromedially just posterior to the ischiadic peduncle, but its remaining posterior portion is either very thin, or does not extend very far medially or posteriorly when compared with the condition displayed by *T. neglectus*. This uncertain condition is attributable to preservation issues, because both the right and left brevis shelves are incomplete posteriorly, and do not exhibit a true edge. The shape of the shelf, however, is similar on both elements. The morphology of the brevis shelf of RSM P 1225.1 appears to be unique to this specimen.

Pubis: Left and right anterior processes of the pubes are preserved, but on neither side is a pubic shaft represented. The right anterior process of the pubis is preserved from the pubic foramen to the anterior end of the element (Fig. 19). The left anterior process of the pubis is preserved from its articulation with the ilium to a position slightly caudad to the anterior end of the element. The pubis is similar to that of other specimens of *Thescelosaurus* (CMN 8537, USNM 7757), and to that of *Parksosaurus* (ROM 804). The proximal aspect is expanded transversely, forming a flat sutural contact dorsally for the ilium (Fig. 19A). Posterolateral to this sutural surface the expanded margin is concave and forms the anteroventral aspect of the acetabulum. Lateral to the contact surface of the ilium is a prominent rounded lateral projection that overhangs a laterally directed concavity of the main body of the pubis. The anterior pubic process is straight (the right side is shown as curving ventrally, but this is as a result of reconstruction), and is round in cross section. The element is slightly dorsoventrally depressed and is ovoid anteriorly, with its end being expanded and bulbous. The pubic foramen is open, with its perimeter not completely encircling the foramen (Fig. 19C, D). This condition is variable in *Hypsilophodon* (Galton, 1974b), *Orodromeus* (Scheetz, 1999), and *Thescelosaurus* (C.M. Brown, pers. observ., 2008), and its correlation with ontogeny is not well understood.

Femur: The femora are almost completely preserved, but the midshafts are fragmentary (Fig. 20). Their structure is very similar to that of USNM 7757 and CMN 8537, only differing in the position of the fourth trochanter and the relative size of the condyles. The greater trochanter occupies the posterior two-thirds of the lateral proximal margin of the femur, and forms a broad curvature dorsally (when viewed laterally) (Fig. 20D, E). It has a flat medial surface, as is the case for *T. neglectus* (USNM 7757), *Parksosaurus* (ROM 804), *Orodromeus* (MOR 294, 473, 623), and

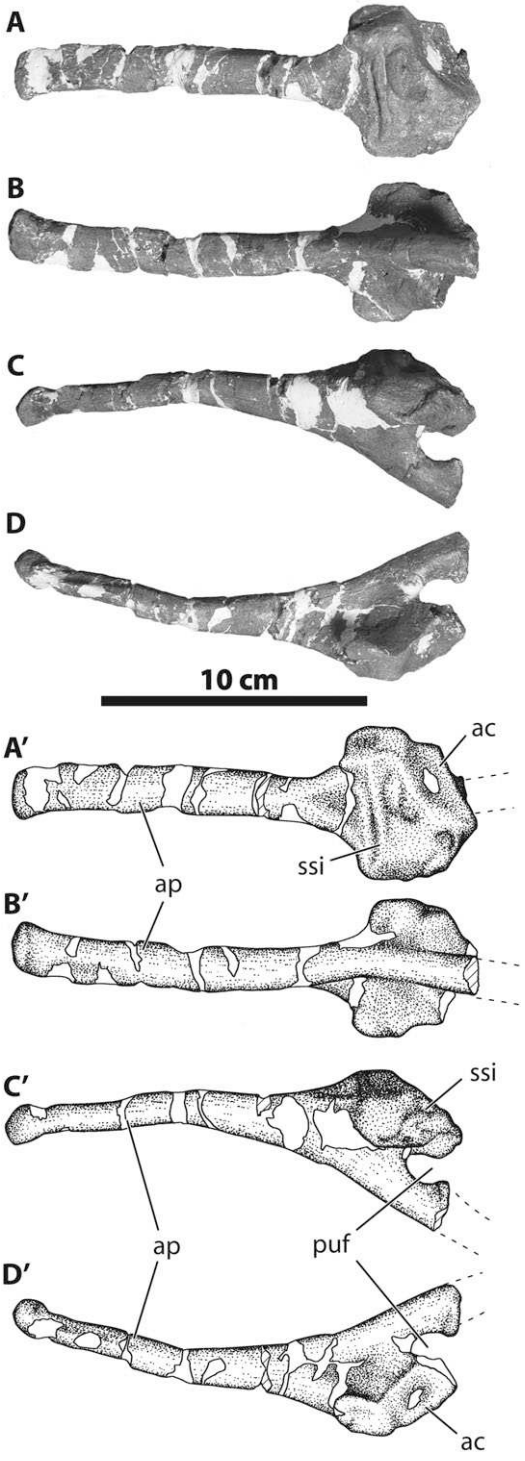

Figure 19. Right pubis of the holotype of ***Thescelosaurus assiniboiensis* sp. nov.**, RSM P 1225.1, in dorsal (A), ventral (B), medial (C), and lateral (D) views. Dashed lines indicate the extrapolated margins of the element. See list in text for an explanation of anatomical abbreviations. Primes indicate illustrations of photographed elements. Hatched areas represent incomplete bone surface. White areas represent plaster reconstruction.

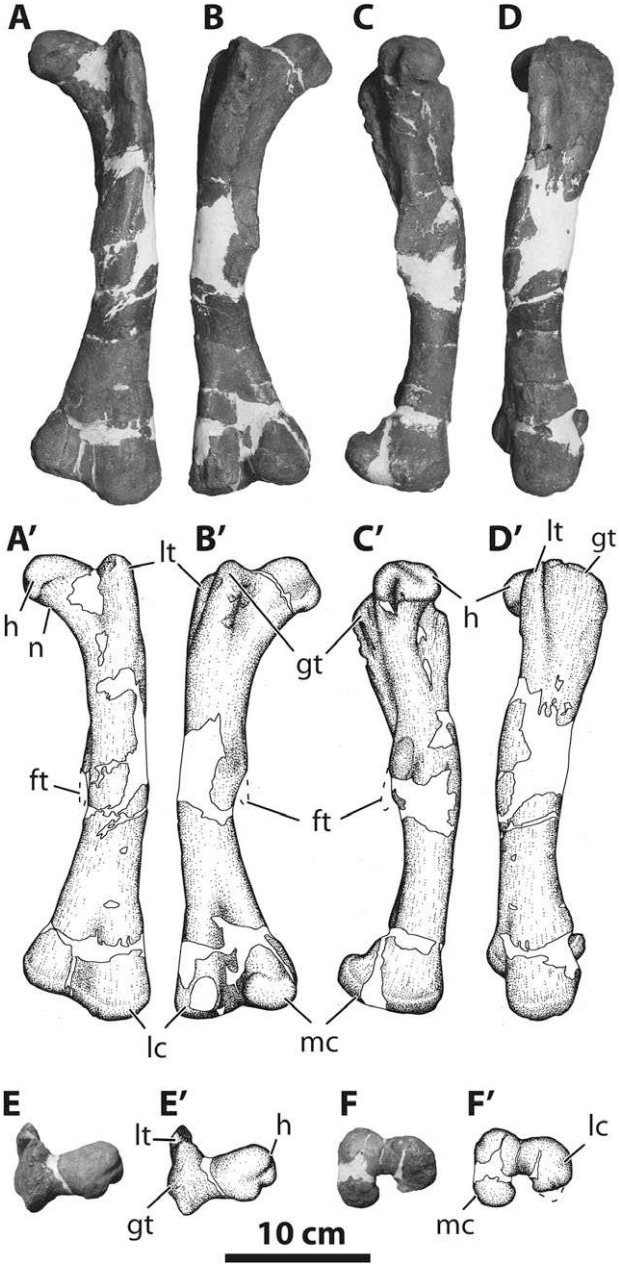

Figure 20. Left femur of the holotype of ***Thescelosaurus assiniboiensis* sp. nov.**, RSM P 1225.1, in anterior (A), posterior (B), medial (C), lateral (D), proximal (E), and distal (D) views. Dashed lines indicate the extrapolated margins of the element. See list in text for an explanation of anatomical abbreviations. Primes indicate illustrations of photographed elements. Hatched areas represent incomplete bone surface. White areas represent plaster reconstruction.

Hypsilophodon (NHMUK R 196, 5830). The lesser trochanter occupies the anterior third of the proximal surface, and is separated from the greater trochanter by a distinct vertical groove. Relative to the greater trochanter, the lesser trochanter is displaced laterally, as it is in USNM 7757 and *Hypsilophodon*. The greater and lesser trochanters are not divided medially. Posteriorly, there is a vertical groove between the lateral margin of the greater trochanter and the head of the femur (Fig. 20B, E).

The fourth trochanter is not completely preserved on either femur, but its base is evident on both and lies entirely on the proximal half of the femur (Fig. 20B, C). Its distal tip, however, probably extended distal to the midpoint of the shaft. The proximal extremity of this trochanter lies further proximally than it does in USNM 7757, and more closely resembles the position of *Parksosaurus*. Anteromedial to the base of the fourth trochanter lies a prominent oval muscle scar marking the insertion of the musculus caudifemoralis longus (Galton, 1974b) (Fig. 20C). The distal end of the femur is expanded transversely and posteriorly into two distinct condyles, separated anteriorly by an extremely shallow intercondylar groove that is much deeper and more distinct posteriorly (Fig. 20A, B, F). The medial condyle extends farthest distally and is more massive than the lateral condyle, a condition that is opposite to that reported for the holotype of *T. neglectus* (USNM 7757; Gilmore, 1915), but is similar to that of *Hypsilophodon* (NHMUK R 5830) and *Dryosaurus* (Galton, 1981). In *Orodromeus* there is evidence of ontogenetic change in the morphology of the distal femoral condyles, with the smaller specimen (MOR 407) having subequal condyles, and the larger specimen (MOR 473, 623) possessing a larger medial condyle (Scheetz, 1999).

Tibia: Both left and right tibiae are preserved in fused articulation with their respective fibulae, calcanea, astragali, and the left lateral distal tarsal (although the distal ends of the fibulae remain articulated at the ankle, their shafts and proximal ends are broken off and are no longer articulated with the tibia) (Fig. 21). The morphology of the tibia is most similar to that displayed by CMN 8537. The tibia is relatively long, being only slightly shorter than the femur, giving a femur : tibia length ratio of 1.07 on the left side (it should be noted, however, that reconstruction of the elements probably affects recorded length, and that the right side is too fragmentary to measure). The tibia is expanded anteroposteriorly proximally, and transversely distally, giving a twisted appearance to the shaft, with the longest dimensions of the expansions lying at an angle of 65° relative to each other.

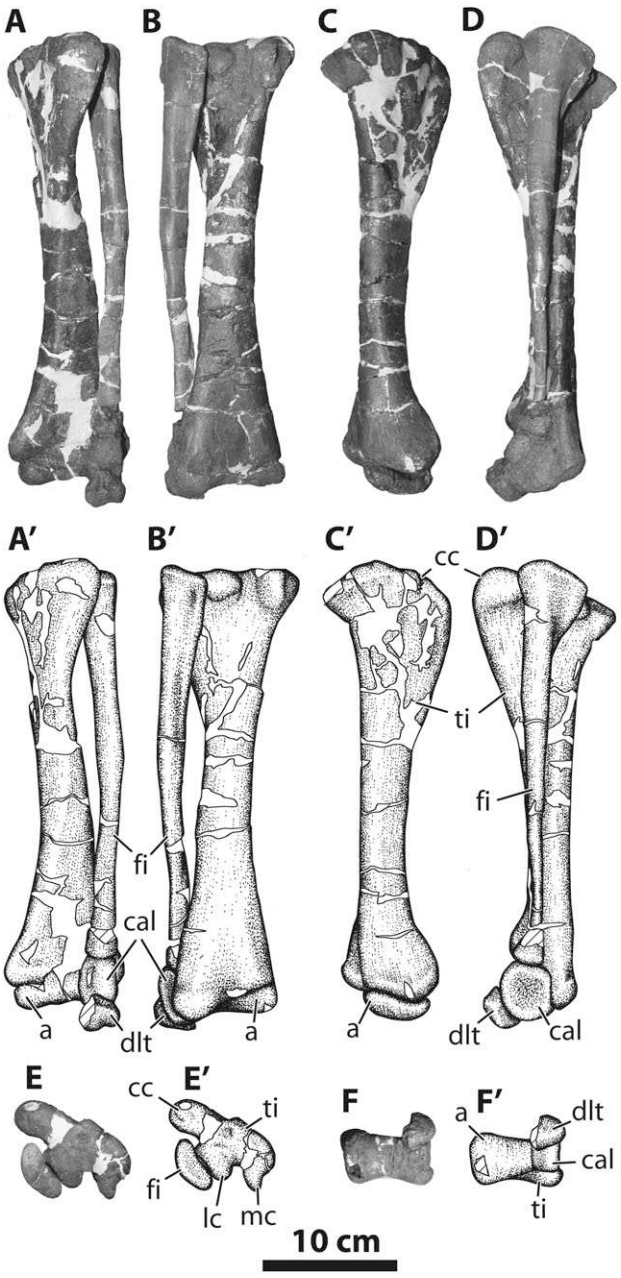

Figure 21. Left tibia, fibula, astragalus calcaneum, and distal lateral tarsal of the holotype of ***Thescelosaurus assiniboiensis*** **sp. nov.**, RSM P 1225.1, in anterior (A), posterior (B), medial (C), lateral (D), proximal (E), and distal (F) views. See list in text for an explanation of anatomical abbreviations. Primes indicate illustrations of photographed elements. Hatched areas represent incomplete bone surface. White areas represent plaster reconstruction.

The proximal expansion of the tibia is characterized by two posteriorly projecting cotyles of approximately equal size, with the lateral one flanked by a laterally directed epicondyle (Fig. 21E). There is a prominent

but relatively narrow anterolaterally projecting cnemial ('prenemial', Gilmore, 1915; Parks, 1922; 'praecnemial', Hulke, 1882) crest, which projects further anteriorly than does either cotyle posteriorly. It is as distinct as that of *Dryosaurus* (YMP 1876) and *Camptosaurus* (USNM 5818), a condition that is similar to that of other specimens of *Thescelosaurus* (USNM 7757, CMN 8737) and of *Parksosaurus* (MOR 804), but is markedly different from that of *Hypsilophodon* (NHMUK R 8530) and *Orodromeus* (PU 23250). Posteriorly, the two cotyles are divided by a deep intercotylar groove. Further distally the shaft cross section changes from subtriangular to elliptical, with the sharper apex directed laterally. At the transversely expanded distal end, the medial malleolus expands anteroposteriorly into a flat medial surface (Fig. 21E, D, F). The lateral surface of the tibia, however, is not expanded in the anteroposterior plane, resulting in the distal end having a triangular cross section, with the apex facing laterally. The distal articular end is smoothly convex and spool shaped.

Fibula: The fibula is relatively long and thin, as it is in most ornithopods, and does not differ significantly from that of other specimens of *Thescelosaurus* (Fig. 21). The left and right fibulae are preserved almost in their entirety. Proximally the fibula is slightly concave medially, and convex laterally, resulting in a semicircular cross section and an anteroposteriorly expanded head. Distally the element thins and becomes more ovoid in cross section, and then becomes almost flat, being flattened anteroposteriorly and expanded transversely. The extreme distal end is swollen, and is round in cross section. Distally the lateral malleolus of the fibula articulates with the lateral edge of the anterior surface of the tibia, as is the case in CMN 8537 and USNM 7757, but contrary to the suggestion of Sternberg (1940) who implied that the fibula articulates only with the lateral face of the tibia in CMN 8537.

Pes: The pes of RSM P 1225.1 is similar to that of *Thescelosaurus* (USNM 7757; Gilmore, 1915), and differs only in being more gracile in form. Distally, the medial two-thirds of the distal end of the tibia articulate with the astragalus, whereas laterally the lateral margin passes posterior to the calcaneum, resulting in the latter abutting the anterior surface of the tibia (Fig. 21). The fibula is closely appressed to the anterior surface of the tibia, and articulates with the calcaneum distally. The left pes is well preserved and disarticulated but the proximal elements of the right are fused.

The right astragalus is preserved in its entirety, but the left is less complete. Both are preserved in articulation with their respective tibiae (Fig. 21). The astragalus is closely appressed to the medial two-thirds of the distal portion of the tibia. It is concave proximally and convex distally. Its transverse width and anteroposterior length exceed its proximodistal height. The astragalus is thicker both proximodistally and anteroposteriorly in its medial extremity than its lateral extremity (Fig. 21B). Laterally it thins towards its contact with the calcaneum. Its posterior face is sharp and thin, whereas its anterior face curves dorsally and wraps over the anterior face of the tibia.

The calcaneum is preserved and articulated on both sides. It is block-like, and its proximodistal dimension exceeds its transverse width. In lateral view it is rounded distally and anteriorly, but its articulation with the fibula dorsally and the tibia posteriorly are squared off (Fig. 21D). Its lateral surface is concave, whereas its medial surface tapers on all sides to form the spool-shaped mesotarsal articular surface, in conjunction with the astragalus. Unlike the condition in *T. garbanii* (LACM 33542) (Morris, 1976), but as for *T. neglectus* (USNM 7757), the calcaneum is not reduced and participates in the mesotarsal ankle joint.

The distal lateral tarsal is preserved in articulation with the left calcaneum (only the lateral portion preserved); the right is isolated. The element is trapezoidal when viewed distally, with the anterior and posterior surfaces approximately equal in length. The lateral surface is shorter and rounded, whereas the medial surface is as long as the anterior and posterior surfaces, and is flat where it contacts the medial distal tarsal. The transverse width of this element exceeds its proximodistal height by about two-fold, and bears a concave surface proximally, into which fits the convex distal surface of the calcaneum. The distal medial tarsal is disarticulated from the astragalus on both the left and right sides. The left is isolated and preserved almost in its entirety. The right is broken and only partially preserved, with its lateral extremity articulated with the calcaneum and its medial extremity isolated. The element is squarish when viewed distally, with rounded edges. It is noticeably thinner proximodistally than the distal lateral tarsal, and bears a concave surface proximally and a slightly convex surface distally. The distinct notch for receipt of metatarsal III, noted by Gilmore (1915) for USNM 7757, is absent.

Metatarsals: Right metatarsals I, II, and III are preserved and fused together with their proximal surface obscured; metatarsal IV is isolated. Left metatarsals I–IV are preserved in isolation and, with the exception of metatarsal I, are better preserved than their right counterparts (Fig. 22). As is usual for ornithopods, the foot consists of three main weight-

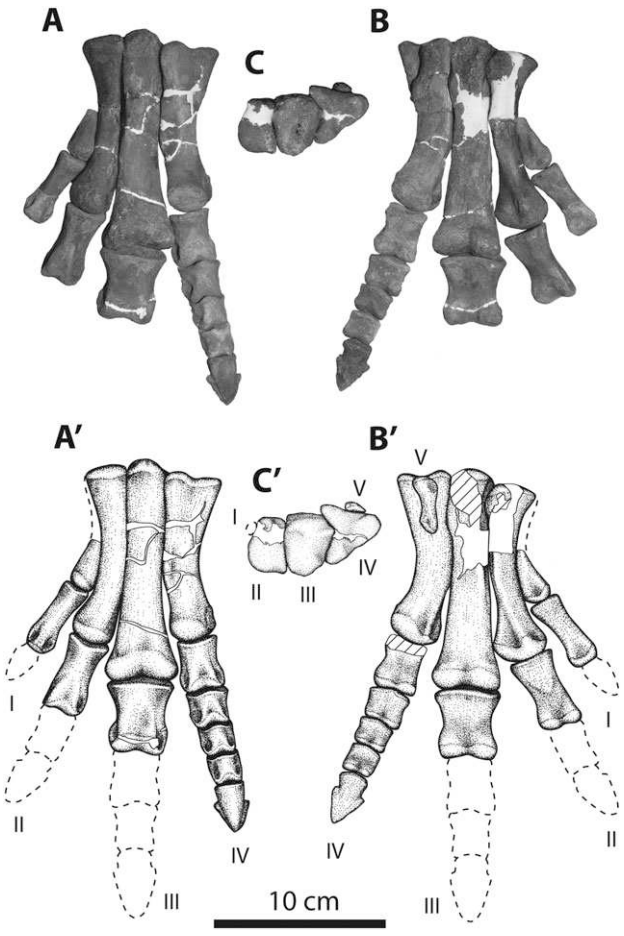

Figure 22. Left pes of the holotype of ***Thescelosaurus assiniboiensis* sp. nov.**, RSM P 1225.1, in dorsal (A), plantar (B), and proximal (C) views. Dashed lines indicate the extrapolated margins of the pes. See list in text for an explanation of anatomical abbreviations. Hatched areas represent incomplete bone surface. White areas represent plaster reconstruction. Roman numerals denote digit number.

bearing metatarsals (II, III, and IV), with metatarsal III being the most robust. Metatarsal I is reduced and metatarsal V is vestigial.

As in *T. neglectus* (USNM 7757), metatarsal I is reduced in size relative to metatarsals II, III, and IV, being approximately half the length of metatarsal III and two-thirds that of metatarsals II and IV. It is thin and slightly oblong in cross section, and is taller plantodorsally than it is transversly wide. There is no evidence of a proximal expansion (although the proximal extremity is not preserved on either side). The element increases in girth distally and its distal end is greatly expanded and bulbous, bearing a convex articular surface, concave ventral and lateral surfaces, and a convex medial surface that is continuous with the dorsal surface.

Metatarsal II is a medially curving and mediolaterally compressed element, slightly longer than metatarsal IV (Fig. 22). The proximal articular surface is simple, higher than wide, and convex, with a flat lateral and rounded medial face (Fig. 22C). The shaft is D-shaped in cross section, with its rounded medial surface sharply contrasting with the flat lateral surface that articulates with metatarsal III for two-thirds of its length. Ridges dorsolaterally and ventrolaterally, at approximately the midpoint of the shaft, demarcate the flat lateral surface and its articulation with metatarsal III. The distal surface is expanded and convex distally. Collateral pits mark the sides and a distinct concave surface lies ventrally.

Metatarsal III is robust, and flares proximally and distally (Fig. 22). The proximal articular surface is oblong, taller than wide, and convex (Fig. 22C). The proximal aspect of the lateral surface exhibits two adjacent triangular articular facets where it abuts metatarsal IV. These are wide proximally, occupy slightly less than the height of the metatarsal, and taper distally until they disappear at about the midpoint of the shaft. Using the horizontal plane as a reference point, the more dorsal of these facets faces dorsolaterally at an angle of approximately 45°, and the ventral one faces ventrolaterally at an angle of approximately 45°. Together they produce a 90° apex projecting laterally that fits snugly into a corresponding proximal medial trough in metatarsal IV. Metatarsals III and IV are closely apposed for the proximal half of the length of metatarsal III (Fig. 22). In contrast to the lateral surface, the medial articular surface of metatarsal III is flat and vertical, corresponding to a flat articular surface on the lateral side of metatarsal II to which it is closely appressed for about two-thirds of its length. A longitudinal ridge traverses the ventromedial edge of this contact, but the remaining shaft is simple, ovoid, and wider than tall. The distal end of metatarsal III flares both transversely and dorsoventrally to form two condyles separated by a shallow intercondylar groove, forming a ginglymous, spool-shaped articular surface. The medial condyle is slightly larger than the lateral condyle, and the entire articular surface is wider than high. A shallow fossa is present on the lateral and medial sides of the condyles, with the lateral one being deeper and more prominent.

Metatarsal IV is shorter and more robust than metatarsal II, but is similarly expanded (Fig. 22). Its roughly triangular proximal articular surface is slightly concave, with a faint trough extending dorsoventrally through its middle (Fig. 22). The proximal aspect of the medial surface is invaginated, forming a right-angled embayment into which the lateral surface of metatarsal III fits. This right-angled groove extends one-third of the way along the medial side of

the shaft. Ventrally the shaft is flat, with the surface trending medially towards its distal end (Fig. 22B). Dorsally the shaft is flat proximally, but becomes convex at mid-shaft (Fig. 22A). The distal end is expanded dorsoventrally, with a convex ball-like distal surface, collateral pits, and slightly convex dorsal and ventral surfaces.

As in other specimens of *Thescelosaurus* (e.g. USNM 7757), metatarsal V is markedly reduced and is represented by a small splint of bone about half the length of metatarsal I (Fig. 22B, C). It is dorsoventrally depressed, and its proximal and distal ends are expanded transversely. No evidence of phalanges is present on this digit, as is the case for all other specimens of *Thescelosaurus*.

Phalanges: The pedal phalangeal formula for *Thescelosaurus* and its relatives is 2-3-4-5-0, and although not fully preserved, RSM P 1225.1 presents no evidence that it differs from this pattern (Fig. 22). The phalanges are more gracile, but otherwise do not differ significantly from those of *T. neglectus* (USNM 7757), but are described here because the description of these elements for *T. neglectus* (USNM 7757) is not highly detailed. Elements of both the left and right sides are preserved: the left is more complete and is described (Fig. 22).

Only the first phalanx of digits I, II, and III are preserved. I-1 is elongate and slightly wider transversely than tall (Fig. 22). The proximal articular surface is triangular and slightly concave, with the apex directed dorsally. The shaft is subtriangular in cross section, with a slightly expanded distal end bearing distinct collateral pits. II-1 is similar in length and morphology to I-1, but is twice as robust. Proximally the concave cotyle is taller than its transverse width, and is D-shaped in cross section, with a flat ventral surface and an arched dorsal surface. Distally the element is expanded transversely into two condyles that are higher than wide. They exhibit distinct collateral pits and spool-like articular surfaces. III-1 is similar in length and morphology to I-1, but is twice as robust. Proximally the concave cotyle is taller than its transverse width, and is D-shaped in cross section, with a flat ventral surface and an arched dorsal surface. Distally the element is expanded transversely into two condyles that are higher than wide. They exhibit distinct collateral pits and spool-like articular surfaces.

The complete phalangeal series for digit IV, consisting of four non-terminal phalanges and one ungual, is preserved (Fig. 22). All phalanges are triangular in cross section proximally, with the apex positioned dorsally, and bear distinct collateral pits distally (Fig. 22A). The first phalanx differs from the others in having one concavity on the proximal articular surface, and in being longer than wide, and slightly taller than wide. The remaining three non-terminal phalanges possess two concave articular facets proximally divided by a vertical keel, are equal in length and width, and are slightly less than equal in height. Proximally the midline keel results in posterior projections of the dorsal and ventral edges of the articular surface. The ungual compares closely to that described for *Thescelosaurus* (USNM 7757). It is arrowhead shaped in dorsal view, is dorsoventrally flattened, and is twice as wide as it is tall. Proximally it is slightly convex and D-shaped, with the ventral surface being flat. Further distally the ventral surface is flat and dorsally it is gently convex. The lateral edges are sharp but irregular. Extending along the dorsolateral surface are two distinct and deep grooves that do not meet up at the anterior extremity, which is pointed and not rounded.

Systematic analysis

Given the distinct morphology of *T. assiniboiensis* sp. nov., and the convoluted phylogenetic history of the taxon *Thescelosaurus*, a cladistic analysis was conducted in order to resolve the position of *T. assiniboiensis* sp. nov. relative to other species of *Thescelosaurus*, and understand the effect this new species may have on the hypothesized phylogenetic position of the genus *Thescleosaurus*.

Cladistic methodology

The data set used in this analysis was originally developed by Scheetz (1999), and subsequently modified by Varricchio *et al*. (2007) and Boyd *et al*. (2009). We further modified the data set by adding one new out-group (*Herrerasaurus*), removing eight phylogenetically uninformative characters (characters 83, 125–127, 129, and 131–133; Boyd *et al*. 2009), splitting four characters (characters 96, 102, 104, and 110; Boyd *et al*. 2009) into nine characters (characters 95–97, 103–104, 106–107, and 113–114; Appendix 1), adding an additional character state to three characters (characters 13, 41, and 60; Appendix 1), adding three new characters (characters 138–140; Appendix 1), and incorporating additional character observations for some taxa. Additionally, five specimen-level terminal taxa referred to *Thescelosaurus* sp. by Boyd *et al*. (2009) were removed (CMN 8537, LACM 33543, MOR 979, NCSM 15728, and SDSM 7210), leaving only the type series of *T. neglectus* (USNM 7757 and 7758) and the holotypes of *T. garbanii* (LACM 33542) and *T. assiniboiensis* sp. nov. (RSM P 1225.1). The resulting data set contains 140 characters for 23 terminal taxa (Appendix 2). The analysis was conducted using the implicit enumera-

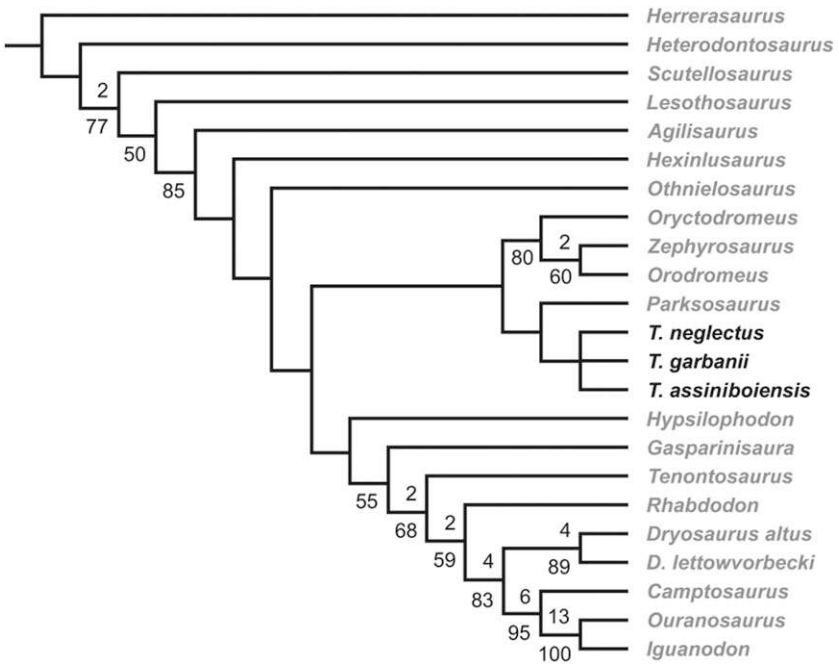

Figure 23. The single most-parsimonious tree (tree length 361 steps) recovered from the cladistic analysis using the implicit enumeration search option in TNT. Bootstap values (1000 replicates) above 50% are reported below the branches, and Bremer support values greater than 1 are reported above.

tion search option in the TNT 1.1 (Goloboff, Farris & Nixon, 2008). All characters were run unordered, and the tree was rooted using the terminal taxon *Herrerasaurus*. Branches were collapsed if their minimum length equalled zero. Bootstrap (1000 replicates) data and Bremer support value data were obtained using PAUP* 4.0b10 (Swofford, 2002), with the same settings as the primary analysis.

Cladistic results

Analysis of this data set resulted in the recovery of a single most-parsimonious tree of 361 steps (Fig. 23). The structure of the tree topology agrees closely with that of Boyd *et al*. (2009), except that *Heterodontosaurus* is recovered as the most basal ornithischian taxon included in this analysis, which is consistent with the results of other recent analyses (Butler *et al*., 2008; Butler *et al*., 2010). All three species of *Thescelosaurus* form a monophyletic group, but the interrelationships of these taxa remain uncertain, largely as a consequence of the fragmentary nature of the holotype of *T. garbanii*, which impedes character optimization within this clade (Fig. 23). However, all three taxa are considered valid based on the presence of distinct apomorphic traits in each (see Boyd *et al*. 2009; and discussion below). As was the case for Boyd *et al*. (2009), *Thescelosaurus* is recovered as the sister taxon of *Parksosaurus*, and these two taxa form a clade to the exclusion of a clade of smaller, earlier Cretaceous basal ornithopods composed of *Orodromeus*, *Oryctodromeus*, and *Zephyrosaurus*.

Autapomorphies of *Thescelosaurus assiniboiensis* sp. nov.

Several cranial autapomorphies of *T. assiniboiensis* sp. nov. are recognized. The supraoccipital exhibits a prominent median foramen posteriorly, coursing from the dorsal surface of the region roofing the mylencephalon to the dorsal surface of the supraoccipital (Fig. 11F). The external opening of this foramen is located in a shallow fossa (Fig. 11B, F). This foramen was noted and illustrated by Galton (1997: labelled as 'f_4' in fig. 4 and pl. II). In the absence of more extensive material, Galton (1997) was only able to contrast this condition with that found in LACM 33543, hindering the recognition of its taxonomic significance. Butler *et al*. (2008) suggested this foramen may be autapomorphic for *Thescelosaurus*. Further analysis and comparison has revealed the complete absence of this foramen in all other specimens of *Thescelosaurus* (CMN 8537, LACM 33543, NCSM 15728). Additionally, it is absent from all other ornithischians. Because it is not present in any extant animals, and is not expressed in other known species, hypotheses regarding the functional role of this feature are problematic. It is unlikely that it transmitted nerves. The

pattern of cranial nerves in amniotes is highly conserved and consists of paired structures as opposed to single median structures (de Beer, 1937; Hopson, 1979). Superficially, this foramen resembles the pineal foramen in size and its median dorsal position, but its location within the supraoccipital rather than the parietal, and its posterior placement, dorsal to the location of the myelencephalon rather than the diencephalon, precludes this assignment. A more likely hypothesis is that it conducted circulatory vessels.

In addition to the morphology of the supraoccipital, the squamosal of *T. assiniboiensis* sp. nov. is distinct from that of *T. neglectus*, all other specimens of *Thescelosaurus*, and from that of other ornithischian taxa. The postorbital process of the squamosal is relatively longer and narrower than that of the paratype of *T. neglectus* (NMNH 7758; Boyd *et al*., 2009), and all other skeletons referable to *Thescelosaurus*, and the dorsal surface of the postorbital–squamosal suture exhibits several anteroposterior ridges and grooves (Fig. 6A). Additionally, in both dorsal (Fig. 6A) and lateral (Fig. 6D) views, the posterior margin of the squamosal is convex and rounded. This is distinct from the condition seen in the paratype of *T. neglectus* (USNM 7758; Boyd *et al*., 2009:Fig. 5), all other specimens of *Thescelosaurus* (Boyd *et al*., 2009), and the basal ornithopods *Hypsilophodon* and *Orodromeus*. In contrast, these taxa exhibit a concave posterior surface of the squamosal in dorsal view, and a concave and angular surface in lateral view. The convex posterior margin of the squamosal is preserved on both the left and right sides of the holotype of *T. assiniboiensis* sp. nov., and is clearly distinct from that of other taxa.

It is uncertain as to whether the anteroposterior ridges on the dorsal surface of the postorbital suture represent an autapomorphic condition. They are distinct and clear on the left suture, but are missing from the right, and the suture is more sunken by comparison. This suggests that there may be asymmetry in the distribution of these ridges and grooves. An alternative interpretation of this morphology is that the ridges and grooves seen on the left suture are actually not representative of the sutural contact, as suggested by Galton (1995), but rather represent a thin veneer of the postorbital, which is closely apposed to, and indistinguishable from, the squamosal. To address this ambiguity, further specimens are needed.

This investigation has also revealed the first recognizeable postcranial autapomorphies of *Thescelosaurus*. The anterior dorsal ribs possess several morphological features not seen in other basal ornithopods. Proximally, the neck of each rib is highly curved, whereas the remaining shaft is relatively straight (Fig. 16A, B). In the straighter distal region the shafts are laterally compressed, and most present a concave surface laterally (Fig. 16D). The posterior margins of the distal half of the shafts are characterized by the presence of a distinct rugose texture and a flat surface, contrasting with the anterior or leading edge, which is thinner and smooth (Figs 16B, E and 17). These rugose posterior margins roughly correlate with the point of juncture with the mineralized intercostal plates described for *Thescelosaurus* and other basal ornithopods (Boyd *et al*., 2008; Butler & Galton, 2008). These plates lie in close proximity to, but do not fuse with, the posterior surface of the ribs (Boyd *et al*., 2008).

The truncation of the brevis shelf anterior to the posterior end of the ilium may also be diagnostic for *T. assiniboiensis* sp. nov. Both left and right ilia show a brevis shelf much thicker than that of the holotype of *T. neglectus* (USNM 7757), and which is truncated anterior to the posterior margin of the ilium (Fig. 18). Because of the poor preservation of the brevis shelf in RSM P 1225.1, it is unclear whether this morphology represents a unique condition of *T. assiniboiensis* sp. nov. Additional specimens are needed to permit this question to be answered.

Plesiomorphies of *Thescelosaurus assiniboiensis* sp. nov.

Thescelosaurus assiniboiensis sp. nov. exhibits some postcranial features that are more similar to those of *Parksosaurus* and *Orodromeus* than to those *T. neglectus*. The blade of the ilium of *T. assiniboiensis* sp. nov. is highest directly dorsal to the acetabulum, and gradually decreases in height posteriorly until it reaches the low and rounded posterior margin (Fig. 18A). This is in sharp contrast to the morphology of the ilium of the holotype of *T. neglectus* (USNM 7757), and all other known *Thescelosaurus* specimens (AMNH 5031, AMNH 117, AMNH 5889, CMN 8537, NCSM 15728, MOR 979, MOR 1185), in which the dorsal margin of the ilium is relatively horizontal until it projects dorsally as it approaches the posterior margin. The morphology exhibited by *T. assiniboiensis* sp. nov. is very similar to that seen in *Parksosaurus* (ROM 804) and *Orodromeus* (MOR 294, MOR 623), with sloping dorsal margins and a rounded posterior extremity, and therefore is likely to represent the plesiomorphic condition for the larger clade containing these taxa.

In addition to the iliac blade, the brevis shelf projects medially in RSM P 1225.1, lying almost in the frontal plane (Fig. 18B), with only a minor ventrally dipping component. Again, this is more similar to the condition seen in both *Parksosaurus* (ROM 804) and *Orodromeus* (MOR 294, MOR 623), and is distinct from the condition in other *Thescelosaurus* speci-

mens (CMN 8537, NCSM 15728, USNM 7757), which have a significant ventrally sloping aspect to the medially projecting brevis shelf.

DISCUSSION

PALAEOBIOLOGY AND SYSTEMATICS OF *THESCELOSAURUS ASSINIBOIENSIS* SP. NOV.

Thescelosaurus assiniboiensis sp. nov. represents the smallest ornithischian dinosaur recovered from the Frenchman Formation of Saskatchewan, and may represent the smallest ornithischian from the late Maastrichtian of North America. This time interval is generally characterized by large dinosaurs, in many cases, the largest to evolve within their respective lineages, such as *Tyrannosaurus rex* and *Triceratops horridus*. Although *T. neglectus* represents a noted size increase from the putative sister taxon of *Thescelosaurus*, *Parksosaurus warreni*, the holotype of *T. assiniboiensis* sp. nov. is of equal size to the holotype and only known specimen of *Parksosaurus* (ROM 804). This suggests that although many of the latest Maastrichtian dinosaur taxa show a potential size increase, the small herbivore niche probably remained occupied.

In RSM P 1225.1 the neurocentral sutures of the anterior dorsals are not fused, leaving their neural arches dissociated from their respective centra. The posterior dorsals, although articulated, retain visible sutural lines throughout the series, whereas the neurocentral sutures are firmly fused in the sacral and caudal vertebrae, with suture lines being obliterated. The lack of fusion of the neurocentral sutures is a common occurrence in *Thescelosaurus*, regardless of the absolute size of the animal (MOR 1106, 1164, 1165, NCSM 15728, and SDSM 7210). The closure of neurocentral sutures serves as a conserved size-independent indicator of ontogeny in extant crocodilians, and has been suggested to have developed similarly in extinct crocodilian relatives (Brochu, 1996). Irmis (2007), however, found that this trend was not uniformly expressed across phytosaur ontogeny, and suggested that its consistency should not be assumed for extinct archosaurs. Although as yet inadequately documented, the retention of open neurocentral sutures occurs more broadly than solely in *Thescelosaurus*, and is common in many basal ornithopod specimens, presumed to be at, or near, adult size [*Camptosaurus* (USNM 4697), *Dryosaurus* (CM 21786), *Hypsilophodon* (NHMUK R 196), *Orodromeus* (MOR 623), *Zephyrosaurus* (MCZ 4392)], as well as in several undescribed North American basal ornithopod taxa (C.M. Brown, pers. observ.). Two hypotheses can be erected to explain this occurrence: firstly, sutural closure is ontogenetically conserved, as it is in extant crocodilians, and the sample of basal ornithopod specimens is disproportionately represented by juvenile material; secondly, and alternatively, neurocentral sutural fusion in many basal ornithopod taxa is either not tightly correlated with ontogeny or is ontogenetically postdisplaced, and sutures may remain open for the majority of the life of the animal. A more extensive investigation of this phenomenon and testing of these hypotheses, in conjunction with the exploration of other aspects of the ontogeny of *Thescelosaurus*, is currently underway.

All autapomorphies of *T. assiniboiensis* sp. nov., as well as two synapomorphies (posterior half of ventral edge of jugal offset ventrally and covered laterally with obliquely inclined ridges, and frontals wider midorbitally than across posterior margin) and two potential synapomorphies (presence of a Y-shaped indentation on the dorsal edge of opisthotics and palpebral dorsoventrally flattened and rugose along the medial and distal edges) of *Thescelosaurus*, are preserved in the cranial skeleton of the holotype (RSM P 1225.1). The postcranial skeleton of this specimen, however, preserves many of the features that are more similar to those of *Parksosaurus* and *Orodromeus* than to the other species of *Thescelosaurus*, specifically in the ilium and femur. These are interpreted here as plesiomorphies. The regional segregation of character occurrence (the cranial skeleton preserving derived characters, and the postcranial skeleton preserving putatively ancestral characters) suggests that cranial synapomorphies of *Thescelosaurus* initially differentiated this genus from *Parksosaurus*, and that many characters associated with the postcranial skeleton were acquired within *Thescelosaurus*, and may have arisen in association with increased body size.

As was found by Boyd *et al*. (2009), our cladistic analysis recovered a clade composed exclusively of basal ornithopods from the Cretaceous of North America (Fig. 23). It is subdivided into an earlier Cretaceous small-bodied clade (*Orodromeus*, *Oryctodromeus*, and *Zephyrosaurus*), and a larger-bodied later Cretaceous clade (*Thescelosaurus* and *Parksosaurus*). This topology greatly reduces the ghost lineages for many of these taxa (most notably *Thescelosaurus*) that were implied in previous phylogenetic hypotheses (Sereno, 1986; Weishampel & Heinrich, 1992). Additionally, the monophyly of the Cretaceous North American taxa suggests that they may represent an exclusively North American radiation of basal ornithopods during the Cretaceous, a pattern not previously recognized. Further work incorporating newly discovered taxa and examining taxa that fall outside of this clade can be used to test this hypothesis, and may reveal this radiation to

encompass more taxa, and to be more widespread than is currently understood.

THESCELOSAURUS IN THE FRENCHMAN FORMATION

The occurrence of a new species of *Thescelosaurus* from the Frenchman Formation necessitates a review of other material referred to *Thescelosaurus* from the formation. Three other specimens of *Thescelosaurus*, exhibiting a large size range, have been retrieved from this unit. Unfortunately, none of these preserves cranial material and therefore cannot be identified at the specific level. The large articulated specimen RSM P 2415.1 does, however, preserve both ilia. They exhibit the distinctive dorsal kink at the posterior margin common to *T. neglectus* (USNM 7757) and other specimens of *Thescelosaurus* (MOR 979, NCSM 15728). This character may prove to be diagnostic for *T. neglectus*. If this is the case, it indicates the presence of both *T. neglectus* and *T. assiniboiensis* sp. nov. in the Frenchman Formation, and suggests spatial and temporal overlap of these two taxa. The discovery of additional diagnostic material referable to *Thescelosaurus*, as well as an increased understanding of the stratigraphy of the Frenchman Formation, are required to explore these questions further.

The discovery of a multitaxa bone bed within the Frenchman Formation (the 'convenience store' locality) has yielded isolated limb elements from several individuals of *Thescelosaurus*, all of very small size. All limb elements preserved are smaller than their respective elements in RSM P 1225.1, which is the smallest known associated, reasonably complete skeleton of *Thescelosaurus*. The simplest interpretation is that this site preserves a rich sample of juvenile specimens of *Thescelosaurus*. All material of *Thescelosaurus* recovered from the Frenchman Formation, with the exception of RSM P 2415.1, is smaller than the smallest specimens recovered from the Hell Creek, Lance, and Scollard formations (RSM P 1225.1 and CMN 22039). This suggests a general trend towards the preservation of ontogenetically young individuals of *Thescelosaurus* in the Frenchman Formation, a pattern repeated for *Tyrannosaurus*, for which large volume of juvenile and subadult material has been collected and reported (RSM P 2347.1, partial fragmentary juvenile skeleton; 2693.1, juvenile metatarsal; 2990.1, subadult lacrimal; 2416.82, juvenile metatarsal), and for *Triceratops* (RSM P 2299.1, subadult supraorbital horncore; 2613.1, subadult supraorbital horncore; 2982.1, juvenile skull) (Tokaryk, 1997b; Snively & Longrich, 2009). Given the sample size of the collected material from the Frenchman Formation, the volume of juvenile material is proportionally much larger than that retrieved from the Hell Creek, Lance, and Scollard formations. At present, however, it remains uncertain whether this represents a biological signal, or is the result of preservational biases based on associations of lithology and ontogeny (Goodwin & Horner, 2010).

ABUNDANCE OF BASAL ORNITHOPODS DURING THE LATE MAASTRICHTIAN IN NORTH AMERICA

It is evident that direct interpretation of faunal assemblages from historically collected specimens, rather than systematic surveys, are biased, and are potentially misleading. It has been shown that the nature of taphonomic accumulations is often a function of the depositional environment (Bown & Kraus, 1981; Behrensmeyer, 1982, 1988; Retallack, 1984, 1988; Badgley, 1986; Koster, 1987; Smith, 1993; White, Fastovsky & Sheehan, 1998). Additionally, White *et al*. (1998) illustrate the relationship between vertebrate faunal elements and the fluvial architectural elements that deposited them. As well as the potential bias introduced by differences in the preservational environments represented by the Frenchman Formation, and contemporaneous formations, differences in historical sampling intensity between the Frenchman Formation and more thoroughly studied formations (e.g. Hell Creek and Lance formations) may induce an additional source of bias into faunal comparisons (Vavrek & Larsson, 2010; Butler *et al*., 2011a). For these reasons, conclusions regarding the relative abundance of *Thescelosaurus* within the Frenchman Formation are considered preliminary; however, the patterns observed to date are provocative enough to warrant further discussion.

Thescelosaurus, although not rare, is not a dominant member of more southern Hell Creek beds. White *et al*. (1998), in their study of dinosaur diversity in the Hell Creek Formation, reported that fossils of 'hypsilophodontids' (of which *Thescelosaurus* is the only member known from the late Maastrichtian of North America) ranked fifth in total abundance among the dinosaurian taxa surveyed, comprising about 3% of the dinosaur fauna based on *in situ* articulated, associated, and isolated elements. This fauna is mostly dominated by neoceratopsians and tyrannosaurids, as well as hadrosaurids and ornithomimids, all of these being more common than *Thescelosaurus* (White *et al*., 1998). Lehman (1987) suggested a relative abundance of around 2% for pooled samples of hypsilophodontids and pachycephalosaurs in the '*Triceratops* fauna' of the combined Lance, Hell Creek and Frenchman formations, and the data set of Lyson & Longrich (2011) suggests *Thescelosaurus* represents 5% of all articulated dinosaur skeletons in the Hell Creek Formation.

The relative abundance of *Thescelosaurus*, based on the current study, in the Frenchman Formation of Saskatchewan does not reflect this pattern, and instead, *Thescelosaurus* represents one of the most abundant, if not the most abundant, dinosaurian taxon. Four skeletons of *Thescelosaurus* have been found (CMN 22039; RSM P 1225.1, 2415.1 and 3123.1), compared with two ceratopsid skeletons (EM 16.1 and RSM P 1163) and several partial skulls, two hadrosaur skeletons (CMN 9509 and RSM P 2610.1), and a single tyrannosaur skeleton (RSM P 2523.8) (Tokaryk, 1997a, b, 2009). No articulated or associated specimens of pachycephalosaurs or ankylosaurs are known. If this, albeit small, sample size is at all representative of the true fauna, then *Thescelosaurus* is a much more abundant taxon in the Frenchman fauna [~31%, based on the data set of Lyson and Longrich (2011) with CMN 22039 and RSM P 3123.1 added to it] than it is in generally time-equivalent faunas, either further inland (Scollard Formation) or further south (Hell Creek Formation). Material collected from the 'convenience store' locality further supports this pattern. Here, *Thescelosaurus* makes up 42% of the preserved tetrapod elements (14/38), and is the only ornithischian represented. The remainder of the assemblage consists of turtles (~24%), theropods (~21%), crocodilians (~8%), and champsosaurs (~5%). Although we do not suggest that the 'convenience store' locality is absolutely representative of the true faunal composition of the Frenchman Formation, it is noteworthy that similar types of localities from time-equivalent faunas do not recover this pattern, reinforcing the observation of the increased abundance of *Thescelosaurus* within the Frenchman Formation. These observed differences in faunal composition between the Frenchman Formation and contemporaneous formations might be evidence for either latitudinal (relative to Hell Creek) or coastal (relative to Scollard) faunal provinciality during the latest Maastrichtian. However, much more work is needed to clarify our understanding of late Maastrichtian faunal provinciality, and the effect of different sampling and lithological biases between formations (Barrett, McGowan & Page, 2009; Vavrek & Larsson, 2010; Butler *et al*., 2011a; Lyson & Longrich, 2011).

Interestingly, a possible parallel may exist between basal ornithopods in North America, specifically the Frenchman Formation, and rhabdodontids from Europe. Deposits representing the Late Cretaceous of Southern France have revealed localities in which the euornithopod *Rhabdodon* is the most common dinosaurian taxon (Pincemaill, Bufferaut & Quillevere, 2006), and *Zalmoxes* is common in both multispecies bone beds and microvertebrate sites in late Maastrichtian deposits in Romania (Weishampel *et al*., 2003).

Late Maastrichtian ornithischian diversity

Several investigations into dinosaur diversity have suggested a marked decrease in the diversity of non-avian dinosaurs from the Campanian to the Maastrichtian, preceding their end-Cretaceous mass extinction by 7–10 million years (Clemens, Archibald & Hickey, 1981; Sloan *et al*., 1986; Dodson & Tatarinov, 1990; Archibald, 1992; Clemens, 1992; Sullivan, 2006; Barrett *et al*., 2009). This is by no means universally accepted, and other studies indicate stable patterns of diversity through the Maastrichtian (Russell, 1984; Dodson, 1990; Fastovsky *et al*., 2004). Another suggestion is that the observed diversity decrease may be an artefact of the fossil record (Wang & Dodson, 2006; Butler *et al*., 2011a). The issue of a perceived or real diversity decrease in the Maastrichtian is still debated, and is likely to remain contentious for some time. What is certain, however, is that in terms of collected material there is a drop in the generic and specific diversity of dinosaurs, most significantly ornithischians, through the Maastrichtian (Clemens, 1992; Sullivan, 2006).

In contrast, the recognition of a new species of *Thescelosaurus* from late Maastrichtian deposits of North America increases the total number of known species to three: *T. neglectus*, *T. garbanii*, and *T. assiniboiensis* sp. nov. *Parksosaurus*, the putative sister taxon of *Thescelosaurus* (Boyd *et al*., 2009), is the only basal ornithopod known from early Maastrichtian deposits (Horseshoe Canyon Formation of Alberta: Parks, 1926) (Fig. 24). This increase in basal ornithopod diversity during the latest Maastrichtian runs counter to the trend seen in most other ornithischians from the Campanian to the late Maastrichtian in North America (Scannella & Horner, 2010). Parallels are again evident in the apparent absence of a diversity decline in basal ornithopods in the Maastrichtian of Europe (Fig. 24). Although less robustly documented than the North American trends, the basal ornithopods, such as *Zalmoxes* and *Rhabdodon*, are common, geographically widespread, and exhibit a stable diversity through this time period, whereas other ornithischian taxa show a putative decrease (Weishampel *et al*., 2003; Sullivan, 2006). The basal ornithopods *Rhabdodon priscus* Matheron, 1869 and *Rhabdodon septimanicus* Buffetaut and Le Loeuff, 1991 are known from the Campanian and early Maastrichtian of southern France, northern Spain, and Austria (Buffetaut & Le Loeuff, 1991; Garcia *et al*., 1999), and *Zalmoxes robustus* (Nopcsa 1900) and *Zalmoxes shqiperorum* Weishampel, Jianu, Cziki & Norman, 2003 from the late Maastrichtian of

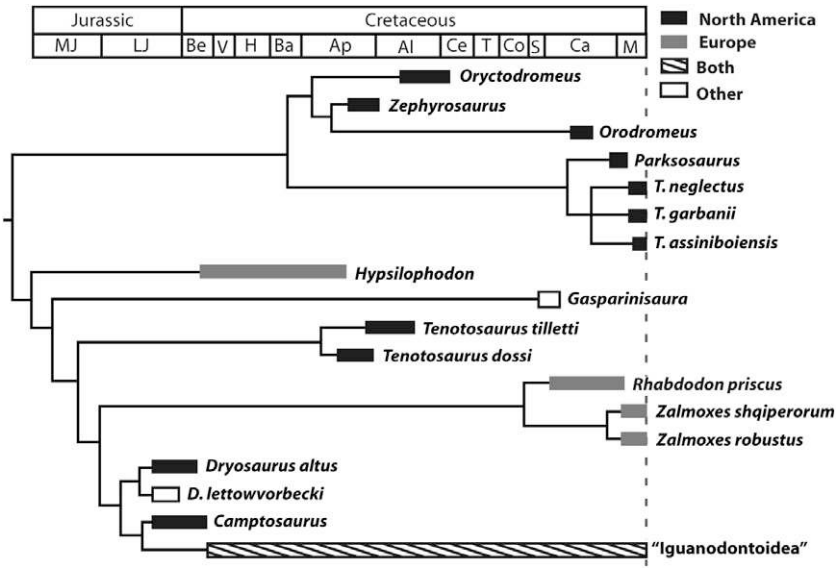

Figure 24. Time-correlated phylogeny for basal ornithopod taxa illustrating relative abundance through time. Note the Maastrichtian radiation of *Thescelosaurus* in North America and *Zalmoxes* in Europe. The iguanodontian radiation is represented as a single line because of size constraints. Al, Albian; Ap, Aptian; Ba, Barremian; Be, Berriasian; Ca, Campanian; Ce, Cenomanian; Co, Coniacian; H, Hauterivian; LJ, Late Jurassic; M, Maastrichtian; MJ, Middle Jurassic; S, Santonian; T, Turonian; V, Valanginian. Modified from Weishampel *et al*., 2003.

Romania (Weishampel *et al*., 2003; Codrea & Godefroit, 2008) and possibly the Campanian of Austria (Sachs & Hornung, 2006). Such examples suggest that although overall global ornithischian diversity appears to decrease during the Maastrichtian, prior to the end-Cretaceous mass extinction, the diversity of taxa systematically basal to the dominant ornithopod herbivorous fauna of the Campanian appears to increase in both North America and Europe. Many studies have attempted to address the overall patterns of Late Cretaceous faunal diversity, sometimes on a global scale, and often in terms of factors such as body size and aquatic versus terrestrial habitats (Clemens *et al*., 1981; Archibald & Macleod, 2007). Few studies, however, have endeavoured to understand differences in diversity patterns between dinosaur clades at varying taxonomic levels, an avenue of research that deserves more detailed consideration in future investigations.

CONCLUSION

Thescelosaurus assiniboiensis sp. nov. is assigned to the taxon *Thescelosaurus* based on three synapomorphies: posterior half of ventral edge of jugal offset ventrally and covered laterally with obliquely inclined ridges; frontals wider midorbitally than across posterior margin; and distal portions of anterior dorsal rib shafts highly laterally compressed, with concave lateral and rugose posterior surfaces. It is diagnosed by two autapomorphies: a supraoccipital with a prominent medial foramen located posterodorsally, and a squamosal with convex posterior and dorsal borders. The type specimen also exhibits features that appear to be plesiomorphic, including the position of the fourth trochanter of the femur and the shape of the ilium. The recovery of an exclusively Cretaceous North American clade of basal ornithopod taxa suggests that these taxa may represent a previously overlooked North American radiation.

Examination of all *Thescelosaurus* material retrieved from the Frenchman Formation to date suggests that it is representative of small, presumably juvenile, individuals. Preliminary data for *Tyrannosaurus* and *Triceratops* also indicate an abnormally large proportion of putatively juvenile individuals. This fauna is seemingly rich in juveniles when compared with the Hell Creek and Lance formations. In addition, the faunal assemblage from the Frenchman Formation suggests that *Thescelosaurus* is one of the most common dinosaurian taxa present.

The identification of a third species of *Thescelosaurus* from the late Maastrichtian of North America indicates that this taxon was more diverse than previously recognized. Basal ornithopods show an increase in diversity from the Campanian through the late Maastrichtian, in contrast to the trend displayed by most other ornithischian clades. Further research into the diversity and abundance of *Thescelosaurus* during the Maastrichtian, combined with more

detailed investigations into the diet and lifestyle of this taxon, may reveal the causal factors associated with this apparent rich diversity and abundance.

ACKNOWLEDGEMENTS

We thank the following people for many discussions and contributions to this project: D. Evans, M. Ryan, J. Theodor, D. Brinkman, P. Galton, J. Anderson, E. Snively, T. Tokaryk, H. Bryant, W. Long, K. Brink, L. O'Brien, D. Weishampel, R. Sissons, D. Larson, N. Campione, P. Currie, N. Longrich, R. Scheetz, W. Sloboda, P. Wise, H. Jamniczky, D. Henderson, D. Tanke, R. Furr, M. Vickaryous, C. Meister, D. Fraser, H. Knoll, and members of the University of Calgary Vertebrate Morphology and Palaeontology Research Group (RATZ labs). H.-D. Sues and an unnamed reviewer, as well as P. Hayward (editor), provided feedback and suggested revisions that greatly improved this article. V. Arbour, D. Bailey, H. and N. Brink, P. Currie, D. Evans, R. Hynes, E. Koppelhus, J. Northover, E. Ross, S. Sewlal, C. White, and D. Zariski provided temporary lodging during collections visits.

Access to specimens was facilitated by: C. Mehling (AMNH); M. Feuerstack, K. Shepherd, A. McDonald, and E. Ross (CMN); J. Horner and B. Baziak (MOR); V. Schneider and D. Russell (NCSM); P. Barrett, S. Chapman, and S. Maidment (NHMUK); D. Evans and K. Seymour (ROM); H. Bryant, T. Tokaryk, and W. Long (RSM); S. Shelton (SDSM); D. Winkler (SMU); and M. Brett-Surman and M. Carrano (USNM).

This research was supported by generous funding from: ACCESS Alberta; a Queen Elizabeth II Graduate Scholarship; an Alberta Graduate Student Scholarship from the Alberta Government; a University of Calgary Research Services Travel Grant; three University of Calgary Graduate Research Scholarships; two Dr Anthony Russell Distinguished Faculty Achievement Graduate Scholarships in Zoology; a Canadian Society of Zoologists Travel Grant; two Dinosaur Research Institute Student Project Grants; and two Dinosaur Research Institute Rene Vandervelde SVP Travel Grants to Caleb Brown; as well as an NSERC Discovery Grant to Anthony Russell.

REFERENCES

Archibald JD. 1992. Dinosaur extinction: how much and how fast? *Journal of Vertebrate Paleontology* **12:** 263–264.

Archibald JD, MacLeod N. 2007. *Dinosaurs, extinction theories for Encyclopedia of Biodiversity*. Amsterdam: Elsevier, 1–9.

Badgley C. 1986. Taphonomy of mammalian fossil remains from Siwalik rocks of Pakistan. *Paleobiology* **12:** 119–142.

Barrett PM, McGowan AJ, Page V. 2009. Dinosaur diversity and the rock record. *Proceeding of the Royal Society of London Series B* **276:** 2667–2674.

de Beer G. 1937. *The development of the vertebrate skull*. Oxford: Clarendon Press.

Behrensmeyer AK. 1982. Time resolution in fluvial vertebrate assemblages. *Paleobiology* **8:** 211–227.

Behrensmeyer AK. 1988. Vertebrate preservation in fluvial channels. *Palaeogeography, Palaeoclimatology, Palaeoecology* **63:** 183–199.

Bellairs AdA, Kamal AM. 1981. The chondrocranium and the development of the skull in recent reptiles. In: Gans C, ed. *Biology of the reptilia, volume 11: morphology F*. Toronto: Academic Press, 1–247.

Bown TM, Kraus MJ. 1981. Lower Eocene alluvial paleosols (Willwood Formation, northwest Wyoming, USA) and their significance for paleoecology, paleoclimatology, and basin analysis. *Palaeogeography, Palaeoclimatology, Palaeoecology* **34:** 1–30.

Boyd CA, Cleland TP, Novas FE. 2008. Histology, homology, and function of intercostals plates of ornithischian dinosaurs. *Journal of Vertebrate Paleonotology* **28** suppl.**:** 55A.

Boyd CA, Brown CM, Scheetz RD, Clarke JA. 2009. Taxonomic revision of the basal neornithischian taxa *Thescelosaurus* and *Bugenasaura*. *Journal of Vertebrate Paleontology* **29:** 758–770.

Braman DR, Sweet AR. 1999. Terrestrial palynomorph biostratigraphy of the Cypress Hills, Wood Mountain, and Turtle Mountain areas (Upper Cretaceous – Paleocene) of western Canada. *Canadian Journal of Earth Sciences* **36:** 725–741.

Brinkman DB. 2003. A review of nonmarine turtles for the late Cretaceous of Alberta. *Canadian Journal of Earth Science* **40:** 557–571.

Brochu CA. 1996. Closure of neurocentral sutures during crocodilian ontogeny: implications for maturity in fossil archosaurs. *Journal of Vertebrate Paleontology* **16:** 49–62.

Bryant HN, Russell AP. 1992. The role of phylogenetic analysis in the inference of upreserved attributes of extinct taxa. *Philosophical Transaction of the Royal Society of London, Series B* **337:** 405–418.

Bubien-Waluszewska A. 1981. The cranial nerves. In: King AS, McLelland J, eds. *Form and function in birds, volume 2*. Toronto: Academic Press, 385–438.

Buffetaut E, Le Loeuff J. 1991. Une nouvelle espece de *Rhabdodon* (Dinosauria, Ornithischia) du Crétacé supérieur de l'Hérault (Sud de France). *Comptes Rendus De l'Académie Des Sciences* **312:** 934–948.

Butler RJ. 2005. The 'fabrosaurid' ornithischian dinosaurs of the Upper Elliot Formation (Lower Jurassic) of South Africa and Lesotho. *Zoological Journal of the Linnaean Society* **145:** 175–218.

Butler RJ, Galton PM. 2008. The 'dermal armour' of the ornithopod dinosaur *Hypsilophodon* from the Wealden (Early Cretaceous: Barremian) of the Isle of Wight: a reappraisal. *Cretaceous Research* **29:** 636–642.

Butler RJ, Upchurch P, Norman DB. 2008. The phylogeny of the ornithischian dinosaurs. *Journal of Systematic Palaeontology* **6:** 1–40.

Butler RJ, Galton PM, Porro LA, Chiappe LM, Henderson D, Erickson GM. 2010. Lower limits of ornithischian dinosaur body size inferred from a new jurassic heterodontosaurid from North America. *Procedding of the Royal Society B* **277:** 375–381.

Butler RJ, Benson RBJ, Carrano M, Mannion PD, Upchurch P. 2011a. Sea level, dinosaur diversity and sampling biases: investigating the 'common cause' hypothesis in the terrestrial realm. *Proceeding of the Royal Society of* London *Series B* **278:** 1165–1170.

Butler RJ, Jin L, Chen J, Godefroit P. 2011b. The postcranial osteology and phylogenetic position of the small ornithischian dinosaur *Changchunsaurus parvus* from the Quantou Formation (Cretaceous: Aptian-Cenomanian) of Jilin Province, northeastern China. *Palaeontology* **54:** 667–683.

Clemens WA. 1992. Dinosaur diversity and extinction. *Science* **256:** 159.

Clemens WA, Archibald JD, Hickey LJ. 1981. Out with a whimper not a bang. *Paleobiology* **7:** 293–298.

Codrea VA, Godefroit P. 2008. New Late Cretaceous dinosaur findings from northwestern Transylvania (Romania). *Comptes Rendus Palevol* **7:** 289–295.

Cooper MR. 1985. A revision of the ornithischian dinosaur *Kangnasaurus coetzeei* Haughton, with a classification of the Ornithischia. *Annals of the South African Museum* **95:** 281–317.

Currie PJ. 1997. Braincase anatomy. In: Currie PJ, Padian K, eds. *Encyclopedia of dinosaurs*. Toronto: Academic Press, 81–84.

Currie PJ, Rigby JKJ, Sloan RE. 1990. Theropod teeth from the Judith River Formation of southern Alberta, Canada. In: Carpenter K, Currie PJ, eds. *Dinosaur systematics: approaches and perspectives*. Cambridge: Cambridge University Press, 107–125.

Dodson P. 1990. Counting dinosaurs: how many kinds were there? *Proceedings of the National Academy of Science* **87:** 7908–7612.

Dodson P, Tatarinov LP. 1990. Dinosaur paleobiology; Part III, Dinosaur extinction. In: Weishampel DB, Dodson P, Osmólska H, eds. *The dinosauria*. Los Angeles, CA: University of California Press, 55–62.

Eberth DA. 2004. Revising the Edmonton Group: a framework for assessing biostratigraphy and climate change. In Allen H, ed. *Alberta Palaeontological Society Eighth Annual Symposium*. Mount Royal College, Calgary, Alberta, 7–10.

Evans DC. 2005. New evidence on brain-endocranial cavity relationships in ornithischian dinosaurs. *Acta Palaeontologica Polonica* **50:** 617–622.

Fastovsky DE, Huang Y, Hsu J, Martin-MaNaughton J, Sheehan PM, Weishampel DB. 2004. Shape of Mesozoic dinosaur richness. *Geology* **32:** 877–880.

Fisher PE, Russell DA, Stoskopf MK, Barrick RE, Hammer M, Kuzmitz AA. 2000. Cardiovascular evidence for an intermediate to high metabolic rate in an ornithichian dinosaur. *Science* **288:** 503–505.

Fox RC. 1997. Late Cretaceous and Paleocene mammals, Cypress Hills Region, Saskatchewan, and mammalian evolution across the Cretaceous-Tertiary Boundary. In: McAnally LM, ed. *Canadian paleontology conference, field trip guidbook no. 6*. St. John's, NL: Geological Association of Canada, 70–85.

Galton PM. 1973. Redescription of the skull and mandible of *Parksosaurus* from the late Cretaceous with comments on the family Hypsilophodontidae (Ornithischia). *Life Science Contributions Royal Ontario Museum* **89:** 1–21.

Galton PM. 1974a. Notes on *Thescelosaurus*, a conservative ornithopod dinosaur from the Upper Cretaceous of North America, with comments on ornithopod classification. *Journal of Paleontology* **48:** 1048–1067.

Galton PM. 1974b. The Ornithischian Dinosaur *Hypsilophodon* from the Wealden of the Isle of Wight. *Bulletin of the British Museum (Natural History) Geology* **25:** 1–152.

Galton PM. 1981. *Dryosaurus*, a hypsilophodontid dinosaur from the Upper Jurassic of North America and Africa; postcranial skeleton. *Palaeontologische Zeitschrift* **55:** 271–312.

Galton PM. 1989. Crania and endocranial casts from ornithopod dinosaurs of the families Dryosauridae and Hypsilophodontidae (Reptilia; Ornithischia). *Geologica Et Palaeontologica* **23:** 217–239.

Galton PM. 1995. The species of the basal hypsilophodontid dinosaur *Thescelosaurus* Gilmore (Ornithischia: Ornithopoda) from the late Cretaceous of North America. *Neues Jahrbuch Für Geologie Und Paläontologie, Abhandlungen* **198:** 243–311.

Galton PM. 1997. Cranial anatomy of the basal hypsilophodontid dinosaur *Thescelosaurus neglectus* Gilmore (Ornithischia: Ornithopoda) from the Upper Cretaceous of North America. *Revue De Paléobiologie* **16:** 321–348.

Galton PM. 1999. Cranial anatomy of the hypsilophodontid dinosaur *Bugenasaura infernalis* (Ornithischia, Ornithopoda) from the Upper Cretaceous of North America. *Revue De Paléobiologie* **18:** 517–534.

Garcia G, Pincemaill M, Vianey-Liaud M, Marandat B, Lorenz E, Cheylan G, Cappetta H, Michaux J, Sudre J. 1999. Découverte du premier squelette presque complet de *Rhabdodon priscus* (Dinosauria, Ornithopoda) du Maastrichtien inférieur de Provence. *Comptes Rendus De l'Académie Des Sciences – Series IIA – Earth and Planetary Science* **328:** 415–421.

Gilbert MM, Tokaryk TT, Cuggy MB. 2010. New amiid material from the Frenchman Formation (Late Cretaceous) of Saskatchewan, Canada. *Canadian Palaeontological Conference*. Halifax, Nova Scotia. 15.

Gilmore CW. 1913. A new dinosaur from the Lance Formation of Wyoming. *Smithsonian Miscellaneous Collections* **61:** 1–5.

Gilmore CW. 1915. Osteology of *Thescelosaurus*, an orthopodous dinosaur from the Lance Formation of Wyoming. *Proceedings of the United States National Museum* **49:** 591–616.

Goloboff PA, Farris JS, Nixon K. 2008. TNT, a free program for phylogenetic analysis. *Cladistics* **24:** 774–786.

Goodwin MB, Horner JR. 2010. Historical collecting bias and the fossil record of *Triceratops* in Montana. In: Ryan M, Chinnery-Algeier BJ, Eberth DA, eds. *New perspectives on horned dinosaurs: the Royal Tyrrell Museum Ceratopsian Symposium*. Bloomington: Indiana University Press, 551–563.

Hamblin AP, Abrahamson BW. 1996. Stratigraphic architecture of 'Basal Belly River' cycles, Foremost Formation, Belly River Group, subsurface of southern Alberta and southwestern Saskatchewan. *Bulletin of Canadian Petroleum Geology* **44:** 654–673.

Hopson JA. 1979. Paleoneurology. In: Gans C, Northcutt RG, Ulinski P, eds. *Biology of the Replilia, Neurology A*. New York: Academic Press, 39–146.

Horner JR. 2001. *Dinosaurs under the big sky*. Missoula: Mountian Press Publishing Company.

Hulke JW. 1882. An attempt at a complete osteology of *Hypsilophodon foxii*; a British Wealden Dinosaur. *Philosophical Transactions of the Royal Society of London* **173:** 1035–1962.

Iordansky NN. 1973. The skull of the Crocodilia. In: Gans C, ed. *Biology of the reptilia, volume 4; morphology D*. New York: Academic Press, 201–260.

Irmis RB. 2007. Axial skeleton ontogeny in the Parasuchia (Archosauria: Pseudosuchia) and its implications for ontogenetic determination in archosaurs. *Journal of Vertebrate Paleontology* **27:** 350–361.

Jin L, Chen J, Zan S, Butler RJ, Godefroit P. 2010. Cranial anatomy of the small ornithischian dinosaur *Changchunsaurus parvus* from the Quantou Formation (Cretaceous: Aptian-Cenomanian) of Jilin Province, northeastern China. *Journal of Vertebrate Paleontology* **30:** 196–214.

Johnston PA, Fox RC. 1984. Paleocene and late Cretaceous mammals from Saskatchewan, Canada. *Palaeontographica, Abteilung A* **186:** 163–122.

Koch T. 1973. *Anatomy of the chicken and domestic birds*. Ames, IA: The Iowa State University Press.

Koppelhus EB, Braman DR. 2010. Upper Cretaceous palynostratigraphy of the Dry Island Area. *Canadian Journal of Earth Science* **47:** 1145–1158.

Koster EH. 1987. Vertebrate taphonomy applied to the analysis of ancient fluvial systems. In: Ethridge FG, Flores RM, Harvey MD, eds. *Recent developments in fluvial sedimentology*. Tulsa: Society of Economic Paleontologists and Mineralogists, Special Publication, *No. 39*. 159–168.

Kupsch WO. 1957. Frenchman Formation of eastern Cypress Hills, Saskatchewan, Canada. *Bulletin of the Geological Society of America* **68:** 413–420.

Larson DW, Brinkman D, Bell PR. 2010. Faunal assemblages from the upper Horseshoe Canyon Formation, an early Maastrichtian cool-climate assemblage from Alberta, with special referance to the *Albertosaurus sarcophagus* bonebed. *Canadian Journal of Earth Science* **47:** 1159–1181.

Lehman TM. 1987. Late Maastrictian paleoenvironments and dinosaur biogeography in the western interior of North America. *Palaeogeography, Palaeoclimataology, Palaeontology* **60:** 187–217.

Lerbekmo JF. 1999. Magnetostratigraphy of the Canadian Continental Drilling Program Cretaceous-Tertiary (K-T) Boundary Project core holes, western Canada. *Canadian Journal of Earth Sciences* **36:** 705–715.

Lerbekmo JF, Coulter KC. 1985. Late Cretaceous to early Tertiary magnetostratigraphy of a continental sequence: Red Deer Valley, Alberta, Canada. *Canadian Journal of Earth Sciences* **22:** 567–583.

Lyson RT, Longrich NR. 2011. Spatial niche partitioning in dinosaurs from the latest Cretaceous (Maastrichtian) of North America. *Procedding of the Royal Society B* **278:** 1158–1164.

McIver EE. 2002. The paleoenvironment of *Tyrannosaurus rex* from southwestern Saskatchewan, Canada. *Canadian Journal of Earth Sciences* **39:** 207–221.

Morris WJ. 1976. Hypsilophodont dinosaurs: a new species and comments on their systematics. In: Churcher CSe, ed. *Athlon. Essays on palaeontology in honour of Loris Shano Russell*. Toronto: Toronto University Press, 93–113.

Norman DB. 1980. On the ornithischian dinosaur *Iguanodon bernissartensis* from the Lower Cretaceous of Bernissart (Belgium). *Bulletin De l'Institut Royal Des Sciences Naturelles De Belgique* **178:** 1–103.

Norman DB, Sues H-D, Witmer LM, Coria RA. 2004. Basal ornithopoda. In: Weishampel DB, Osmólska H, Dodson P, eds. *The dinosauria (2nd edition)*. Berkeley: University of California Press, 393–412.

Novas FE, Cambiaso AV, Ambrosio A. 2004. A new basal iguanodontian (Dinosauria, Ornithischia) from the Upper Cretaceous of Patagonia. *Ameghiniana* **41:** 75–82.

Ostrom JH. 1961. Cranial morphology of the hadrosaurian dinosaurs of North America. *Bulletin of the American Museum of Natural History* **122:** 33–186.

Owen R. 1842. *Report on British fossil reptiles, part II. Report of the British Association for the Advancement of Science for 1841*. **9:** 60-204.

Parks WA. 1922. *Parasaurolophus walkeri*, a new genus and species of crested trachodont dinosaur. *University of Toronto Studies, Geological Series*, **13:** 1–32.

Parks WA. 1926. *Thescelosaurus warreni*, a new species of orthopodous dinosaur from the Edmonton formation of Alberta. *University Toronto Studies, Geological Series* **21:** 1–42.

Pearson R. 1972. *The avian brain*. New York: Academic Press.

Pincemaill M, Bufferaut E, Quillevere F. 2006. Description ostéologique de l'arrière-crâne de *Rhabdodon* (Dinosauria, Euornithopoda) et implications phylogénétiques. *Bulletin De La Societe Geologique De France* **177:** 97–104.

Prieto-Marquez A. 2010. Global phylogeny of Hadrosauridae (Dinosauria: Ornithopoda) using parsimony and Bayesian methods. *Zoological Journal of the Linnaean Society* **159:** 435–502.

Retallack G. 1984. Completeness of the rock and fossil record: some estimates using fossil soils. *Paleobiology* **10:** 59–78.

Retallack G. 1988. Down-to-Earth approaches to vertebrate paleontology. *Palaios* **3:** 335–344.

Russell DA. 1984. The gradual decline of the dinosaurs – fact or fallacy. *Nature* **306:** 360–361.

Sachs S, Hornung JJ. 2006. Juvenile ornithopod (Dinosauria: Rhabdodontidae) remains from the Upper Cretaceous (Lower Campanian, Gosau Group) of Muthmannsdorf (Lower Austria). *Geobios* **39:** 415–425.

Scannella JB, Horner JR. 2010. *Torosaurus* Marsh, 1891, is *Triceratops* Marsh, 1889 (Ceratopsidae: Chasmosaurinae): synonymy through ontogeny. *Journal of Vertebrate Paleontology* **30:** 1157–1168.

Scheetz RD. 1998. Phylogeny of basal ornithopod dinosaurs and the dissolution of the Hypsilophodontidae. *Journal of Vertebrate Paleontology* **18** (suppl.)**:** 75A.

Scheetz RD. 1999. Osteology of *Orodromeus makelai* and the phylogeny of basal ornithopod dinosaurs. Unpublished Ph.D. dissertation, Montana State University.

Seeley HG. 1887. On the classification of the fossil animals commonly named Dinosauria. *Proceedings of the Royal Society of London* **43:** 165–171.

Sereno PC. 1986. Phylogeny of the bird-hipped dinosaurs (Order Ornithischia). *National Geographic Research* **2:** 234–256.

Sereno PC. 1998. A rational for phylogenetic definitions, with application to the higher-level taxonomy of Dinosauria. *Neues Jahrbuch Für Geologie Und Paläontologie Abhandlungen* **210:** 41–83.

Sloan RE, Rigby J, Keith J, Van Valen LM, Gabriel D. 1986. Gradual dinosaur extinction and simultaneous ungulate radiation in the Hell Creek Formation. *Science* **232:** 629–633.

Smith RMH. 1993. Vertebrate taphonomy of the Late Permian floodplain deposits in the southwestern Karoo Basin of South Africa. *Palaios* **8:** 45–67.

Snively E, Longrich NR. 2009. *A small juvenile tyrannosaurid specimen from the Frenchman Formation (Maastrichtian) of Saskatchewan. Frenchman Formation Terrestrial Ecosystem Conference*. Eastend, Saskatchewan: Royal Saskatchean Museum Contribution to Science, Number 12, 46.

Starck D. 1979. Cranio-cerebral relations in recent reptiles. In: Gans C, ed. *Biology of the reptilia, volume 9: neurology A*. Toronto: Academic Press, 1–36.

Sternberg CM. 1940. *Thescelosaurus edmontonensis*, n. sp., and classification of the Hypsilophodontidae. *Journal of Paleontology* **14:** 481–494.

Sues H-D. 1980. Anatomy and relationships of a new hypsilophodontid dinosaur from the Lower Cretaceous of North America. *Palaontographica Abt. A* **169:** 51–72.

Sues H-D. 1997. Hypsilophodontidae. In: Currie PJ, Padian K, eds. *The encyclopedia of dinosaurs*. San Diego, CA: Academic Press, 356–358.

Sues H-D, Norman DB. 1990. Hypsilophodontidae, *Tenontosaurus* and Dryosauridae. In: Weishampel DB, Dodson P, Osmólska H, eds. *The dinosauria*. Berkeley: University of California Press, 498–509.

Sullivan RM. 2006. The shape of Mesozoic dinosaur richness: a reassessment. In: Lucas SG, Sullivan RM, eds. *Late Cretaceous vertebrates from the Western Interior*. Albuquerque: New Mexico Museum of Natural History and Science, 403–405.

Swofford DL. 2002. *Phylogenetic Analysis Using Parsimony* (and other methods). 4.0b10*. Sunderland, MA: Sinaur Associates.

Tokaryk TT. 1997a. Preliminary review of the non-mammalian vertebrates from the Frenchman Formation (Late Maastrichtian) of Saskatchewan. In: Mckenzie-McAnally L, ed. *Canadian Paleontology Conference Field Trip Guidebook No. 6, Upper Cretaceous and Tertiary Stratigraphy and Paleontology of Southern Saskatchewan*. St. John's, NL: Geological Association of Canada, 34–44.

Tokaryk TT. 1997b. First evidence of juvenile ceratopsians (Reptilia: Ornithischia) from the Frenchman Formation (late Maastrichtian) of Saskatchewan. *Canadian Journal of Earth Sciences* **34:** 1401–1404.

Tokaryk TT. 2009. *Head-hunting in Saskatchewan: the history of Triceratops. Frenchman Formation Terrestrial Ecosystem Conference*. Eastend, Saskatchewan: Royal Saskatchewan Museum Contribution to Science Number, 12, 61-62.

Tokaryk TT, Brinkman D. 2009. *Turtles from the Frenchman Formation and latitudinal patterns of distribution of turtles in the late Maastrichtian. Gaffney Turtle Symposium*. Drumheller, Alberta: Royal Tyrrell Museum, 178–179.

Tokaryk TT, Bryant HN. 2004. The fauna from the *Tyrannosaurus rex* excavation, Frenchman Formation (Late Maastrichtian), Saskatchewan *Summary of Investigations 2004, Volume 1*. Saskatchewan Geological Survey, Saskatchewan Industry Resources, Misc. Rep. 1-12.

Tokaryk TT, James PC. 1989. *Cimolopteryx* sp. (Aves, Charadriiformes) from the Frenchman Formation (Maastrichtian), Saskatchewan. *Canadian Journal of Earth Sciences* **26:** 2729–2730.

Tokaryk TT, Snively E. 2009. Workshop: the fauna of the Frenchman Formation. Frenchman Formation Terrestrial Ecosystem Conference. Eastend, Saskatchewan: Royal Saskatchewan Museum Contribution to Science Number 12. 64–67.

Varricchio DJ, Martin AJ, Katsura Y. 2007. First trace and body fossil evidence of a burrowing, denning dinosaur. *Proceedings of the Royal Society B* **274:** 1361–1368.

Vavrek MJ, Larsson HCE. 2010. Low beta diversity of Maastrichtian dinosaurs of North America. *Proceddings of the National Acadamy of Science* **107:** 8265–8268.

Wang SC, Dodson P. 2006. Estimating the diversity of dinosaurs. *Proceedings of the National Academy of Science* **103:** 13601–13605.

Weishampel DB, Heinrich RE. 1992. Systematics of Hypsilophodontidae and basal Iguanodontia (Dinosauria: Ornithopoda). *Historical Biology* **6:** 159–184.

Weishampel DB, Jianu C-M, Csiki Z, Norman DB. 2003. Osteology and phylogeny of *Zalmoxes* (n. g.), an unusual euornithopod dinosaur from the latest Cretaceous of Romania. *Journal of Systematic Palaeontology* **1:** 65–123.

White PD, Fastovsky DE, Sheehan PM. 1998. Taphonomy and suggested structure of the dinosaurian assemblage of

the Hell Creek Formation (Maastrichtian), eastern Montana and western North Dakota. *Palaios* **13:** 41–51.

Winkler DA, Murry PA, Jacobs LL. 1998. The new ornithopod dinosaur from the Proctor Lake, Texas, and the destruction of the family Hypsilophodontidae. *Journal of Vertebrate Paleontology* **18** (suppl.): 87A.

Witmer LM. 1995. The extant phylogenetic bracket and the importance of reconstructing soft tissues in fossils. In: Thompson JJ, ed. *Functional morphology in vertebrate palaeontology*. Cambridge: Cambridge University Press, 19–33.

APPENDIX 1

Description of characters used for the phylogenetic analysis of basal ornithopod relationships

1. Length of jugal wing on quadrate greater than 20% quadrate length (0), less than 20% (1).
2. Quadrate notch absent (0), present (1).
3. Length of the articulation between the quadrate and quadratojugal greater than or equal to 50% length of quadrate (0), between 50% and 25% (1), contact 25% or less (2).
4. Dorsal head of the quadrate recurved posteriorly (0), straight (1).
5. Pterygoid wing on quadrate greater than 25% length of quadrate (0), less than 25% (1).
6. Jugal or quadratojugal meets the quadrate near the distal end (0), above distal end (1), well above distal end (2).
7. Ventral condyles of quadrate dorsomedially sloped or horizontal (0), dorsolaterally sloped (1).
8. Pterygoid wing emerges at the dorsal head of the quadrate (0), below the dorsal head of the quadrate (1).
9. The ventral extent of the jugal wing ends at or near distal condyles of quadrate (0), above distal condyles (1), well above the distal condyles (2).
10. Groove on the base of the posterior side of the pterygoid wing of the quadrate absent (0), groove or fossa present (1).
11. Lateral pit in mid-quadrate shaft present (0), absent (1).
12. Ventral process on squamosal less than 30% length of the quadrate (0), greater than 30% (1).
13. Quadrate leans posteriorly (0), oriented vertically (1), leans anteriorly (2).
14. Jugal fails to articulate with quadrate (0), jugal articulates with quadrate (1).
15. Quadratojugal height normal to short (0), tall and narrow (1).
16. Quadratojugal foramen absent (0), present (1).
17. Exoccipital contributes to part of occipital condyle (0), occipital condyle entirely composed of basioccipital (1).
18. Orbital edge of postorbital smooth (0), striated and rugose orbital edge (1).
19. Postorbital non-robust (0), robust postorbital (1).
20. Orbital margin of the postorbital arcuate (0), anteriorly directed inflation along upper half of the orbital margin of the postorbital (1).
21. Socket for the head of the laterosphenoid occurs along frontal–postorbital suture (0), only in postorbital (1), socket absent (2).
22. Combined width of frontals less than 150% frontal length (0), greater than 150%.
23. Frontals arched over the orbits (0), dorsally flattened frontals (1).
24. Frontal contacts orbit along more than 25% of total frontal length (0), less than 25% (1).
25. Ratio of frontal length to nasal length greater than 120% (0), between 120 and 60% (1), less than 60% (2).
26. Frontals positioned over all of orbit (0), frontals only over the posterior half of orbit (1).
27. Six premaxillary teeth (0), five premaxillary teeth (1), no premaxillary teeth (2).
28. Oral margin of the premaxila non-flared (0), slightly flared oral margin of the premaxilla (1), everted oral margin of the premaxilla (2).
29. Posterolateral recess in the posterior end of the premaxilla for receipt of the anterolateral boss of the maxilla absent (0), present (1).
30. Premaxilla does not contact lacrimal (0), premaxilla contacts lacrimal (1).
31. Non-packed maxillary teeth (0), lack of space between adjacent maxillary teeth up through the occlusional margin (1).
32. Maxillary and dentary teeth not inset (0), maxillary and dentary teeth at least modestly inset (1).
33. Maxillary tooth roots straight (0), curved (1).
34. Cingulum present on maxillary tooth crowns (0), no cingulum on maxillary teeth (1).
35. Distinct neck present below maxillary crown (0), crown tapers to root (1).
36. Maxillary teeth independently occlude (0), maxillary teeth form a continuous occlusal surface (1).
37. Maxillary teeth lingually concave (0), lingually convex (1).
38. Maxillary teeth with centrally placed apical ridge (0), posteriorly set apical ridge (1).
39. Maxillary teeth equally enamelled on both sides (0), enamel restricted to one side (1).
40. Anterior end of the maxilla exhibits a spike-like process that inserts into the posterior end of the premaxilla (0), anterior end of maxilla bears an anterodorsal sulcus to receive the posterior portion of the premaxilla (1).

41. Maxillary crowns relatively low and spade-like, rectangular, or triangular (0), high diamond-shaped maxillary tooth crowns (1), maxillary tooth crowns laterally compressed and recurved posteriorly (2).
42. Jugal contacts antorbital fenestra (0), jugal excluded from bordering antorbital fenestra (1).
43. Greatest posterior expanse of the jugal greater than one-quarter skull height (0), less than one-quarter skull height (1).
44. Jugal horn or boss absent (0), present (1).
45. Anterior process of jugal straight (0), dorsally curved (1).
46. Maxillary process on the medial side of jugal medially projected and modestly arched (0), presence of a straight groove for insertion of the posterior flange of the jugal (1), anteromedially projected and arched (2).
47. Ectopterygoid articular facet on medial jugal consists of a deep groove (0), rounded scar (1).
48. In lateral view anterior end of jugal ends above maxilla (0), inserts within maxilla (1).
49. Jugal forms an oblique to right angle bordering the anteroventral corner of the infratemporal fenestra (0), acute angle (1).
50. Jugal barely touches lacrimal (0), jugal meets lacrimal with more contact (1), lacrimal–jugal butt joint (2).
51. Position of the anterior tip of dentary positioned high (0), mid height (1), near lower margin of dentary (2), below lower margin (3), well below lower margin (4).
52. Apical ridge on dentary teeth anteriorly or centrally positioned (0), posteriorly positioned (1).
53. Dentary tooth crowns possess primary and some secondary ridges (0), dentary crown possess primary, secondary, and tertiary ridges (1).
54. Dentary teeth possess ridges on both sides of crown (0), ridges on only one side (1).
55. Dentary teeth with enamel on both sides (0), enamel primarily on one side (1).
56. Dentary crowns possess denticles supported by ridges (0), not all denticles supported by ridges (1).
57. Dentary teeth possess a modest cingulum (0), no cingulum on dentary teeth (1).
58. Dentary tooth roots round in cross section (0), oval (1), squared (2), squared and grooved (3).
59. Dentary tooth roots straight (0), curved (1).
60. Dentary tooth crowns rectangular, triangular, or leaf-shaped (0), dentary tooth crowns lozenge-shaped (1), dentary tooth crowns laterally compressed and recurved posteriorly (2).
61. Dentaries straight in dorsal view (0), dentaries arched medially (1).
62. Post-coronoid elements make up 35–40% of the total length of the lower jaw (0), 25–35% (1), less than 25% (2).
63. Proportion of dentary height (just anterior to the rising coronoid process) to length of dentary 15–20% (0), 20–35% (1).
64. Predentary possesses a single posteroventral process (0), posteroventral process paired or bifurcate (1).
65. External mandibular fenestra present (0), absent (1).
66. Surangular foramen absent (0), present (1).
67. Dorsal margin of the surangular convex or diagonal (0), concave in lateral view (1).
68. Nuchal crest on supraoccipital present (0), absent (1).
69. Supraoccipital forms greater than 5% of the margin of the foramen magnum (0), less than 5% (1), does not contribute to dorsal margin (2).
70. Basioccipital ventral keel absent (0), present (1).
71. Foramen magnum occupies over 30% of the width of occipital condyle (0), 20–30% (1), less than 20% of occipital condyle (2).
72. Floor of braincase on basioccipital flat (0), arched (1).
73. Median ridge on floor of braincase on the basioccipital absent (0), present (1).
74. Basioccipital tubera extend further ventrally than the basisphenoid (0), level (1).
75. Basisphenoid shorter than basioccipital (0), equal in size (1), longer than basioccipital (2).
76. Foramen for cranial nerve V notches the anteroventral edge of the prootic (0), foramen nearly or completely enclosed in prootic (1).
77. Cervical vertebrae plateocoelous to amphicoelous (0), opisthocoelous (1).
78. Neural spine anteriorly positioned or centred over the dorsal centrum (0), posteriorly positioned (1).
79. Transition in dorsal ribs between a near-vertical orientation of the tuberculum and capitulum to a horizontal orientation occurs within ribs 2–4 (0), 5–6 (1), 6–8 (2).
80. Twelve dorsal vertebrae (0), 15 dorsal vertebrae (1), 16 dorsal vertebrae (2), 17 dorsal vertebrae (3).
81. Four sacral vertebrae (0), five sacral vertebrae (1), six sacral vertebrae (2), seven sacral vertebrae (3).
82. Sacral neural spines less than twice the height of the centrum (0), neural spines between two and two and a half times the height of the centrum (1), greater than two and a half times (2).
83. Pubis does not articulate with the sacrum (0), pubis supported by sacral rib (1), pubis supported by sacral centrum (2).

84. Caudal ribs borne on centrum (0), on neurocentral suture (1), on neural arch (2).
85. Ossified hypaxial tendons on the tail absent (0), present (1).
86. First caudal vertebrae bears longest rib (0), longest rib posterior to the first (1).
87. Caudal neural spines positioned over centrum (0), neural spines extend beyond own centrum (1).
88. Scapular spine low or broad (0), sharp and pronounced (1).
89. Coracoid width divided by length less than 60% (0), between 70 and 100% (1), greater than 100% (2).
90. Coracoid foramen enclosed within coracoid (0), open along coracoid–scapula suture (1).
91. Sternals cresent-shaped (0), hatchet-shaped (1).
92. Olecranon process on ulna low (0), moderately developed (1), relatively high (2).
93. Shaft of ulna triangular or oval in cross section (0), cylindrical (1).
94. Shaft of ulna straight (0), bowed (1).
95. Four phalanges in manual digit III (0), three phalnages (1).
96. Three phalanges in manual digit IV (0), two phalanges (1).
97. Three or more phalanges in manual digit V (0), two phalanges (1), one phalanx (2), none (3).
98. Unfused carpus (0), fused carpus (1).
99. Acetabulum high to normal (0), vertically short and long (1).
100. Ischiac peduncle of ilium not supported by sacral rib (0), ischiac peduncle articulates with sacral rib (1).
101. Shaft on ischium flat and blade-like (0), bar-like (1).
102. Distal end of ischium lacks an expanded foot (0), distal foot present (1).
103. Ischium obturator process absent (0), present (1).
104. Obturator process on ischium placed 60% or further down shaft (0), 50% (1), 40% (2), 30% or closer.
105. Pubic peduncle of ischium larger than iliac peduncle (0); iliac peduncle of ischium as large or larger than pubic peduncle (1).
106. Anterior process of pubis absent (0), present (1).
107. Anterior process of pubis rod-like or sword-like in lateral view (0), anterior process dorsoventrally expanded (1).
108. Anterior process of pubis straight when present (0), upturned anterior process (1).
109. Femur lacks a neck-like constriction below the femoral head (0), constriction present (1).
110. Lesser trochanter of femur lower or equal to greater trochanter (0), higher than greater trochanter (1).
111. Lesser trochanter of femur anterior and medial of greater trochanter (0), anterior and somewhat lateral to lesser trochanter (1).
112. Greater trochanter of femur laterally convex (0), laterally flattened (1).
113. Anterior intercondylar groove on the distal end of femur absent (0), present (1).
114. Anterior intercondylar groove on the distal end of femur modestly developed (0), anterior intercondylar groove well developed (1).
115. Lateral distal condyle width divided by medial distal condyle width on femur approximately 100% (0), 80–60% (1), 59–50% (2), 49–40% (3), 39–30% (4), 29–20% (5).
116. Both proximal lateral condyles on the tibia equal in size (0), fibular condyle smaller (1), only one lateral condyle present (2).
117. Cnemial crest of tibia rounded (0), sharply defined (1).
118. Midshaft of tibia triangular in cross section (0), round in cross section (1).
119. Fibula shaft elliptical or round in cross section (0), D-shaped in cross section (1).
120. Astragalus bears a short ascending process (0), triangular and tooth-like (1), spike-like (2), relatively large (3).
121. Posterior side of astragalus low (0), high (1).
122. Anterior side of astragalus high (0), moderate (1), low (2).
123. Angle between the tibial and fibular articular facets on the calcaneum greater then 120° (0), less than 120° (1).
124. Medial distal tarsal blocky in dorsal view (0), thin and rectangular (1), round (2).
125. Medial distal tarsal does not articulate over the proximal end of metatarsal II (0), medial distal tarsal articulates over a least a portion of the proximal end of metatarsal II (1).
126. Lateral distal tarsal square in dorsal view (0), kidney shaped (1).
127. Four functional digits (i.e. bear phalanges) in the pes (0), three functional digits in the pes (1).
128. Premaxillae unfused (0), fused (1).
129. Palpebral dorsoventrally flattened and rugose along the medial and distal edges: absent (0); present (1).
130. Frontals wider across posterior end than at midorbital level (0), wider at midorbital level (1).
131. Presence of a Y-shaped indentation on the dorsal edge of opisthotics: absent (0); present (1).
132. Angle formed by a line drawn along the ventral edge of the braincase (occipital condyle, basal tubera, and basipterygoid processes) and a line drawn through the centre of the trigeminal foramen and the posterodorsal hypoglossal foramen: greater than 15° (0); less than 15° (1).

133. Dorsolaterally directed process on the lateral surface of the surangular: absent (0); present (1).
134. Ratio of femur length to tibia length: less than one (0); greater than one (1).
135. Presence and structure of a horizontal ridge on the maxilla: absent or smooth when present (0); present with at least the posterior portion covered by a series of obliquely inclined ridges (1).
136. Posterior half of ventral edge of jugal offset ventrally and covered laterally with obliquely inclined ridges: absent (0); present (1).
137. Foramen in the prefrontal positioned dorsomedial to the articulation surface for the palpebral that opens into the orbit: absent (0); present (1).
138. Dorsalmost extent of ilium above acetabulum (0), posterior to acetabulum (1).
139. Brevis shelf angled medially in horizontal plane (0), oriented ventromedially (1).
140. Distal portions of anterior dorsal rib shafts circular or oval in transverse section (0), highly laterally compressed with a concave lateral and rugose posterior surfaces (1).

APPENDIX 2

Character codings for the 23 terminal taxa used in the analysis shown in Fig. 23. Modified from Boyd *et al*. (2009). Question marks indicate lack of information for that taxon.

	10	20	30	40	50	60	70	80	00	100	110	120	130	140
Herrerasaurus	?00000??20	?020000000	?010202000	00?1101-0?	20?00???02	----0-1??2	?00-000000	??????00??	000?0000?0	?2000?3000	00??00--00	00?-000101	0???0000??	???1??????
Heterodontosaurus	?00000??0?	000000?0?0	?000100?1	11??11?00?	00010??001	0001101100	0010000000	???0?0??00	0??0000?1?	?200001100	010-00-00?	100-0?0???	???0000000	0000000?0
Scutellosaurus	??????????	??????0000	??????00??	00?0000000	0?????????	0000000000	0?000?????	??????????	1???0??010	?0?????0??	00??1???00	00100????0	???????00??	???0??????
Lesothosaurus	000000000?	0000000000	0000000000	0000000100	00000??001	0000000000	0000000000	00??10????	2???0?0?10	?000??2000	000-00-000	000-00???3	?0010?0000	00?00000??
Agilisaurus	?001??????	???000????	?000101 1??	01?000?10?	01?01??110	??????????	????10????	?????????1	1??10??0?0	????????11	0012?10100	100-?????0	????0?0000	??000000??
Hexinlusaurus	0000??????	??10000001	?00010???0	?1?000?10?	01100???11	1?0??????0	1?0????00?	0?????00?1	1??1??1?10	?0000?10??	0012010000	100-??0?01	???11?0?00	???0000???
Othnielosaurus	??????????	??????0000	?00??0????	0100000 10?	0???0???1?	1000000000	1?001????0	101???00?1	10010?1010	00?0?01001	0012010010	100-1?00?2	1011110 0??	???0??????
Oryctodromeus	001???1000	??????????	??????111?	010000???0	0??001??1?	200????0?00	1?0????001	110??11121	3022?11110	?100?????1	?????10010	110-?10010	0???????1??	0??0?0?0?0
Zephyrosaurus	0010001001	01?0??0101	0010?0101?	1100001?00	0?11100 00?	?000000000	1?1????001	110120000?	??210?1110	?00??????1?	0???????10	11101?0010	0201100100	00?0000???
Orodromeus	0010001101	0100000101	1000?0111?	0100000000	0111000002	2000000000	1010110101	1101110001	2021001110	011000?011	0011010010	110-100012	0001100000	??00000000
Parksosaurus	001?01?010	1000000000	?01010???0	01?0001 10?	01000???11	?000000000	011011??0?	000?0010?2	2?01201010	01?0?????1	0010110110	110-0?0000	0011100??0	??00000000
Hypsilophodon	0000020 02?	?000010 0?0	0000101000	1100111110	01000??111	2011110010	111011?001	01?010?001	2011211011	010100?001	0010010010	100-210001	0011110000	0000000?0
Gasparinisaura	1000?2??2?	?000 11?000	??00??????	11?111?1??	11?00??1?1	3?????????	?01?110000	2?????????	1011101010	???0?????1	0?12110011	110-120100	0212111 00?	??0000?1??
Tenontosaurus	0000100?00	0011010??0	1010102 2?0	1111111110	01000??111	2001111211	001111?121	20?0001112	1101101010	00011??011	0112111110	1011320100	0211100000	0001000 1??
Rhabdodon	?010?10000	1?????????	??????200?	11?1?11100	0?????????	1001101210	1?11111??1	?000??01??	21210?1000	?101?????1	110-1???10	1011220 0?0	12?2011 0??	???????0?0
Dryosaurus altus	0120020100	?011000??0	1000102200	1111111111	1000010001	2111111111	1011101001	2000011111	2102001001	0100???111	1113011111	1011310 0?3	1011111000	0000000 1??
Dryosaurus lettowvorbecki	1120020121	1011000???	?000102201	??????????	???0010101	2111111111	1011111001	2100211 1?1	2?12011001	0101??????	1113011111	10113????3	1?1?0?1000	0000000 1??
Camptosaurus	01?0120120	1111?00010	1011102201	1111111111	1100001111	3111111311	1111111000	2011000102	2201?11011	0101101111	1113111110	1011?20100	120?0?1000	0101000 1??
Iguanodon	1101120120	1010101?10	2111212201	1111111111	1100021112	4111111311	1201111020	2000201123	2211011021	12?0110111	1113111110	1011521100	1202011000	01?1?????0
Ouranosaurus	110112002?	?010101010	1111212201	11?????1?1	?010021112	3111????11	1100111120	00002?1123	22?0??1021	1210???111	0113111100	1011421100	1212??1000	0001000 1?0
Thescelosaurus neglectus	??????????	???????101	??????????	??????????	??????????	??????????	??????????	???????0?2	1?0?1?1???	?000001001	00??110110	1110??00??	0?1?1?0??1	???1???111
Thescelosaurus assinaboiensis	??????????	??????000?	0010?0????	?1????????	??????????	??????????	???????111	011100?0??	1???1?1???	????????01	?????10110	1110??0000	00A1?00?11	11?1?1?001
Thescelosaurus garbanii	??????????	??????????	??????????	??????????	??????????	??????????	??????????	??????????	??????????	??????????	??????????	??10??0000	00?11?0???	??????????